LUCAS DE SOUZA SOARES

TÉCNICO-FUNCIONALIDADE DE QUITOSANO EM MEIOS AQUOSOS ÁCIDOS FLUIDOS OU GELIFICADOS

Tese apresentada à Universidade Federal de Viçosa, como parte das exigências do Programa de Pós-Graduação em Ciência e Tecnologia de Alimentos, para obtenção do título de *Doctor Scientiae*.

VIÇOSA
MINAS GERAIS – BRASIL
2019

Ficha catalográfica preparada pela Biblioteca Central da Universidade Federal de Viçosa - Câmpus Viçosa

T
S676t
2019

Soares, Lucas de Souza, 1989-
Técnico-funcionalidade de quitosano em meios aquosos ácidos fluidos ou gelificados / Lucas de Souza Soares. – Viçosa, MG, 2019.
xviii, 132f. : il. (algumas color.) ; 29 cm.

Inclui apêndices.
Orientador: Eduardo Basílio de Oliveira.
Tese (doutorado) - Universidade Federal de Viçosa.
Inclui bibliografia.

1. Colóides. 2. Dispersão. 3. Emulsões. I. Universidade Federal de Viçosa. Departamento de Tecnologia de Alimentos. Programa de Pós-Graduação em Ciência e Tecnologia de Alimentos. II. Título.

CDD 22 ed. 660.2945

LUCAS DE SOUZA SOARES

TÉCNICO-FUNCIONALIDADE DE QUITOSANO EM MEIOS AQUOSOS ÁCIDOS FLUIDOS E GELIFICADOS

Tese apresentada à Universidade Federal de Viçosa, como parte das exigências do Programa de Pós-Graduação em Ciência e Tecnologia de Alimentos, para obtenção do título de *Doctor Scientiae*.

APROVADA: 26 de abril de 2019.

Alvaro Vianna Novaes de Carvalho Teixeira
(Coorientador)

Jane Sélia dos Reis Coimbra
(Coorientadora)

Vagner Tebaldi de Queiroz

Alexandre Gurgel

Eduardo Basílio de Oliveira
(Orientador)

“Mas é preciso ter manha
É preciso ter graça
É preciso ter sonho sempre
Quem traz na pele essa marca
Possui a estranha mania
De ter fé na vida”
(Milton Nascimento/Fernando Brant)

AGRADECIMENTOS

À Universidade Federal de Viçosa (UFV), ao Departamento de Tecnologia de Alimentos (DTA) e ao Programa de Pós-Graduação em Ciência e Tecnologia de Alimentos (PPGCTA), pela oportunidade e pelos recursos investidos durante o curso.

À Coordenação de Aperfeiçoamento de Pessoal de Nível Superior (CAPES), pela concessão da bolsa de estudos e pela concessão de recursos financeiros ao PPGCTA-UFV (Código 001).

À Fundação de Amparo à Pesquisa do Estado de Minas Gerais (FAPEMIG), pela concessão de recursos financeiros ao projeto (CAG - APQ-00566-14; Valor total da concessão: R$ 48.300,00).

Ao professor Eduardo Basílio de Oliveira, por todos os ensinamentos e pelas orientações feitas durante a elaboração e realização do projeto. Pela confiança, apoio, dedicação e cuidado e, sobretudo, por acreditar em mim como profissional.

Aos professores Alvaro Vianna Novaes de Carvalho Teixeira e Jane Sélia Coimbra dos Reis, pelo excelente convívio, pelos valiosos ensinamentos e pela preciosa colaboração como co-orientadores desse trabalho.

Aos professores Alexandre Gurgel (DEQ) e Vagner Tebaldi de Queiroz (DQF - UFES *Campus* Alegre), pela participação na banca de defesa e pelas sugestões dadas para a conclusão do trabalho.

Ao professor Frederico Augusto Ribeiro de Barros, pela gentileza ao avaliar o texto do projeto de tese e pelas considerações realizadas.

Aos professores Elson Santiago de Alvarenga (DEQ) e Luciano de Moura Guimarães (DEF) pelos ensinamentos compartilhados durante o meu exame de qualificação e pela generosa parceria.

Aos professores Eber Antonio Alves Medeiros e Nilda de Fátima Ferreira Soares, por terem disponibilizado os equipamentos alocados no laboratório por eles coordenado e por sua a gentil colaboração nas atividades.

Às professoras Laura Fernandes de Melo Correia e Érica Nascif Rufino Vieira, pelo carinho, atenção e amizade.

Aos colegas dos laboratórios de Operações e Processos (LOP) e Estudos de Materiais Alimentares (LEMA), pela colaboração e ótima convivência. Em especial, aos estimados: Ana Paula Hanke de Oliveira, Angélica Ribeiro da Costa, Douglas Fernando Balbino, Kely de Paula Correa, Maurício Palmeira Chaves de Souza, Michele Harumi Omura, Thais Jordânia Silva, Thomás Valente de Oliveira, Vitor Alledi da Rocha e Zoila Rosa Nieto Galván.

Ao amigo-irmão Gustavo Leite Milião, pelo incentivo diário, pelas longas conversas científico-filosóficas e por todas as contribuições nos experimentos.

Aos bolsistas de Iniciação Científica e aos estagiários que colaboraram na realização dos experimentos (Bruna Tonole, Jéssica Silva Gomes, Beatriz Borges Pinto Pereira, Gabriel Batalha de Souza, Rayza Badiani Perim e Bárbara Gomes Teixeira).

Aos amigos Alessandra Casagrande Ribeiro, Carini Aparecida Lelis, Dandara Lima Brasil, Letícia Rocha Ferreira, Luana Virgínia Souza, Nayara Benedito Martins da Silva, Richard Marins da Silva, Thamiris Caroline Dutra, pelas reflexões, apoio e incentivo.

Aos meus pais, Tânia e Márcio, aos meus irmãos, Athos e Gabriel, pelo apoio e incentivo ao longo dessa jornada.

A todos que de alguma forma contribuíram para a realização deste trabalho.

BIOGRAFIA

LUCAS DE SOUZA SOARES, filho de Márcio Augusto Soares e Tânia Fernandes de Souza, nasceu em Coronel Fabriciano, Minas Gerais, em 20 de setembro de 1989.

Em março de 2005 ingressou no curso técnico em Agropecuária, na Escola Agrotécnica de Alegre, concluindo-o em dezembro de 2007.

Em março de 2008 iniciou a graduação em Engenharia de Alimentos, na Universidade Federal do Espírito Santo, concluindo-o em julho de 2013. Durante a graduação foi bolsista da Pró-Reitoria de Extensão, entre março de 2009 e fevereiro de 2011, sob a supervisão do professor Heberth de Paula. Atuou, também, como bolsista de iniciação científica, entre março de 2011 e julho de 2011, sob a orientação da professora Consuelo Domenici Roberto, do Departamento de Engenharia de Alimentos. Foi monitor da disciplina de Microbiologia (novembro de 2012 a abril de 2013), sob a supervisão da professora Elisabete Fantuzzi, do Departamento de Produção Vegetal. Foi monitor da disciplina de Bromatologia e Composição de Alimentos e Microbiologia de Alimentos, entre setembro de 2012 e julho de 2013, sob a supervisão do professor Wagner Miranda Barbosa.

Em julho de 2013 ingressou no Curso de Mestrado do Programa de Pós-Graduação em Ciência e Tecnologia de Alimentos, na UFV, concluindo-o em fevereiro de 2015.

Em março de 2015 ingressou no Curso de Doutorado do Programa de Pós-Graduação em Ciência e Tecnologia de Alimentos, na UFV, submetendo-se à defesa de sua tese em abril de 2019.

SUMÁRIO

LISTA DE FIGURAS

LISTA DE TABELAS

RESUMO

SOARES, Lucas de Souza, D.Sc., Universidade Federal de Viçosa, abril de 2019. **Técnico-funcionalidade de quitosano em meios aquosos ácidos fluidos ou gelificados**. Orientador: Eduardo Basílio de Oliveira. Coorientadores: Alvaro Vianna Novaes de Carvalho Teixeira e Jane Sélia dos Reis Coimbra.

Quitosano é reconhecidamente um polissacarídeo com ação hipocolesterolêmica obtido pela desacetilação parcial (≥ 50%) da quitina, que é um biopolímero extraído principalmente de crustáceos processados pela indústria pesqueira. Este biopolímero tem sido usado em várias aplicações biotecnológicas. Entretanto, a prévia dispersão deste biopolímero é necessária para a exploração de suas técnico-funcionalidades. Meios aquosos contendo o ácido acético são comumente utilizados para dispersar o quitosano, uma vez que os grupos amino (NH_2) existentes em suas cadeias podem ser protonados (NH_3^+), o que favorece a repulsão inter-cadeia e, portanto, sua dispersão. Assim, o estudo de dispersões aquosas de quitosano e de interações intermoleculares específicas entre esse biopolímero e outros ácidos orgânicos além do acético torna-se relevante, a fim de ampliar a aplicabilidade do quitosano como ingrediente ou aditivo em formulações fluidas ou gelificadas, em particular as alimentícias. Então, este estudo foi estruturado em três grandes vertentes. Inicialmente, dispersões de quitosano contendo os ácidos acético (AA), glicólico (AG), propiônico (AP) ou lático (AL) foram analisadas. O aumento da concentração de ácido reduziu o pH e a viscosidade das dispersões, além do |ζ potencial| das partículas dispersas. Por outro lado, a condutividade elétrica e a densidade das dispersões aumentaram, assim como o diâmetro hidrodinâmico das cadeias dispersas. A uma mesma concentração de ácido, esses efeitos foram ligeiramente mais pronunciados para as dispersões contendo AG ou AL, sendo tal comportamento atribuído a interações atrativas mais intensas das cadeias do quitosano com os contra-ânions glicolato ou lactato. Portanto, concluiu-se que os ácidos glicólico, propiônico ou lático são adequados para dispersar o quitosano em meios aquosos e, em termos físico-químicos, podem substituir o ácido acético que tem sido tipicamente usado para tal finalidade. Em uma segunda abordagem, emulsões O/A contendo

diferentes concentrações de quitosano, previamente disperso em soluções aquosas de AA, AG, AP ou AL, foram preparadas usando homogeneização ultrassônica. O aumento da concentração de quitosano promoveu o aumento do índice de consistência e do módulo de armazenamento das emulsões, além de reduzir o aumento do diâmetro médio de suas gotículas e prevenir a separação de fases das emulsões expostas aos ciclos de centrifugação, congelamento-descongelamento ou congelamento-descongelamento-aquecimento. Assim, constatou-se que o quitosano atuou como agente espessante e estabilizante nas formulações das emulsões ácidas, sendo seu desempenho influenciado pela concentração de biopolímero, mas não pelo tipo de ácido. Por fim, hidrogéis de amido ou de carragena contendo uma substituição parcial desses agentes gelificantes por quitosano foram preparados usando solução de ácido lático adicionada do corante amarelo crepúsculo (INS 110). Hidrogéis parcialmente substituídos por quitosano não apresentaram diferenças significativas para os parâmetros de cor, nem alterações expressivas nas propriedades visco-elásticas, quando comparadas aos materiais preparados exclusivamente com carragena ou amido. Além disso, a substituição parcial do amido por quitosano reduziu drasticamente a liberação do INS 110, para uma solução de sacarose em contato com os hidrogéis durante 316 h. Dessa forma, o desempenho técnico-funcional do quitosano em meio aquoso ácido contendo diferentes ácidos orgânicos foi demonstrado nesta tese. Somados às biofuncionalidade já conhecidas do quitosano, os resultados aqui apresentados prenunciam o impacto promissor desse biopolímero para aplicações alimentícias, uma vez que: *i)* ácidos orgânicos alimentares que não o acético podem ser utilizados para dispersá-lo em meio aquoso; e *ii)* ele exerce as funções de espessante de dispersões aquosas e estabilizante de emulsões, além de potencializador de cor em hidrogéis (sem alterar sua reologia).

ABSTRACT

SOARES, Lucas de Souza, D.Sc., Universidade Federal de Viçosa, April, 2019. **Techno-functionality of chitosan in fluid or gelled acidic aqueous media**. Adviser: Eduardo Basílio de Oliveira. Co-advisers: Alvaro Vianna Novaes de Carvalho Teixeira and Jane Sélia dos Reis Coimbra.

Chitosan is known to be a hypocholesterolemic polysaccharide obtained by the partial deacetylation (≥ 50%) of chitin, which is a biopolymer extracted mainly from crustaceans processed by the fishing industry. This polysaccharide has been used in several biotechnological applications. However, the prior dispersion of this biopolymer is necessary for the exploitation of its techno-functionalities. Aqueous media containing acetic acid are commonly used to disperse chitosan, since the existing amino groups (NH_2) in their chains can be protonated (NH_3^+), which favors inter-chains repulsion and therefore their dispersion. Thus, the study of chitosan aqueous dispersions and specific intermolecular interactions between this biopolymer and other organic acids rather than acetic becomes relevant in order to extend the applicability of chitosan as an ingredient or additive in fluid or gelled formulations, in particular foodstuff. Then, this study was structured in three broad parts. Initially, chitosan dispersions containing acetic (AA), glycolic (GA), propionic (PA) or lactic (LA) acids were analysed. The increase in acid concentration reduced the pH and viscosity of the dispersions in addition to the |ζ potential| of the dispersed particles. On the other hand, the electrical conductivity and density of the dispersions increased, as did the hydrodynamic diameter of the dispersed chains. At the same acid concentration, these effects were slightly more pronounced for dispersions containing GA or LA, being such behavior attributed to more intense attractive interactions of chitosan chains with glycolate or lactate counter-anions. Therefore, in physicochemical terms, glycolic, propionic or lactic acids are suitable for chitosan dispersion in aqueous media, and they may be properly used to replace acetic acid, which has typically been used for such purpose. Additionally, O/W emulsions containing different chitosan concentrations, previously dispersed in AA, GA, PA or LA aqueous solutions, were prepared using ultrasonic homogenization. The increased chitosan concentration promoted an augment in

the consistency index and the storage modulus of emulsions. In addition, there was an attenuation of the increase in hydrodynamic average diameter of oil droplets, and a prevention of emulsions phase separation, when exposed to centrifugation, freeze-thawed or freeze-thawed-heated cycles. Thus, chitosan acted as a thickening and/or stabilizing agent in the acid emulsion formulations, being its performance influenced by the biopolymer concentration, and not by the acid type. Finally, starch or carrageenan hydrogels containing a partial replacement of these gelling agents by chitosan were prepared using lactic acid solution added with Yellow sunset dye (INS 110). Hydrogels partially substituted by chitosan presented neither significant differences for color parameters nor expressive changes in viscoelastic properties, comparing to materials prepared exclusively with carrageenan or starch. In addition, the partial replacement of starch by chitosan drastically reduced the release of INS 110 to a sucrose solution in contact with the hydrogels, during 316 h. Thus, the technico-functional performance of chitosan in aqueous acid medium containing different organic acids was demonstrated in this thesis. In addition to the known bio-functionality of chitosan, the results presented here show the promising impact of this biopolymer for food applications, since: *i)* organic food acids rather than acetic acid may be used to disperse this biopolymer in aqueous medium; and *ii)* chitosan exerts the functions of aqueous dispersion thickener, emulsion stabilizer, and color enhancer in hydrogels (without altering its rheology).

1. INTRODUÇÃO GERAL

A busca por novas matérias-primas é uma das estratégias que visam à diversificação e/ou melhoria de formulações alimentícias. Polissacarídeos pouco usuais na indústria de alimentos são alvos de estudos e testes, pois podem trazer aos produtos vantagens do ponto de vista nutricional, sensorial e/ou técnico-funcional, quando comparados aos convencionalmente utilizados (goma guar, pectina e outros). Dentre esses polissacarídeos pouco usuais, o quitosano pode ser destacado.

Quitosano é o nome do polissacarídeo biodegradável, biocompatível com tecidos humanos e atóxico, obtido pela desacetilação parcial (≥ 50%) da quitina, que é um biopolímero encontrado nas carapaças de camarões, caranguejos e outros artrópodes marinhos ou na parede celular de alguns fungos. Grupos amino (NH_2) existentes nas cadeias do quitosano podem ser protonados em meios aquosos ácidos, o que favorece a sua dispersão e propicia a sua exploração em aplicações biotecnológicas. O quitosano é empregado como excipiente para liberação controlada de fármacos e outras substâncias bioativas, suporte para a fabricação de próteses ósseas e dérmicas ou, ainda, adsorvente de lipídios para tratamentos pró-emagrecimento e hipocolesterolêmico. No setor alimentar, o quitosano tem uma atuação mais restrita, sendo principalmente utilizado na produção de coberturas comestíveis para frutas e na fabricação de filmes para embalagens. Contudo, a sua utilização como ingrediente ou aditivo de alimentos fluidos não é comum.

A utilização do quitosano como ingrediente ou aditivo pode ser uma alternativa inovadora para a produção de iogurtes, molhos e sobremesas, uma vez que em alimentos ácidos ele poderia desempenhar uma função biofuncional (restringindo a absorção de lipídios pelo trato gastrointestinal) e outra técnico-funcional (estabilizante, gelificante e carreador de compostos, por exemplo), simultaneamente. Meios aquosos contendo o ácido acético são comumente utilizados para dispersar o quitosano, o que poderia ser uma desvantagem para aplicações em produtos alimentícios, devido ao cheiro e sabor desagradável desse composto. Na literatura, foram encontrados poucos relatos que tratam de dispersões do quitosano e/ou do seu desempenho técnico-funcional em meios aquosos contendo outros ácidos que não o acético.

Assim, o estudo das dispersões de quitosano, bem como uma prévia compreensão das interações intermoleculares entre o quitosano e ácidos orgânicos presentes nos meios aquosos, torna-se relevante. Além disso, o emprego do quitosano

em alimentos fluidos ou gelificados e, até mesmo, em sistemas-modelo que reproduzam condições comuns às deles é uma temática que deve ser estudada amplamente, a fim de verificar se o quitosano pode desempenhar um papel técnico-funcional nesses sistemas. Tendo em vista o contexto apresentado, essa tese objetivou estudar a técnico-funcionalidade do quitosano em meios aquosos ácidos fluidos ou gelificados.

Dessa forma, o presente documento foi estruturado como segue:

i) Um capítulo intitulado “Estudo Bibliográfico” em que é feita uma apresentação do quitosano, em termos de estrutura e função. Na sequência, são apresentadas definições sobre dispersões, emulsões e hidrogéis, além de estudos que propuseram a utilização do quitosano em cada um desses sistemas coloidais. Este capítulo objetiva fornecer bases teóricas para a compreensão de como o trabalho experimental visa responder à problemática apresentada. Além disso, espera-se demonstar o caráter inovador da proposta e dos resultados de cada capítulo experimental.

ii) Em seguida, é apresentado o artigo científico intitulado *Insights on physicochemical aspects of chitosan dispersion in aqueous solutions of acetic, glycolic, propionic or lactic acid* (doi:10.1016/j.ijbiomac.2019.01.106), aceito para publicação no periódico **International Journal of Biological Macromolecules**. Nesse trabalho, as propriedades físicas (pH, condutividade elétrica, densidade e viscosidade) de dispersões de quitosano contendo os ácidos acético, glicólico, propiônico ou lático foram analisadas comparativamente. Avaliou-se, também, o diâmetro hidrodinâmico médio e potencial ζ das cadeias de quitosano dispersas nesses meios aquosos ácidos. Ademais, estudaram-se as interações intermoleculares do quitosano com os ácidos utilizando a técnica de FT-IR.

iii) No terceiro capítulo é apresentado um manuscrito de artigo científico com título provisório *Chitosan dispersed in aqueous solutions of acetic, glycolic, propionic or lactic acid as a thickener/stabilizer agent of O/W emulsions produced by ultrasonic homogenization*, a ser submetido a um periódico de circulação interncional. Nesse estudo, emulsões contendo diferentes concentrações de quitosano, previamente disperso em soluções de ácido acético, glicólico, propiônico ou lático, foram preparadas usando homogeneização ultrassônica, a fim de avaliar o desempenho do biopolímero sobre o espessamento e/ou estabilização desses sistemas, em função do tempo de armazenamento ou de diferentes estresses ambientais.

iv) Por fim, no quarto capítulo, é também apresentado um manuscrito de artigo científico com título provisório *Partial replacement of gelling agents by chitosan: impact on the color, viscoelastic properties, and release of Yellow sunset (INS 110) from carrageenan or starch hydrogels*, a ser submetido a um periódico de circulação interncional. Analisou-se o aspecto visual, a cor e as propriedades reológicas de hidrogéis de amido ou de carragena contendo uma substituição parcial desses agentes gelificantes por quitosano. Em seguida, estudou-se a liberação do corante amarelo crepúsculo (INS 110) presente nos hidrogéis para uma solução de sacarose em contato com eles.

Espera-se que os resultados apresentados possam se juntar a mais relatos da literatura da área e contribuir para difundir as aplicações desse biopolímero no setor de alimentos formulados. Dessa forma, o objetivo geral dessa tese foi avaliar a técnico-funcionalidade do quitosano em meios aquosos contendo os ácidos acético, glicólico, propiônico ou lático fluidos (dispersões e emulsões) ou gelificados (hidrogéis).

Capítulo I

Estudo Bibliográfico

Abreviações e símbolos

AA	ácido acético
AC	ácido cítrico
AG	ácido glicólico
AL	ácido lático
AMM	massa molar alta (kDa)
AP	ácido propiônico
AS	alginato de sódio
BMM	massa molar baixa (kDa)
CE	condutividade elétrica ($mS \cdot cm^{-1}$ ou $\mu S \cdot cm^{-1}$)
CH	Chitosan
CMQ	carboxi-metil-quitosano
d_h	diâmetro hidrodinâmico médio (nm)
$d_{3,2}$	diâmetro médio da área da superfície da partícula (nm)
$d_{4,3}$	diâmetro médio do volume da partícula (nm)
EMP	emulsão primária
GA	grau de acetilação (%)
GD	degree de desacetilação (%)
GX	goma xantana
GP	B-glicerofosfato
G'	módulo de armazenamento (Pa)
G"	módulo de perda (Pa)
HAP	homogenizador de alta pressão
HUS	homogeneizador ultrassônica
K	índice de consistência ($Pa \cdot s^n$)
MM	massa molar (kDa)
MMM	massa molar média (kDa)
n	Índice de comportamento (adimensional)
pH	potencial hidrogeniônico
SDS	dodecil sulfato de sódio
TD	tetradecano
z-ave	diâmetro médio de cumulants (nm)
ΔG_{int}	variação da energia livre de Gibbs associada à região interfacial
ΔA_{int}	variação da área interfacial
γ	tensão interfacial ($mN \cdot m^{-1}$)
ζ	potencial zeta (mV)
η	viscosidade (Pa·s)
$\eta_{ap_{17,6}}$	viscosidade de taxa de cisalhamento = 17,6 s^{-1} (Pa·s)
η_0	viscosidade na taxa de cisalhamento zero (Pa·s)
τ	tensão de cisalhamento (Pa)
τ_{MAX}	valor máximo da tensão de cisalhamento (Pa)
$\dot{\gamma}$	taxa de cisalhamento (s^{-1})

1. Quitosano

Quitosano é um polissacarídeo obtido pela desacetilação parcial da quitina [poli-β(1→4)-2-acetamida-2-deóxi-D-glicopiranose], que é um biopolímero presente nas carapaças de crustáceos (camarões, lagostas, caranguejos, por exemplo) ou nas paredes celulares de alguns gêneros de fungos [1,2]. Contudo, a matéria-prima predominantemente utilizada para a extração industrial da quitina são as carapaças de artrópodes processados pela indústria pesqueira [3,4]. A quitina é o segundo polissacarídeo mais abundante no meio ambiente, sendo superada apenas pela celulose [5,6]. O processamento das carapaças de crustáceos para a obtenção da quitina é feito em três etapas principais [5]: *i*) desproteinação usando uma solução de hidróxido de sódio (10% m/v), 60-70 ºC, por 1 h; *ii*) desmineralização usando uma solução de ácido clorídrico (10% v/v), 50-60 ºC, por 1-2 h; e *iii*) despigmentação usando uma solução de permanganato de potássio (0,02% m/v), 60 ºC, por 2 h. A partir da quitina, o quitosano é produzido usando uma solução de hidróxido de sódio (50% m/v), a 100 ºC, por 2-5h, [1,2]. Na Figura 1 é apresentada uma comparação entre as estruturas moleculares da quitina, do quitosano e da celulose.

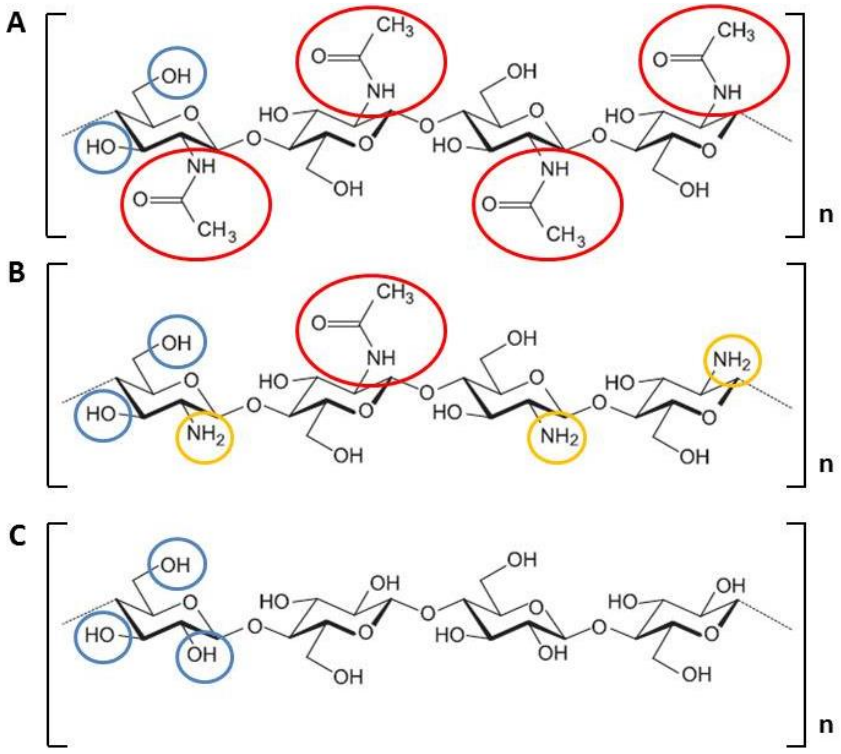

Figura 1 - Estruturas moleculares da quitina (A), do quitosano (B) e da celulose. Adaptado de Chiappisi & Gradzielski (2015).

Na Figura 1 têm-se as representações de um fragmento da quitina, quitosano e celulose, que se repetem “n” vezes para formarem essas macromoléculas. Observa-se que as cadeias de

quitina são formadas exclusivamente por monômeros de N-acetil-D-glicosamina (Figura 1 - A), enquanto as de celulose, por D-glicose (Figura 1 - C). Estruturalmente, esses dois monômeros são semelhantes, porém há a substituição da hidroxila (OH) do carbono C2 da glicose por um grupo acetamido ($NHCOCH_3$) no N-acetil-D-glicosamina. No quitosano (Figura 1 - B) a maioria dos grupos acetamido são convertidos em grupo amino (NH_2) durante o processo de desacetilação e as cadeias desse biopolímero são formadas por monômeros de D-glicosamina e, em menor percentual, N-acetil-D-glicosamina [2,5].

O quitosano apresenta-se como um pó pouco denso, esbranquiçado, opaco e inodoro, em condições ambientais (25 ^{o}C e 1 atm). Ressalta-se que no mercado existem produtos distintos entre si (cor, dispersibilidade, percentual de impurezas, dentre outras) que são chamados de "quitosano", devido à ausência de uma formalização sobre as características que o biopolímero deve apresentar. Algumas empresas que produzem insumos para laboratório conseguem, atualmente, uma padronização do quitosano comercializado utilizando uma mistura de matérias-primas e condições pré-estabelecidas para a reação de desacetilação. Entretanto, o custo desse quitosano é alto, o que poderia inviabilizar aplicações na indústria de alimentos.

A partir do exposto, duas características são fundamentais para definir e classificar os produtos da reação de desacetilação da quitina: *i*) massa molar; e *ii*) grau de desacetilação. Assim, a avaliação da massa molar e do grau de desacetilação do quitosano é recomendada, uma vez que influenciam diretamente nas propriedades físico-químicas e no desempenho técnico-funcional do biopolímero. Segundo a Sigma-Aldrich (2019), o quitosano pode ser classificado em temos de massa molar como baixa (50 a 190 kDa), média (190 a 310 kDa) e alta (≥ 310 kDa) [4,9,10]. Além disso, os quitosanos disponíveis para comercialização geralmente apresentam *GD* entre 75% e 85% [3]. A presença de grupos funcionais reativos em cada uma das unidades monoméricas desacetiladas (grupo NH_2 na posição C2 e grupos OH nas posições C6 e C3) permitem que interações intermoleculares entre o quitosano e outras moléculas possam ocorrer [1].

A dispersão do quitosano em água pura ou meios aquosos alcalinos não é comum, porém este biopolímero é capaz de se dispersar em soluções ácidas (pH ≤ 6,4) [11]. Os grupos amino presentes no quitosano são progressivamente protonados em meios aquosos ácidos, (Equação 1), o que aumenta a polarizabilidade das cadeias poliméricas e a repulsão eletrostática entre elas e, consequentemente, possibilita a sua hidratação.

$$\mathrm{RNH_2} + \mathrm{H^+} \leftrightarrows \mathrm{RNH_3}^+ \quad (1)$$

A dispersibilidade do quitosano em meio aquoso está condicionada à concentração do ácido, bem como à sua estrutura molecular. Nesse caso, o contra-ânion liberado pelo ácido pode interagir com as cadeias protonadas e atenuar a sua dispersão [12]. O quitosano disperso em meios aquosos ácidos pode causar o espessamento desses sistemas [13,14], sendo a magnitude dependente da massa molar e do *GD* do biopolímero [3]. Contudo, estudos reportam que

quitosano com *GD* > 70% apresentam maiores taxas de dispersão, quando comparados com produtos da reação de desacetilação próximos a 50% [1,8].

O quitosano é reconhecidamente um biopolímero com baixa toxicidade, biodegradável, biocompatível com tecidos humanos e ambientalmente amigável [15–18]. Tais propriedades possibilitam seu emprego em diversas aplicações biotecnológicas [19–22]. Na área médico-farmacêutica, por exemplo, esse biopolímero é aplicado como excipiente para liberação controlada de substâncias bioativas [23,24] e como material para a fabricação de próteses ósseas e dérmicas [25]. As aplicações desse biopolímero no setor de alimentos apresentam-se limitadas a produção de filmes plásticos e revestimentos comestíveis, com o intuito de limitar o contato do alimento com o oxigênio atmosférico e estender a conservação do produto [19,21,26,27], como agente clarificador para a produção de bebidas, ou ainda para a imobilização de enzimas. Em termos fisiológicos, o quitosano atua como um adsorvente de lipídios no trato gastrointestinal de humanos [28], sendo o seu consumo, sozinho ou associado a fibras vegetais, indicado para indivíduos em dietas hipocolesterolêmicas e/ou pró-emagrecimento.

No Brasil, o consumo do quitosano é permitido pela Resolução n. 18 (ANVISA), de 30 de abril de 1999, que trata do consumo de alimentos funcionais (BRASIL, 1999). De acordo com essa Resolução o quitosano é uma

> "*... fibra dietética que pode ser utilizada com alegações de redução da absorção de gordura e colesterol, desde que o consumo diário do produto forneça, no mínimo, 3 g de quitosano se o alimento for sólido ou 1,5 g se o alimento for fluido.*"

De acordo com a Resolução n. 18 (ANVISA), a recomendação para a ingestão do quitosano encontra-se restrita no Brasil ao seu papel como pró-emagrecedor e hipocolesterolêmico. Ressalta-se que a permissão para o uso de ingredientes e aditivos alimentares faz parte de um processo de avaliação e constante reavaliação, que está baseada em alegações científicas sobre as suas propriedades biofuncionais e o seu impacto na saúde do consumidor. Dessa forma, a realização de estudos que proponham a adição do quitosano em formulações pode contribuir para a ampliação de seu uso em produtos alimentícios. Em especial, sistemas-modelo aplicados ao estudo do papel que o quitosano desempenha em meios aquosos ácidos (dispersões, emulsões e hidrogéis) são de interesse em pesquisa e desenvolvimento, uma vez que reproduzem várias características de alimentos formulados. Nas próximas seções serão apresentados alguns estudos que propõem o estudo do papel técnico-funcional do quitosano.

2. Dispersões aquosas

Em meios aquosos ácidos, o quitosano forma dispersões coloidais, uma vez que suas cadeias protonadas passam a interagir entre si e com as moléculas de água [3,29]. Assim, do

ponto de vista físico-químico, as cadeias dispersas do quitosano são consideradas partículas coloidais eletricamente carregadas dispersas em meio aquoso. Conforme ocorre com outros hidrocoloides, o balanço das interações quitosano-quitosano e quitosano-água irá impactar as propriedades físicas (densidade, viscosidade, índice de refração, por exemplo) das dispersões. Alterações em tais propriedades podem engendrar ganhos em termos de técnico-funcionalidade, quando essas macromoléculas são adicionadas intencionalmente em produtos, a fim de desempenhar um papel específico. Na Tabela 1 são apresentados alguns exemplos de estudos que propuseram a avaliação de dispersões de quitosano ou das suas cadeias dispersas em meios aquosos ácidos.

Tabela 1 - Descrição de estudos de dispersões de quitosano ou de suas cadeias dispersas em meios aquosos ácidos.

Descrição do material	Tratamentos	Análises	Resultado	Referência
Quitosano (*GD* = 75% ou *GD* = 94%)	Dispersões contendo 0,20%; 1,00%, e 2,00% (m/v) em solução de ácido clorídrico (100 mmol·L^{-1})	Viscosidade (viscosímetro rotacional); 25 ^{o}C	*GD* = 75% - η (mPa·s): 0,20%: 3; 1,00%: 174; 2,00%: 999 *GD* = 94% - η (mPa·s): 0,20%: 2; 1,00%: 26; 2,00%: 380	[30]
Quitosano (MM = 108 kDa; *GD* 75%)	Dispersões contendo 0,50%; 1,00%, 1,50% e 2,00% (m/m) em solução ácida (1,0% v/v), dos ácidos acético (AA), lático (AL) ou clorídrico (HCl)	Curvas de escoamento (reômetro); 25 ^{o}C	η_0 (Pa·s) 0,5% (m/m): AA: 0;28; LA: 0,28 e HCl: 0,08; η_0 (Pa·s) 1,0% (m/m): AA: 2,1; LA: 2,3 e HCl: 1,1; η_0 (Pa·s) 1,5% (m/m): AA: 9,1; LA: 8,7 e HCl: 6,7; η_0 (Pa·s) 2,0% (m/m): AA: 27,0; LA: 29,0 e HCl: 21,0	[31]
Quitosano MM baixa (BMM; 70 kDa; *GD* 75-85%); quitosano de MM média (MMM; 750 kDa; *GD* 75-85%); quitosano de MM alta (AMM; 750 kDa; *GD* 75-85%)	Dispersão de 2,0% (m/m) de quitosano BMM, MMM ou AMM em solução de ácido glicólico 1,0% (m/m) sob agitação magnética por 2 h	Curvas de escoamento (viscosímetro rotacional): 2,2 até 44,0 (s^{-1}), 25 ^{o}C	$\eta_{ap\ 17,6}$ (mPa·s^{n}) - AMM: 5831 ± 105; MMM: 3263 ± 77; e BMM: 221 ± 12 *n* - AMM: 0,77 ± 0,05; MMM: 0,78 ± 0,02; e BMM: 0,87 ± 0,03	[32]
Quitosanos (MM = 190 kDa; *GD* 75 - 85%)	Dispersões contendo 0,25%; 0,50%; 1,00%, 1,50% e 2,00% (m/m) em solução tampão (ácido acético 0,2 mmol·L^{-1} + acetato de sódio 0,05 mmol·L^{-1}; pH 3,90)	Curvas de escoamento (reômetro); 25 ^{o}C	η_0 (Pa·s) 0,25% (m/m): 0,007; 0,5% (m/m): 0,09; 1,0% (m/m): 0,15; 1,5% (m/m): 0,86; 2,0% (m/m): 1,08	[33]
Quitosanos (MM média; *GD* 76%)	Dispersões contendo 0,25%; 0,50%; 0,75%; 1,00% e 1,25% (m/v) em solução de ácido acético (1,0% v/v)	Viscosidade (reômetro de tensão constante); 25 ^{o}C	η (mPa·s) - 0,25%: 5; 0,50%: 10; 0,75%: 25; 1,00%: 40; e 1,25%: 70	[34]

Descrição do material	Tratamentos	Análises	Resultado	
Quitosanos (MM = 326 kDa; *GD* = 60,5%; 65,4%; 70,8%; 77,3%; ou 86,1%)	Dispersão 0,75% (m/v) em solução de ácido acético (1,0% v/v)	Viscosidade (reômetro de tensão constante); 25 ^{o}C	η (mPa·s) - 60,5%: 14; 65,4%: 13; 70,8%: 12; 77,3%: 14; e 86,1%: 16	[34]
Quitosano - a): 229 kDa e *GD* 75,9%; b): 410 kDa e *GD* 76,9%; c): 600 kDa e *GD* 76,7%; d): 706 kDa e *GD* 76,4%; e e): 880 kDa e *GD* 76,1%	Dispersão 0,75% (m/v) em solução de ácido acético (1,0% v/v)	Viscosidade (reômetro de tensão constante); 25 ^{o}C	η (mPa·s) - a): 14; b): 13; c): 12; d): 14; e e): 16	[34]
Quitosano (MM = 150 kDa; *GD* 75 - 85%)	Dispersão 1,0% (m/v) em tampão acetato de sódio (pH 3,0; 100 mmol·L^{-1}) sob agitação magnética, 12h; Diluição para 0,01% (m/v) (pH 4,5; HCl 0,1 mmol·L^{-1})	Diâmetro hidrodinâmico médio (d_h) Potencial ζ	d_h (nm): 1 a 10 Potencial ζ (mV): 51,3 ± 4,7	[35]
Quitosano (MM = 374 kDa; *GD* 89%)	Dispersão 1,9% (m/m) em solução de ácido acético 2,0% (m/m), 25,0 ± 0,1 ^{o}C	Viscosidade (reômetro oscilatório); 25 ^{o}C	Viscosidade (Pa·s): ≈ 2	[36]
Quitosano (MM = 486 kDa; *GD* 87,2%)	Dispersão 1,0% (m/v) em soluções de ácido acético (AA) ou lático (AL) 1,0% (v/v), sob agitação mecânica, 24h, 25,0 ± 0,1 ^{o}C	Viscosidade (reômetro oscilatório); 0,1 a 100 s^{-1}; 25 ^{o}C Potencial ζ (dispersões de AA, diluídas 1:10)	K (Pa·s^{n}) - AA: 0,036; AL: 0,057 n – AA: 0, 987; AL: 0,947 Potencial ζ: +80,75 ± 2,19	[37]
Quitosano (MM = 540 kDa; *GD* 84,6 ± 5,1%)	Titulação de solução ácida (0 a 71 mmol·L^{-1}) água + 1,0% (m/v); ácidos cítrico (AC) ou lático (AL); 14 adições de 500 µL (1,8 mol·L^{-1}), 25 min.	Condutividade elétrica (CE) pH	CE (µS·cm^{-1}) - AC ≈ 1650 (71 mmol·L^{-1}); AL ≈ 1400 (71 mmol·L^{-1}) pH: AC ≈ 3,5 (71 mmol·L^{-1}); AL ≈ 4,3 (71 mmol·L^{-1})	[12]

Descrição do material	Tratamentos	Análises	Resultado	Referência
Quitosano (MM = 540 kDa; *GD* 84,6 ± 5,1%)	Dispersões 1,0% (m/v) em soluções (100 mmol·L^{-1}) dos AC e AL; agitação 24 h (25 ± 1 ^{o}C) e centrifugação.	Potencial ζ	Potencial ζ (mV): AC: +28,5; AL: +52,1	[12]
Quitosano (MM = 540 kDa; *GD* 84,6 ± 5,1%)	Dispersão 0,1% (m/v) em soluções de ácido lático com pH 3,0; 3,5 e 4,0 sob agitação por 12h, 25,0 ± 0,1 ^{o}C	Viscosidade (25,00 ± 0,02 ^{o}C; viscosímetro Cannon-Fenske 51310)	η (mPa·s) - pH 4,0: 4,05 ± 0,20; pH 3,5: 4,05 ± 0,30; e pH 3,0: 3,72 ± 0,20	[38]
Quitosano (MM = 1.200 ± 500 kDa; *GD* 74.5%)	Dispersão 0,1% (m/v) em soluções de ácido acético (AA), glicólico (AG), propiônico (AP) ou lático (AL) 10 mmol·L^{-1}, sob agitação por 12h, 25,0 ± 0,1 ^{o}C)	Condutividade elétrica (CE) pH Diâmetro médio (d_h) Potencial ζ Viscosidade (reômetro oscilatório): 0,1 - 300,0 (s^{-1}); 25,0 ± 0,1 ^{o}C;	CE (µS·cm^{-1}) - AA: 210,3; GA: 355,3; PA: 196,1 e LA: 345,0 pH - AA: 4,4; GA: 3,5; PA: 4,5 e LA: 3,6 d_h (nm) - AA: 15,3; GA: 16,5; PA: 14,9 e LA: 16,2 Potencial ζ (mV): AA: +77,8; GA: +78,4; PA: +74,5; e LA: +78,2 η (mPa·s): AA: 7,68; GA: 7,12; PA: 7,74; e LA: 7,05	[39]
Quitosano - a): 164 kDa e *GD* 75,0%; b): 141 kDa e *GD* 79,0%; c): 137 kDa e *GD* 83,2%; e d): 118 kDa e *GD* 90,0%	Dispersões 0,2% e 1,0% (m/v) em solução de ácido clorídrico (mmol·L^{-1})	Condutividade elétrica (CE) pH Viscosidade (viscosímetro rotacional); 25 ^{o}C	0,2% (m/v) - CE (mS·cm^{-1}): 1,5; pH 2,5; η (mPa·s): a): 2,6; b): 2,3; c): 3; e d): 1,4. 1,0% (m/v) - CE (mS·cm^{-1}): 8; pH 2,0; η (mPa·s): a): 9,5; b): 6,5; c): 7,5; e d): 7,0.	[40]

Na Tabela 1, exemplos de estudos com dispersões preparadas com quitosanos de diferentes massas molares e *GD* podem ser observadas. O incremento na concentração de polissacarídeo promove o aumento das viscosidades das dispersões, o que destaca o desempenho do quitosano como agente espessante. As expressivas variações nos valores de viscosidade apresentadas, em uma determinada concentração de quitosano, estão relacionadas a características intrínsecas do biopolímero. Quitosanos de diferentes origens, massas molares médias e *GD* apresentam diferentes propriedades físicas, visto que a magnitude do espessamento está condicionada a essas características, como pôde ser observado nos artigos analisados. Embora na literatura considere-se que biopolímeros contendo pelo menos 50% dos grupos acetamido desacetilados podem ser chamados de quitosano, a magnitude das propriedades físico-químicas de meios aquosos contendo quitosanos com 50% e 70% de desacetilação diferem. De fato, quitosanos com *GD* ≥ 70% e com massa molar ≥ 10^3 kDa apresentam melhor dispersibilidade e capacidade espessante.

A maior parte dos trabalhos analisados envolvem o uso de ácido acético ou tampões contendo acetatos, que por possuir um odor desagradável poderiam inviabilizar aplicações do quitosano em produtos alimentícios. O papel do ácido utilizado na dispersão do quitosano não se restringe à redução do pH, uma vez que interações específicas entre os contra-ânions e as cadeias policatiônicas podem causar a atenuação da dispersibilidade máxima do biopolímero. Contudo, interações intermoleculares entre os ácidos e o quitosano não são comumente avaliadas e/ou discutidas. Além disso, concentrações excessivas de ácido podem promover a hidrólise das ligações glicosídicas na cadeias de quitosano, o que pode levar a uma redução da viscosidade dos sistemas contendo o biopolímero. Outra maneira de melhorar a dispersibilidade do quitosano, modificações da sua molécula com grupos hidrofílicos têm sido propostas [18,41]. Tais reações são caras, apresentam baixo rendimento e utilizam reagentes químicos potencialmente tóxicos, que não condizem com a produção de alimentos.

A utilização de meios aquosos contendo ácidos orgânicos com estrutura molecular semelhante à do ácido acético deve ser considerada como uma alternativa para a dispersão do quitosano, a fim de possibilitar aplicações alimentícias para esse biopolímero. Nesse sentido, estudos que proponham a avaliação do desempenho técnico-funcional do quitosano em meios aquosos contendo diferentes ácidos orgânicos são cientificamente relevantes. Interações intermoleculares entre o quitosano e esses ácidos devem ser estudadas, uma vez que elas condicionam a sua a dispersibilidade e as propriedades das dispersões. Dessa forma, informações inéditas podem ser obtidas e podem fomentar a utilização do quitosano no setor de alimentos.

3. Emulsões

Emulsões são sistemas coloidais formados por um líquido disperso sob a forma de gotículas (< 15 μm, geralmente) em outro líquido [42]. O aumento do contato entre duas fases

imiscíveis, que é causado pelo aumento da área interfacial (ΔA_{int}) nesses sistemas, causa o aumento do conteúdo de energia livre de Gibbs (ΔG) do sistema (Equação 2).

$$\Delta G = \gamma \cdot \Delta A_{int} \quad (2)$$

Na Eq. 2, ΔG é a variação da energia livre de Gibbs do sistema, ΔA_{int} é a variação da área interfacial, e γ é a tensão interfacial existente entre as duas fases.

Altas taxas de energia são necessárias para a dispersão das gotículas, uma vez que o aumento na área interfacial é termodinamicamente desfavorável ($\Delta G_{int} > 0$, como decorre da Eq. 2). Neste caso, misturadores de alta taxa de cisalhamento, moinhos coloidais, homogeneizadores de alta pressão e microfluidizadores são os dispositivos comumente usados para promover a ruptura de gotículas e produzir as emulsões [43]. Adicionalmente, as abordagens emergentes incluem o uso de ondas ultrassônicas, membranas e microcanais. As diferentes técnicas de emulsificação objetivam em geral produzir emulsões com gotículas de diâmetro médio < 10 µm.

Ainda de acordo com a Eq. 2, observa-se que reduzir o valor da tensão interfacial (γ) é uma estratégia para facilitar a emulsificação. A redução da γ pode ser alcançada pela adição de surfactantes ao sistema [44]. Comumente, na área de emulsões, os surfactantes são chamados de emulsificantes. Emulsificantes são moléculas anfifílicas, que se posicionam entre os líquidos imiscíveis e reduzem o contato energeticamente desfavorável entre elas [42,43]. Durante a preparação das emulsões, os líquidos imiscíveis são misturados e as moléculas de emulsificante se adsorvem à interface das gotículas formadas. A adição de emulsificantes permite, ainda, a produção de emulsões cineticamente estáveis [45]. Além da contribuição dos surfactantes em geral para a formação da emulsão, pelo abaixamento da γ, emulsificantes especificamente iônicos podem favorecer ainda mais a estabilização cinética desses sistemas, uma vez que os grupos eletricamente carregados em suas estruturas moleculares contribuem para repulsão eletrostática e, até mesmo, estérica entre as gotículas [45,46].

Outra maneira de melhorar a estabilidade cinética das emulsões é pela adição de agentes espessantes [47]. Polissacarídeos (goma xantana, celuloses modificadas, galactomananas, por exemplo) são amplamente utilizados como agente espessante e/ou estabilizante de emulsões, devido à sua capacidade de aumentar a consistência da fase contínua em tais sistemas [48], reduzindo a frequência e intensidade de colisões entre as gotículas dispersas em movimento browniano.

Alguns estudos relatam que polissacarídeos com uso emergente no cenário industrial, como o quitosano, podem apresentar vantagens em termos de textura de produtos e/ou de processos de homogeneização comparados àqueles convencionalmente utilizados como espessantes de emulsões. Ao nosso conhecimento, é pequeno o número de trabalhos que propõem estudar o papel técnico-funcional do quitosano em emulsões. No entanto, alguns exemplos de estudos discorrendo sobre este biopolímero em tal tipo de sistema são apresentados na Tabela 2.

Tabela 2 - Descrição de estudos que avaliaram emulsões contendo quitosano.

Descrição do material	Pré-tratamento	Tratamentos	Homogeneização	Análises/Resultado	Referência
5% óleo de milho + 95% dispersão emulsificante (1,0% (m/v) de lecitina, 0,02% (m/v) de azida sódica em solução de ácido acético 100 mmol·L^{-1}; pH 3,0 - HCl); 0,2% (m/v) de quitosano em tampão acetato (100 mmol·L^{-1}; pH 3,0)	Mistura das fases (misturador mecânico)	Quitosano (0,0% ou 0,04% m/v), pH 3,0 e NaCl (0 mmol·L^{-1}) Quitosano (0,036% m/v), pH (3,0; 4,0; 5,0; 6,0; 7,0 e 8,0) e NaCl (0 mmol·L^{-1}) Quitosano (0,036% m/v), pH 3,0 e NaCl (100 mmol·L^{-1})	+ 1 passagens em HAP (34 MPa)	$d_{4,3}$ (µm) - 0,0%: 1,5; 0.04%: 6,0; Pot. ζ (mV) - 0,0%: -50,0; 0.04%: +50,0 $d_{4,3}$ (µm) - pH 3,0-5,0: 1,5; pH 6,0-8,0: 1,8; Pot. ζ (mV) - pH 3,0-5,0: -55,0; pH 6,0-8,0: -75,0 $d_{4,3}$ (µm) - 100 mmol·L^{-1}: 1,8; Pot. ζ (mV): -23,0	[49]
5% óleo de milho + 95% dispersão emulsificante (1,0% (m/v) de lecitina, 0,02% (m/v) de azida sódica em solução de ácido acético 100 mmol·L^{-1}; pH 3,0 - HCl); 0,2% (m/v) de quitosano em tampão acetato (100 mmol·L^{-1}; pH 3,0)	Mistura das fases (misturador mecânico)	Quitosano (0,036% m/v) x pH (3,0; 4,0; 5,0; 6,0; 7,0 e 8,0) x NaCl (0 e 100 mmol·L^{-1})	Pré-emulsificação (misturador) + 1 passagens em HAP (34 MPa)	$d_{4,3}$ (µm) - 0,0%: 1,0; 0.04%: 1,5; Pot. ζ (mV) - 0,0%: -35,0; 0.04%: +50,0 $d_{4,3}$ (µm) - pH 3,0-5,0: 1,0; pH 6,0-8,0: > 8,0; Pot. ζ (mV) - pH 3,0-5,0: -40,0; pH 6,0-8,0: -45,0 $d_{4,3}$ (µm) - 100 mmol·L^{-1}: 1,3; Pot. ζ (mV): +23,0	
20% óleo de milho + 80% dispersão emulsificante (20 mmol·L^{-1} SDS em solução de HCl; pH 3,0)	Pré-emulsificação + 6 passagens HAP (34 MPa)	Diluição 0,0 - 1,0% (m/v) de quitosano em tampão acetato (100 mmol·L^{-1}; pH 3,0)	HUS (2 min, 20 kHz e 40% de amplitude)	$d_{3,2}$ (µm): 0,2 até 1,0 Potencial ζ (mV): -45,0 até +50,0	[50]
20% óleo de milho + 80% dispersão emulsificante (Tween 20 2,5% (m/v) em solução de HCl; pH 3,0)	Pré-emulsificação + 6 passagens HAP (34 MPa)	Diluição 0,0 - 1,0% (m/v) de quitosano em tampão acetato (100 mmol·L^{-1}; pH 3,0)	HUS (2 min, 20 kHz e 40% de amplitude)	$d_{3,2}$ (µm): 0,3 até 0,5 Potencial ζ (mV): -10,0 até +40,0	

Descrição do material	Pré-tratamento	Tratamentos	Homogeneização	Análises/Resultado	Referência
Emulsão-primária (EMP): 20% (m/m) de óleo + 80% (m/m) dispersão emulsificante [Tween 80 0,8% (m/m)], em solução de ácido acético (pH 6.0)	Mistura das fases (misturador mecânico)	Emulsão secundária: 5% (m/m) de óleo + 20% (m/m) EMP + 75% (m/m) dispersão de quitosano (0,0%; 0,5% e 1,0% m/m)	1 passagem em HAP (34 MPa)	z-ave (nm) - 0,0%: 300; 0.5%: 350; e 1.0%: 380 Potencial ζ (mV) - 0,0%: -13,0; 0.5%: -10,0; e 1.0%: -5,0	[51]
Emulsão-primária (EMP): 20% (m/m) de óleo de atum + 80% (m/m) dispersão emulsificante [Tween 80 0,8% (m/m)], em solução de ácido acético (pH 6.0)	Pré-emulsificação (misturador) + 1 passagem em HAP (34 MPa)	Emulsão secundária: 5% (m/m) de óleo + 20% (m/m) EMP + 75% (m/m) dispersão de quitosano (0,0%; 0,5% e 1,0% m/m)	HUS (amplitude = 15%, frequência = 23 KHz, t = 15 min)	z-ave (nm) - 0,0%: 300; 0.5%: 300; e 1.0%: 300 Potencial ζ (mV) - 0,0%: -13,0; 0.5%: -10,0; e 1.0%: -5,0	[51]
5,0% (m/m) carvona, 1,0% (m/v) CLR10 + quitosano (0,00 e 1.00% m/m) em tampão acetato (100 mmol·L^{-1}; pH 4.0)	-	-	6 passagens em HAP (69 MPa)	z-ave (nm) - 0,0%: 100; 1,0%: 300 Potencial ζ (mV) - 0,0%: -50; 1,0%: +40	[52]
Tetradecano (TD) + quitosano (CH) disperso em soluções ácidas (50 mmol·L^{-1}; HCl, AA, AP). TD:CH = 187 (15:0,08); 875(35:0,04); 3500 (35:0,01); e 7000 (35:0,005)	-	-	HUS (20 kHz, 10,7 W/mL; 30 s)	d_h (μm) - HCl: 187: 3,1; 875: 4,1; 3500: 4,5; e 7000: 4,8; AA: 187: 2,2; 875: 2,7; 3500: 3,1; e 7000: 3,3; AP: 187: 2,2; 875: 2,5; 3500: 2,9; e 7000: 3,3	[53]
10,0% óleo de girassol + 90,0% [0,1% (m/v) em soluções de ác. lático pH 3,0; 3,5 e 4,0 adicionadas de Tween 20 1,0% (m/v)]	Misturador (24.000 r/min, 1 min)	-	6 passagens HAP (69 MPa)	d_h (nm) - 0,0%: 360; 0,1%: 45 e 360; Pot. ζ - 0,0%: -1;0; 0,1%: +50,0; η (mPa·s) - 0,0%: 1,2; 0,1%: 3,0	[38]

Em geral, os estudos apresentados na Tabela 2 destacaram o desempenho do quitosano no aumento da viscosidade da fase continua de emulsões. Além do seu papel como agente espessante, observa-se a existência de interações entre as cadeias de quitosano e o filme interfacial das gotículas (inferidas pelo aumento do diâmetro e da modificação dos valores de potencial ζ). Tais interações podem ter contribuído para a repulsão eletrostérica entre as gotículas e, consequentemente, para o aumento da estabilidade cinética das gotículas de óleo das emulsões O/A. Ademais, alguns estudos propuseram a avaliação de emulsões contendo quitosano submetidas a uma variação dos fatores extrínsecos (pH, força iônica e temperatura), a fim de explicar como as interações polissacarídeo-interface se estabelecem nas condições pré-determinadas e como elas podem contribuir para o aumento da estabilidade cinética.

Emulsões preparadas exclusivamente com quitosano (sem a adição de um agente interfacial) mostram, também, uma estabilidade cinética macroscópica que variou entre minutos e horas. Embora esses trabalhos tenham sugerido que o quitosano exerceu alguma contribuição no sistema como emulsificante, características intrínsecas do biopolímero como massa molar (> 100 kDa), rigidez da cadeia polimérica e ausência de grupamentos explicitamente hidrofóbicas predizem que a sua contribuição para a redução da tensão interfacial é pequena. Nesse caso, acredita-se que a estabilização do sistema deu-se pela sua ação espessante.

Em todos os casos analisados, a adição do quitosano pareceu melhorar a estabilidade cinética dos sistemas. Contudo, nota-se a necessidade da realização de estudos que proponham a análise de emulsões contendo diferentes concentrações de quitosano em sua fase contínua, a fim de relacionar o espessamento desses sistemas com a sua estabilidade, em função do tempo e/ou de estresses ambientais (aumento da temperatura, por exemplo).

Os resultados apresentados na Tabela 2 mostram que o quitosano pode atuar como agente espessante e/ou estabilizante de emulsões. Contudo, na maior parte dos sistemas analisados, o quitosano foi previamente disperso em soluções de ácido acético e/ou tampões acetato. Dessa forma, como no caso das dispersões aquosas, estudos que proponham a preparação e avaliação de emulsões contendo o quitosano disperso em meios aquosos contendo ácidos orgânicos diversos apresentam-se como uma perspectiva científica relevante.

4. Hidrogéis

A gelificação de um sistema pode ser definida, microscopicamente, como o fenômeno em que as macromoléculas (geralmente, polímeros de alta massa molar) são induzidas energeticamente a interagir entre si e formar uma rede sólida tridimensional, que contêm em seus interstícios uma fase líquida [48]. Já macroscopicamente, géis se apresentam como sólidos viscoelásticos, isto é, sistemas com propriedades mecânicas intermediárias às de um líquido perfeitamente viscoso e de um sólido perfeitamente elástico, dependo dos esforços a que são submetidos [54].

Hidrogéis, *i*. *e*. géis em que a fase dispersa é aquosa, podem ser produzidos a partir de biomoléculas (muitas vezes proteínas ou polissacarídeos), que estabelecem interações físicas (interações de hidrogênio, interações eletrostáticas e interações hidrofóbicas, entre outras) ou químicas (ligações dissulfeto, por exemplo) para criar zonas de junção e manter a fase líquida dentro da malha coloidal [55].

Geléias, sobremesas lácteas, iogurtes e produtos cárneos processados são alguns exemplos de alimentos semissólidos com uma estrutura típica de gel. Além disso, a produção de alguns materiais das áreas farmacêutica e cosmética (curativos, bandagens, cremes, entre outros), em escala laboratorial ou comercial, está baseada nos princípios da gelificação [20,21,56,57]. Alginato, carragena e ágar são exemplos de polissacarídeos tradicionalmente utilizados como gelificantes em aplicações biotecnológicas, sendo os mecanismos físico-químicos que regem a formação dos géis específicos para cada um deles. Além desses, o quitosano já é usado pela indústria médico-farmacêutica para a produção de materiais gélicos, visando explorar as suas propriedades mecânicas diferenciadas e a capacidade de carreamento do biopolímero. Em formulações alimentícias, no entanto, a aplicação do quitosano para tais finalidades não é de uso corrente. Na Tabela 3 são apresentados alguns exemplos de estudos que propuseram a preparação de géis contendo quitosano.

Tabela 3 - Descrição de estudos que avaliaram géis contendo de quitosano.

Material	Tratamentos	Condição de gelificação	Análises	Resultado	Referência
Quitosano (CH; *GD* = 72% e MM = 820 kDa) Goma xantana (GX; MM = 100 kDa)	6,5 mg CH/mL de solução de HCl (100 mmol·L^{-1}; pH final ajustado com NaOH ≈5,6) 6,5 mg GX/mL H_2O Mistura das dispersões de CH/GX, congelamento e liofilização	Dispersões 7,0 a 10,0% (m/v) da mistura CH/GX para formar os géis	Varredura de frequência (0,1 – 100 rad·s^{-1}, 25 °C, deformação = 3,0%)	*G'* (Pa) – 0,1 rad·s^{-1}: $1{,}0\cdot10^{1}$ (7,0% m/v); $2{,}0\cdot10^{1}$ (8,0% m/v); $7{,}0\cdot10^{1}$ (9,0% m/v); e $1{,}0\cdot10^{2}$ (10,0% m/v) *G'* (Pa) – 100 rad·s^{-1}: $8{,}0\cdot10^{1}$ (7,0% m/v); $1{,}0\cdot10^{2}$ (8,0% m/v); $2{,}0\cdot10^{2}$ (9,0% m/v); e $3{,}0\cdot10^{2}$ (10,0% m/v)	[58]
Quitosano (CH; *GD* = 82% e MM = 78 kDa) Amido de milho (AM)	Dispersão de CH (1,0% m/m) em solução de ácido acético (100 mmol·L^{-1}); suspensão de AM (20% m/m)	Diluição da dispersão CH (0,1; 0,25 e 0,5% m/m) Mistura CH's/AM sob vácuo; Aquecimento 40 °C – 90 °C Resfriamento até 20 °C	Varredura de frequência (0,1 - 2 rad·s^{-1}, 20 °C, deformação = 1,0%)	*G'* (10^3 Pa) – 1 rad·s^{-1}: ≈9,0 (0,0% m/m CH); ≈6,5 (0,1% m/m CH); ≈5,0 (0,25% m/m CH); ≈5,0 (0,5% m/m CH); e ≈5,5 (1,0% m/m CH);	[59]
Quitosano (CH; *GD* = 90,4% e MM = 112 kDa)	Dispersão de CH 3,0% (m/v) em solução de ácido acético (2,0% m/v)	-	Teste de compressão (deformação = 2%·min^{-1})	τ_{MAX} = 0,03 Pa (ruptura em 20% de deformação)	[60]
Quitosano (CH; *GD* = 90,4% e MM = 112 kDa)	Dispersão de CH 3,0% (m/v) em solução de hidróxido de lítio (4,8% m/m) + ureia (8,0% m/m)	-	Teste de compressão (deformação = 2%·min^{-1})	τ_{MAX} = 1,65 MPa (ruptura em 70% de deformação)	
Quitosano (CH; *GD* = 84,7%)	Dispersão 1,0% (m/v) de CH em solução de ácido acético (50 mmol·L^{-1})	Precipitação com solução de NaOH (até pH ≈9,0)	Lavagem, diálise e gel e secagem (80 °C; vácuo) → Retenção de agua	Conteúdo de água: ≈97,8%	[61]

Material	Tratamentos	Condição de gelificação	Análises	Resultado	Referência
Quitosano (CH; *GD* = 84,7%) Alginato de sódio (AS) β-glicerofosfato (GP)	Modificação estrutural localizada no C6-OH (CM) com amônia quaternária de cadeia longa	CM (1,7% m/m) + GP (CM:CP = 1:1,5)	Viscosidade (2h após a preparação; $\dot{\gamma}$ = 10 s^{-1}; 37 °C)	η (mPa·s): 200 (CM + GP); 300 (CM + AS + GP)	[62]
Quitosano (CH; *GD* = 78%; MM = 213 kDa) β-glicerofosfato (GP) Ácido acético (AA)	CH = 87 mmol·L^{-1} GP/CH = 2,11 AA = 0,6	Titulação de GP sob agitação até a composição apresentada; repouso 24h, 4 °C	Visco-elasticidade (τ = 1 Pa; 25 e 47 °C)	25 °C: 1 Hz (Pa) - *G'* = $3{,}0\cdot10^{2}$ e *G''* = $3\cdot10^{0}$; 10 Hz (Pa) - *G'* = $3{,}0\cdot10^{2}$ e *G''* = $1{,}0\cdot10^{2}$ 37 °C: 1 Hz (Pa) - *G'* = $2{,}0\cdot10^{4}$ e *G''* = $2\cdot10^{3}$; 10 Hz (Pa) - *G'* = $3{,}0\cdot10^{2}$ e *G''* = $7{,}0\cdot10^{3}$	[63]
Quitosano (CH; *GD* = 85,6%; MM = 530 kDa) Alginato de sódio (AS) Bicarbonato de sódio ($NaHCO_3$)	[Dispersão de CH 2,0% (m/v) em ácido acético (1 mol·L^{-1}) + 4,0% (m/v) $NaHCO_3$]; pH 7-8 Dispersão de SA 2,0% (m/v)	Mistuta CH:AS (0,1; 0,2; 0,5; 1,0 e 2,0) + glucona delta-lactona (1 mol·L^{-1})	Visco-elasticidade (γ = 1%; 0,1 – 10 Hz; 37 °C)	1 Hz: *G'* (Pa) - $4{,}0\cdot10^{1}$ (CH:AS 0,1); $1{,}5\cdot10^{2}$ (CH:AS 0,2); $2{,}0\cdot10^{2}$ (CH:AS 0,5); $1{,}0\cdot10^{3}$ (CH:AS 1,0); e $3{,}0\cdot10^{2}$ (CH:AS 2,0) 10 Hz: *G'* (Pa) - $5{,}0\cdot10^{1}$ (CH:AS 0,1); $1{,}5\cdot10^{2}$ (CH:AS 0,2); $8{,}0\cdot10^{2}$ (CH:AS 0,5); $1{,}1\cdot10^{3}$ (CH:AS 1,0); e $4{,}0\cdot10^{2}$ (CH:AS 2,0)	[64]
Carboxi-metil-quitosano (CMQ; 100-300 kDa); Poli(2-hidroxil-etil acrilato); Pesulfato potássio (KPS); N,N-metileno-bisacrilamida	0,15 g·15 mL^{-1} CMQ + $9{,}25\cdot10^{-6}$ mol·15 mL^{-1} KPS + $10{,}4\cdot10^{-3}$ mol·15 mL^{-1} 2-HEA + $5{,}84\cdot10^{-4}$ mol·15 mL^{-1} MBA (3h; 75 °C)	Hidrogel: lavado e seco por 72 horas em um liofilizador (-50 °C)	Visco-elasticidade (1 Hz; 25 °C)	*G'* (Pa): $3{,}0\cdot10^{3}$; *G''* (Pa): $2{,}0\cdot10^{2}$	[65]

Na Tabela 3, alguns processos que envolvem a produção de géis contendo o quitosano estão listados. Tais processos estão baseados em: *i)* adição de uma molécula sequestradora de prótons (β-glicerofosfato, por exemplo), que propicia a redução da repulsão eletrostática entre as cadeias de quitosano possibilitando a transição sol-gel; *ii)* exposição controlada das cadeias de quitosano ao meio alcalino, que causa a precipitação gradual de cadeias de quitosano e um arraste de parte da fase aquosa; *iii)* reações químicas de modificação das cadeias de quitosano inserindo-lhe grupos mais propícios à formação de géis; e *iv*) substituição parcial de polissacarídeos com ação gelificante por quitosano. Nos três primeiros mecanismos apresentados, observa-se a adição de reagentes químicos que podem não ser condizentes com a produção de alimentos, por motivos de segurança e/ou por rejeição por parte dos consumidores.

De fato, a combinação entre polissacarídeos parece ser uma alternativa viável para a produção de géis alimentícios. Contudo, a produção de géis usando a associação de polissacarídeos com ação gelificante (ou não) envolve mecanismos específicos, que podem influenciar a formação, as propriedades reológicas e, consequentemente, as técnico-funcionalidades dos géis. Tomando-se como exemplo: Thompson, Paunov, Horozov e Stoyanov (2017) [66] propuseram melhorar a resistência térmica de géis pela mistura de polissacarídeos ágar e metil-celulose. Assim, géis de ágar (1,0% ou 2,0% m/v) e metil-celulose (1,0% ou 2,0% m/v) ou misturas agar:metilcelulose (1.0% m/v:1.0% m/v) foram analisados. O módulo de armazenamento (*G'*) do gel de ágar-metilcelulose apresentou comportamento constante ($7{,}0 \cdot 10^3$ Pa) entre 25 ^{o}C e 85 ^{o}C, enquanto os valores de *G'* aumentaram nos géis de metilcelulose ($7{,}0 \cdot 10^0$ Pa até $6{,}5 \cdot 10^3$ Pa em 1,0% m/v; $10{,}0^0$ Pa até $10{,}0 \cdot 10^3$ Pa em 2,0% m/v) e diminuíram em gel de ágar ($6{,}0 \cdot 10^3$ Pa até $10{,}0 \cdot 10^0$ Pa em 1,0% m/V; $13{,}0 \cdot 10^3$ Pa até $12{,}0 \cdot 10^0$ Pa em 2,0% m/v), nessa mesma faixa de temperatura. Dessa forma, concluiu-se que o hidrogel de agar-metilcelulose apresentou melhor resistência térmica (componente elástico permaneceu estável entre 25 ^{o}C e 85 ^{o}C), em relação aos géis dos seus polissacarídeos precursores. De acordo com o exemplo, a combinação de polissacarídeos promoveu a melhoria das propriedades reológicas (aumento da elasticidade) e da técnico-funcionalidade (estabilidade térmica) dos géis.

Pode-se, assim, hipotetizar que géis obtidos pela combinação do quitosano com polissacarídeos comumente utilizados como agentes gelificantes podem, também, originar produtos diferenciados, em termos de propriedades viscoelásticas, sensoriais (visuais e textura, principalmente) e/ou técnico-funcionais. Pela busca realizada na literatura, poucos trabalhos propuseram estudar géis de polissacarídeos, obtidos pela adição ou substituição parcial do agente gelificante por quitosano. Além disso, em nenhum dos relatos analisados houve a avaliação de alguma técnico-funcionalidade dos materiais gélicos. Assim, a produção de hidrogéis combinando diferentes polissacarídeos com ação gelificante é um assunto ainda passível de exploração científica, a fim de avaliar se o quitosano é capaz de modular as propriedades reológicas e/ou técnico-funcionais dos produtos.

5. Conclusão e perspectivas

A partir dessa breve análise da literatura, conclui-se que a utilização do quitosano como aditivo na indústria de alimentos deve ser vista como uma possibilidade promissora. Nesse sentido, a substituição de outros polissacarídeos convencionalmente utilizados pelo quitosano em formulações alimentícias seria justificada por suas propriedades técnico-funcionais e biofuncionais. Simultaneamente, essas duas funcionalidades representam uma alternativa inovadora para o desenvolvimento de produtos alimentícios. Pelo menos três problemas tecnológicos precisam ser solucionados para que o uso do quitosano seja possível em escala industrial: *i)* uma definição sobre as características intrínsecas e pureza do quitosano deve ser apresentada e implementada; *ii*) uma padronização dos processos de obtenção do quitosano deve ser atingida; e *iii*) informações sobre sistemas-modelo (dispersões, emulsões, e hidrogéis, por exemplo) contendo quitosano disperso em diferentes ácidos devem estar disponíveis. Assim, os artigos experimentais que serão apresentados a seguir objetivam contribuir com informações novas e relevantes sobre a problemática apresentada.

Capítulo II

Insights on physicochemical aspects of chitosan dispersion in aqueous solutions of acetic, glycolic, propionic or lactic acid

L.S. Soares, R.B. Perim, E.S. Alvarenga, L.M. Guimarães, A.V.N.C. Teixeira, J.S.R. Coimbra, E.B. Oliveira. Insights on physicochemical aspects of chitosan dispersion in aqueous solutions of acetic, glycolic, propionic or lactic acid, International Journal of Biological Macromolecules. 128 (2019) 140–148. doi:10.1016/j.ijbiomac.2019.01.106.

International Journal of Biological Macromolecules 128 (2019) 140–148

Contents lists available at ScienceDirect

International Journal of Biological Macromolecules

journal homepage: http://www.elsevier.com/locate/ijbiomac

Insights on physicochemical aspects of chitosan dispersion in aqueous solutions of acetic, glycolic, propionic or lactic acid

Lucas de Souza Soares [a,*], Rayza Badiani Perim [a], Elson Santiago de Alvarenga [b], Luciano de Moura Guimarães [c], Alvaro Vianna Novaes de Carvalho Teixeira [c], Jane Sélia dos Reis Coimbra [a], Eduardo Basílio de Oliveira [a,*]

[a] Departamento de Tecnologia de Alimentos (DTA), Universidade Federal de Viçosa (UFV), Campus Universitário, 36570-900 Viçosa, MG, Brazil
[b] Departamento de Química (DEQ), Universidade Federal de Viçosa (UFV), Campus Universitário, 36570-900 Viçosa, MG, Brazil
[c] Departamento de Física (DPF), Universidade Federal de Viçosa (UFV), Campus Universitário, 36570-900 Viçosa, MG, Brazil

ARTICLE INFO

Article history:
Received 18 July 2018
Received in revised form 12 January 2019
Accepted 22 January 2019
Available online 23 January 2019

Keywords:
Chitosan
Organic acids
Colloidal dispersions

ABSTRACT

Chitosan is a polysaccharide well-known for its applicability as a biocompatible, biodegradable, and non-toxic material to produce drugs excipients and food coatings. Acidic media are required to disperse chitosan, and aqueous solutions of acetic acid have been typically used for this purpose. However, this acid has several sensory drawbacks. In this study, chitosan was dispersed [0.1 g·(100 mL)$^{-1}$] in aqueous media containing acetic (AA), glycolic (GA), propionic (PA), or lactic (LA) acid, at 10, 20, 30, 40, or 50 mmol·L^{-1}. The increase of acid concentration reduced pH and viscosity of the dispersions, and |ζ potential| of dispersed particles. Conversely, it increased electrical conductivity and density of the dispersions, and hydrodynamic diameter of dispersed particles. At a given concentration, these effects were slightly more pronounced for dispersions formed with GA or LA, compared to AA or PA. FT-IR data suggested more intense attractive interactions of chitosan chains with glycolate and lactate anions, than with acetate and propionate. Chitosan chains interacted more strongly with hydroxylated acids counter-anions than with their non-hydroxylated counterparts, leading to slight quantitative changes of physicochemical properties of these systems. Then, in physicochemical terms, GA, LA or PA are suitable to replace AA when preparing aqueous chitosan dispersions for technological applications.

© 2019 Elsevier B.V. All rights reserved.

1. Introduction

Chitosan is an *N*-deacetylate derivative from chitin [poly-β-(1 → 4)-*N*-acetyl-D-glucosamine], which is a polysaccharide industrially obtained from crustacean shells processed by food industries [1]. Among polysaccharides derived from natural sources, chitosan is the unique carrying amino (–NH_2) groups, conferring to it differentiated physicochemical properties, and enabling several biotechnological applications [2]. The applicability of chitosan in cosmetic or dermatological lotions, wound management as scaffold in skin, cartilage and bone healing, excipient for drug delivery, component in bio-based films, and as hypolipidemic agent has been investigated throughout the last two decades, and confirmed by numerous recent reports [3–6]. This wide range of applications is possible because chitosan is a biocompatible, biodegradable, and non-toxic material [2,6–12].

The exploration of chitosan techno-functionalities needs its previous dispersion in aqueous media, as it occurs with the majority of proteins and polysaccharides [7]. Chitosan requires acidic aqueous media to form dispersions, and aqueous solutions of acetic and/or acetates have been typically used for this purpose [1,8,9]. However, the strong and somewhat nasty flavor of this acid is often a drawback when chitosan dispersions are destined to food or cosmetic formulations. Therefore, a

Abbreviations: A, first constant of Mark-Houwink-Sakurada relationship (dimensionless); A_2, second virial coefficient (cm^3·mol)·g^{-2}; *c*, concentration (g·mL^{-1}); *D*, constant diffusivity (m^2·s^{-1}); DA, acetylation degree (%); DD, deacetylation degree (%); d_h, average hydrodynamic diameter particle (nm); $g^{(2)}(t)$, normalized temporal intensity correlation functions; *k*, optical constant; k_B, Boltzmann constant (1.3806488 · 10^{-23} (m^2·kg)·(s^2·K)$^{-1}$); K_{MHS}, second constant of Mark-Houwink-Sakurada relationship (dL·g^{-1}); $\overline{M}_V$, viscometric-average molar mass (kDa); $\overline{M}_W$, weight-average molar mass (kDa); *n*, Number of predicted/experimental score pairs applying the adjusted model; *q*, scattering vector modulus; PDI, polydispersity index of droplet distribution (dimensionless); pH, hydrogenionic potential (dimensionless); R_G, gyration radius (nm); R^2, coefficient of determination; R_Θ, Rayleigh ratio; SD, standard deviation in hydrodynamic average diameter determination (nm); *T*, temperature (K); Y_i, the i^{th} experimental score applying the adjusted model; $\hat{Y}_i$, the i^{th} score predicted applying the adjusted model; Γ, decay rate in DLS analyses (s^{-1}); β, constant that depends on the number of coherence areas in DLS analyses; ε_o, permittivity of free space (C^2·N^{-1}·m^{-2}); ε_r, dieletric constant of the medium (dimensionless); ζ, zeta potential (m*V*); Θ, scattering angle (°); μ, viscosity (Pa·s); μ_e, electrophoretic mobility (m^2·(V·s)$^{-1}$); ν, speed of particles (m·s^{-1}); τ, shear stress (Pa); $\dot{\gamma}$, shear rate (s^{-1}); $\vec{E}$, electric field (N·C^{-1}); $[\eta]_H$, Huggins intrinsic viscosity (dL·g^{-1}); $[\eta]_K$, Kraemer intrinsic viscosity (dL·g^{-1}); $[\overline{\eta}]$, average intrinsic viscosity (dL·g^{-1}).

* Corresponding authors.
E-mail addresses: lucas.s.soares@ufv.br (L.S. Soares), eduardo.basilio@ufv.br (E.B. de Oliveira).

https://doi.org/10.1016/j.ijbiomac.2019.01.106
0141-8130/© 2019 Elsevier B.V. All rights reserved.

proper physicochemical characterization of aqueous dispersions of chitosan obtained with organic acids other than acetic is a relevant research field. For instance, Amorim et al. [13] studied the dispersibility of chitosan in aqueous solutions containing citric acid or lactic acid, both at different concentrations (25, 50, or 100 mmol·L^{-1}). Protonation enthalpies, ζ potential, pH, and electrical conductivity measurements were analysed together, showing that the concentration and the type of acid influenced both the kinetics of dispersion and the maximal dispersibility of chitosan. Such differences were attributed to the different intermolecular interaction patterns between chitosan and lactate, or chitosan and citrate anions. Even if this study contributed greatly to show that different counter-anions might play different roles in the chitosan dispersion process, the two acids chosen (citric and lactic) have considerably different molecular structures, hampering a more specific understanding of how the structure of the counter-anions impacted, at a molecular level, the biopolymer dispersibility and the resulting dispersions' properties. To the best of our knowledge, the literature lacks further studies about the effects of the type of organic acid (with systematic differences in their molecular structures) on interactions between acid counter-anions and chitosan in aqueous dispersions.

Many organic acids are naturally present in foods (citric fruits, berries, fermented milks, to cite only some emblematic examples), or can be added to food and cosmetic formulations, where they act as antioxidants, preservatives, acid taste enhancers, etc. [10]. Glycolic, propionic (INS 280), and lactic (INS 270) acids are some examples of the many organic acids commonly used with such purposes in commercial products. In particular, these acids may be seen as systematic structural variants of acetic acid (glycolic = acetic + –OH at C2; propionic = acetic + –CH_3 at C2; lactic = acetic + both –OH and –CH_3 at C2). Therefore, the characterization of chitosan dispersions in aqueous solutions of these four acids is not only relevant to assess techno-functional properties of this biopolymer, but also can provide a rational understanding of how intermolecular interactions between chitosan and the acid counter-anions affect such dispersions' properties. Hence, this study was focused on: *i)* studying physical and rheological properties of aqueous dispersions of chitosan in the presence of acetic, glycolic, propionic, or lactic acids, at variable concentrations, and *ii)* relating such properties to intermolecular interactions established between chitosan and the counter-anion released by these acids.

2. Materials and methods

2.1. Materials

Chitosan (Medium Molecular Weight, Sigma-Aldrich Corporation, USA; Product ID = 448877; Batch number = #LBG4282V) from fresh shrimp sells *Pandalus borealis* was used in all the experiments, after additional purification (Section 2.2.1). Organic acids used were: glacial acetic acid (Vetec, Brazil; purity = 99.7%), glycolic acid (Vetec, Brazil; purity ≥98.0%), lactic acid (Impex Quimica, Spain; purity = 85%), and propionic acid (Sigma-Aldrich Corporation, USA; purity ≥99.5%). In all cases, deionized water (QUV3, Millipore, Italy; electrical resistivity ~18 MΩ·cm^{-1} at 25 °C) was used. All the acids were used without further purification.

2.2. Chitosan characterization

2.2.1. Removal of chitosan impurities

In order to eliminate salts residues and water-soluble chitooligosaccharides, firstly chitosan was sequentially washed three times with deionized water, as follows: 1.0 g chitosan was added to 100 mL of water, this mixture was kept under magnetic stirring at room temperature (25.0 ± 1.0 °C) for 60 min, and during this time its electrical conductivity was periodically measured (Termo, Orion 145A+, USA). Next, chitosan was vacuum-filtered using qualitative paper (Cat No 1004 125, Whatman), and the insoluble fraction (washed chitosan) was recovered. After that, the washed chitosan was frozen at −40.0 ± 1.0 °C (Terroni, VERTICAL-40, Brazil), lyophilized (Terroni, LS 3000, Brazil), packed in glass jar, and finally stored at 7 ± 2 °C (Consul, PRATICE 410, Brazil), prior to further use.

2.2.2. Deacetylation degree (DD)

DD was estimated by applying a Fourier-transform infrared (FT-IR) spectroscopy approach [11]. FT-IR analyses were carried out directly on the chitosan powder, using a spectrophotometer (600-IR, Varian, USA) equipped with an attenuated reflectance accessory (GladiATR, PIKE Technologies, USA) over the region of 450–3750 cm^{-1}. The spectrum was normalized relatively to the highest corrected absorbance, and two regions (450–1850 cm^{-1} and 1850–3750 cm^{-1}) were created by splitting the spectrum. Absorbances of peaks present in these two regions were calculated through deconvolution in Lorentzian components by PeakFit (v. 4.12, SeaSolve Software Inc., 1999–2003). Then, acetylation degree (DA) of the chitosan was estimated using Eq. (1) [11,12]:

$$\mathrm{DA}(\%) = \frac{\left(\frac{A_{1320}}{A_{1420}} - 0.3822\right)}{0.03133} \quad (1)$$

In Eq. (1), A_{1320} and A_{1420} are the normalized absorbances of the peaks at wavenumbers 1320 and 1420 cm^{-1}, respectively. Then, DD was obtained by simple difference [DD(%) = 100% − DA(%)].

2.2.3. Viscometric average molar mass ($\overline{M}_V$)

Chitosan [1.0, 2.0, 3.0, 4.0, and 5.0 mg mL^{-1}] was dispersed in a lactic acid solution (50 mmol·L^{-1}), and flow times from each concentration were measured in a Cannon-Fenske viscometer (model 513 20, Schott, Germany). Lactic acid (50 mmol·L^{-1}) was chosen to ensure the dispersion of all chitosan present in aqueous media [13]. Then, the average intrinsic viscosity ($\overline{[\eta]}$) was calculated as described in details elsewhere [13–15]. From these experimental data, the viscometric-average molar mass (M_V) was estimated by the Mark-Houwink-Sakurada (MHS) relationship (Eq. (2)):

$$\overline{[\eta]} = K_{MHS} M_V^a \quad (2)$$

In Eq. (2), a and K MHS are the constants of Mark-Houwink-Sakurada (MHS) relationship.

2.2.4. Weight-average molar mass ($\overline{M}_W$), gyration radius (R_G), and second virial coefficient (A_2)

Chitosan (0.476, 0.909, 1.667, 2.307, 3.333, 4.118, and 5.000 mg·mL^{-1}) was dispersed in a lactic acid solution (50 mmol·L^{-1}). Multiangle Static Light Scattering (MSLS) measurements of chitosan dispersions were performed with a photodiode detector (BI-APD, Brookhaven, USA) and a correlator (TURBOCORR, Brookhaven, USA) equipped with a laser HeNe (75 mW; λ = 632.2 nm; CVI, Melles Griot, USA), coupled with a thermostatic bath (25.0 ± 0.5 °C; Q214M, Quimis, Brazil). Then, dispersions were placed in scattering glass cells, and scattered light intensities were measured at seven angles (40°, 50°, 60°, 70°, 80°, 90°, and 100°). Light intensity measurements were derived according to the classical Rayleigh-Debye relationship (Eq. (3)) [16]:

$$\frac{k \cdot c}{\Delta R_\theta} = \frac{1}{\overline{M}_W}\left(1 + \frac{q^2\left\langle R_G{}^2\right\rangle}{3}\right) + 2A_2 \cdot c \quad (3)$$

In Eq. (3), k is an optical constant, c is the concentration (w/V), ΔR_Θ is the Rayleigh ratio in excess, $\overline{M}_W$ is the weight-average molar mass, q is the scattering vector modulus, $\langle R_G^2 \rangle$ is the root-mean square average radius of gyration, and A_2 is the 2nd virial coefficient.

2.3. Preparation of acidic aqueous dispersions of chitosan

Firstly, a 50 mmol·L^{-1} solution was prepared for each acid (acetic, glycolic, propionic or lactic), which were diluted to obtain 40, 30, 20 and 10 mmol·L^{-1} solutions (thus totaling 20 solutions). Then, chitosan was added to each of these solutions in appropriate amounts to obtain the final concentration of 0.1 g·(100 mL)$^{-1}$ of the biopolymer in each system. The resulting systems were kept under magnetic stirring at 25.0 ± 0.1 °C in a thermostatic bath (TE-184, Tecnal, Brazil), during 12 h, to ensure the chain hydration and dispersion. After that, dispersions were filtered using 0.8 mm cellulose acetate membranes (Millipore, USA), in order to remove any non-dispersed material. The filtrates were transferred to glass tubes recovered with aluminum foil in order to protect against light, then carefully closed in order to avoid contact with external air and, finally, stored at 7.0 ± 1.0 °C in a B.O.D. incubator (SP500, SPlabor, Brazil).

2.4. Evaluation of physicochemical properties

2.4.1. Electrical conductivity, pH, density, and refractive index

Solutions containing acetic (AA), glycolic (GA), propionic (PA), or lactic (LA) acid (10, 20, 30, 40, and 50 mmol·L^{-1}) had their electrical conductivity (Termo, Orion 145A+, USA) and pH (digital potentiometer Hanna, H2221, USA) measured, soon after their preparation. Electrical conductivity and pH of the chitosan dispersions [0.1 g·(100 mL)$^{-1}$] were similarly measured. All of these measurements were carried out at 25.0 ± 1.0 °C. Density (oscillatory densimeter Schmidt Haensch, EDM, Germany; 25.00 ± 0.05 °C) and refractive index (digital Abbe refractometer 972A, Kiltler, Brazil; 25.0 ± 0.5 °C) of the chitosan dispersions were also measured.

2.4.2. Hydrodynamic average diameter (d_h) and ζ potential

Hydrodynamic average diameter (d_h) and ζ potential of dispersed chitosan particles [0.1 g·(100 mL)$^{-1}$] were evaluated by dynamic light scattering (DLS) (Zetasizer Nano-ZS, Malvern Instruments, United Kingdom). Chitosan dispersions were diluted (1:6) with a single channel micropipette (K1-1000B, Kasvi, Brazil), using as diluent the same acid solution employed to prepare each dispersion. Then, the diluted dispersions were placed in a cuvette for analyses, which were all carried out at 25.0 ± 0.1 °C.

Hydrodynamic diameter distributions were obtained by means of the amplitude of the decay rate A(Γ), which is estimated by fitting the normalized temporal intensity correlation functions, $g^{(2)}(t)$, through a NNLS (Non-Negative Least Square) algorithm, according to Eq. (4) [17]. Thus, Γ distribution is turned to d_h by Eqs. (5) and (6):

$$g^{(2)}(t) = 1 + \beta\left[\int_0^\infty A(\Gamma)e^{-\Gamma t}d\Gamma\right]^2 \quad (4)$$

$$\Gamma = q^2 \cdot D \quad (5)$$

$$d_h = \frac{k_B T}{3\pi\mu D} \quad (6)$$

In Eqs. (4)–(6), β is a constant that depends on the number of coherence areas in the detector and Γ is the decay rate, q is the scattering vector modulus, D is the constant diffusivity, k_B is the Boltzmann constant, T is the temperature, μ is the viscosity of the diluent, and d_h is the particle hydrodynamic average diameter for each population. Refractive index and viscosity of each dispersion were used to correct the d_h values. Polydispersity index (PDI) was calculated for each d_h estimated according to Eq. (7) [14]:

$$\mathrm{PDI} = \left(\frac{SD}{d_h}\right)^2 \quad (7)$$

In Eq. (7), SD is the standard deviation corresponding to each d_h value.

ζ potential was estimated from the electrophoretic mobility of dispersed chitosan chains due to a controlled electric field, applied to the systems. Then, the speed and the direction of the particle movement due to this electric field allowed calculating the electrophoretic mobility (Eq. (8)). Finally, the Smoluchowski model for the double electrical layer was considered to calculate the ζ potential values (Eq. (9)):

$$\mu_e = \frac{v}{\left|\vec{E}\right|} \quad (8)$$

$$\mu_e = \frac{\varepsilon_r \varepsilon_o \zeta}{\mu} \quad (9)$$

In Eqs. (8) and (9), μ_e is the electrophoretic mobility, v is the speed of particles, $\vec{E}$ is the electric field, ε_r is the dielectric constant of the medium, ε_o is the permittivity of free space, ζ is the zeta potential, and μ is the viscosity.

2.4.3. Rheological properties

Rheological measurements of acidic chitosan dispersions [0.1 g·(100 mL)$^{-1}$] were performed using a rotational rheometer (Haake Mars II, Thermo Scientific Corporation, Germany), equipped with a stainless steel cone-plate geometry sensor (cone angle = 1°; diameter = 60 mm; gap = 0.052 mm). During the analyses, samples were kept at 25.0 ± 0.1 °C by using an ultrathermostatic bath (Phoenix 2C30P, Thermo Scientific Corporation, Germany). Flow curves were determined by progressively varying the shear rate from 0.1 to 300 s^{-1} in three cycles (1st up cycle, down cycle, and 2nd up cycle; 180 s each cycle) and measuring the corresponding shear stresses.

2.5. Evaluation of intermolecular interactions between chitosan and the organic acids

Intermolecular interactions between chitosan and the acids used to form the dispersions were studied through FT-IR. First, suitable amounts of chitosan were added to 100 mmol·L^{-1} acid solutions (AA, GA, PA, or LA), in order to obtain aqueous biopolymer dispersions with 0.5, 1.0, and 1.5 g·(100 mL)$^{-1}$. Similarly, dispersions containing 1.0 g·(100 mL)$^{-1}$ chitosan in 50, 75, or 100 mmol·L^{-1} acid solutions (AA, GA, PA, or LA) were prepared. All systems were stirred for 24 h, at room temperature, frozen at −40.0 ± 1.0 °C, and then lyophilized. FT-IR analyses were carried out on the lyophilized materials, over the wavenumber interval 450–3750 cm^{-1}. Then, absorbances from FT-IR spectra were calculated through deconvolution in Lorentzian components by PeakFit (v. 4.12, SeaSolve Software Inc., 1999–2003). A control system consisting of washed and lyophilized chitosan only (without acid) was also analysed.

2.6. Data analyses

All measurements were carried out in three repetitions. SAS software (version 9.3, SAS Institute Incorporation, USA; licensed by the Universidade Federal de Viçosa) was used to analyse the experimental data. Newtonian model was fitted to experimental data for $\tau = f(\dot{\gamma})$, from rheological measurements. Coefficient of determination (R^2) and mean absolute percentage error (MAPE) (Eq. (10)) were used to evaluate the adequacy of fitting in all cases.

$$MAPE = \frac{1}{n}\sum_{i=1}^{n}\left|\frac{\left(Y_i - \hat{Y}_i\right)}{Y_i}\right| \cdot 100\% \quad (10)$$

In Eq. (10), Y_i is the i^{th} experimental score, $\hat{Y}_i$ is the i^{th} score predicted applying the adjusted model and n is the number of predicted/experimental score pairs. To be considered adequately fitted to experimental data, models had to present R^2 values ≥0.9 and *MAPE* values ≤10%.

3. Results and discussion

3.1. Chitosan characterization

By using the relationship involving the integral intensities of the FT-IR bands at wavenumbers 1320 cm^{-1} and 1420 cm^{-1} (Eq. (1)) [11,12], DD value of the chitosan used in the present study was estimated as 74.4% (for details, see Supplementary material). This value is somehow inferior to that informed by the manufacturer (81.0%). Indeed, during the chitosan production process, chitin is submitted to high temperatures (~150 °C) and strongly alkaline reaction media; therefore, chitooligosaccharides (chitosans with degrees of polymerization ≤20 and with DD usually ≥95.0%) are produced together, due to hydrolysis of the amide group [18]. As these chitooligosaccharides have been eliminated during the chitosan washing, a small reduction of the average DD value of the remaining chitosan was in fact expected.

The dissimilarity between the DD values provided by the manufacture and the one obtained experimentally emphasizes the importance of checking experimentally the DD of commercial chitosan prior to use. DD's experimental determination become even more significant in the present study because chitosan underwent a preliminary purification. As commented previously, DD value greatly influences biological activities and physicochemical properties of chitosan, including its dispersibility in acidic aqueous media. DD values ≥70.0% have been correlated to high dispersion rates [2,9]. Also noteworthy, other authors have proposed alternative relationships to calculate deacetylation degree (or acetylation degree) of chitosans using spectroscopic analyses [11,12]. One difficulty inherent to such approaches is the fact that the moisture content of chitosan can increase the intensity of bands (above 1750 cm^{-1}), leading to illogical, even negative, values of DD [19]. Then, an exhaustive dehydration of the sample to be analysed, as well as choosing the appropriate set of bands to be taken for DD estimation, is critical for the reliability of the obtained value.

Intrinsic viscosity of chitosan dispersed in lactic acid solution (50 $mmol \cdot L^{-1}$) was estimated as $[\overline{\eta}] = 25.8\ dL \cdot g^{-1}$, from the simple average between $[\eta]_H = 34.3\ dL \cdot g^{-1}$ and $[\eta]_K = 17.3\ dL \cdot g^{-1}$ (for details, see Supplementary material). After DD value calculation, the constants $a = 0.88$ and $K_{MHS} = 8.50 \cdot 10^{-5}\ dL \cdot g^{-1}$ of MHS relationship (Eq. (6)) were easily obtained [20]. Then, the viscometric-average molar mass ($\overline{M}_V$) of chitosan was estimated as 1700 ± 300 kDa. The weight-average molar mass ($\overline{M}_W$) was estimated through multiple-angle light scattering (MSLS) measurements, which gave the value of 1200 ± 500 kDa. The corresponding Zimm plot built by double extrapolation to 0° and 0.0 $mg \cdot mL^{-1}$ from other angles and concentrations of chitosan (for details, see Supplementary material). Differences between $\overline{M}_V$ and $\overline{M}_W$ are frequent, and are associated to different fractions of polymer chains considered in the calculations to average value [21]. $\overline{M}_V$ and $\overline{M}_W$ values also indicate that the previous washing process may have removed chitooligosaccharides from the commercial chitosan.

MSLS measurements also allowed estimating $R_G = 260 \pm 60$ nm and $A_2 = -(5.6 \pm 4.0) \cdot 10^{-5}\ (cm^3 \cdot mol) \cdot g^{-2}$. Both R_G and A_2 values give information about polymer chain compaction in the aqueous media. Gyration radius (R_G) is the average distance between the center of mass of a dispersed polymer chain and arbitrary points on its surface, at a given conformation [22]. R_G value is representing a good decompression and hydration in aqueous medium of the chitosan chains. Negative values of second virial coefficient (A_2), as observed in our results, indicate the effective attractive interaction between the polyelectrolyte chains, despite the positive charge of the chains [23]. This observation suggests that in addition to electrostatic repulsion between chitosan chains dispersed, counter-anions are also interacting with the colloidal network, and can influence A_2 value.

3.2. Physicochemical properties

Chitosan [0.1 $g \cdot (100\ mL)^{-1}$] added to acidic aqueous solution showed fully dispersed when macroscopically/visually assessed. Different physicochemical properties were observed according to the concentration and type of acid present in the different properties analysed. Results for pH and electrical conductivity measurements of the aqueous media without or with chitosan are compiled in Fig. 1. Both increased with the increase of acid concentration from 10 to 50 $mmol \cdot L^{-1}$, regardless of the acid used to form the dispersions. pH values are used to represent H^+ concentration in aqueous media, while electrical conductivity measurements take into account the counter-ion and the protons from organic acid [22]. Modifications in both electrical conductivity and pH values are demonstrating changes in the equilibrium of the dissociation of the acid molecules. According to Fig. 1 – A, which addresses pH results, in the aqueous media without chitosan the increase in acid concentration from 10 to 50 $mmol \cdot L^{-1}$ led to a reduction in pH (3.5 to 3.1 in systems containing AA; 3.0 to 2.5 for GA; 3.6 to 3.1 for PA; and 3.0 to 2.3 for LA). In these cases, systems containing GA and LA presented pH values clearly inferior to the counterparts containing AA and PA, at a given concentration. This observation can be explained by an inductive effect: the carbon atom of the carboxyl group present in GA and LA supports a higher positive charge (when compared to AA and PA), due to the hydroxyl group attached to their C2 carbon, which exerts an attraction on electronic clouds of the molecule towards the oxygen atom of this hydroxyl group. Consequently, protons of GA and LA are more easily released from the –COOH group [24,25]. This is further supported by the pK_a values of these organic acids (AA = 4.75; GA = 3.83; PA = 4.87; and LA = 3.85). Indeed, it is well-known that, the lower the pK_a, the more easily the H^+ is released by organic acids [26]. In Fig. 1 – B, results for electrical conductivity of the systems without chitosan are represented: the increase in acid concentration from 10 to 50 $mmol \cdot L^{-1}$ promoted a raise in electrical conductivity of aqueous media without chitosan (163 to 402 $\mu S \cdot cm^{-1}$ in systems containing AA; 477 to 1124 $\mu S \cdot cm^{-1}$ for GA; 156 to 345 $\mu S \cdot cm^{-1}$ for PA; and 467 to 1118 $\mu S \cdot cm^{-1}$ for LA). Both H^+ cations and the counter-anions released by the organic acids in aqueous media are excellent electrical conductors (small and electrically charged chemical entities). So, in accordance, as the acid concentration increased, the electrical conductivity of the systems also increased. Not surprisingly, values of electrical conductivity were sharply higher in aqueous media containing GA and LA than in the counterparts with AA and PA, at the same concentration. In fact, due to their molecular nature (hydroxyl group at C2) and the consequent lower pK_a values, explained above, GA and LA release their proton more easily than the two other acids (at the same concentration), generating more conductor entities within the medium.

Also in Fig. 1 – A, one can see that pH values of aqueous dispersions of chitosan were slightly higher, compared to the counterpart systems without chitosan, at the same concentration of acid. Dispersions of chitosan containing AA and PA showed higher pH values (Fig. 1 – A) than those seen in GA and LA from 10 to 50 $mmol \cdot L^{-1}$ (4.4 to 3.5 in systems containing AA; 3.5 to 2.5 for GA; 4.5 to 3.6 for PA; and 3.6 to 2.7 for LA). This result for pH was expected, since H^+ cations from aqueous media protonated amino groups present in chitosan chains whose pK_a is ~6.4 [27]. In other words, chitosan added to the acidic aqueous medium causes an equilibrium shift, resulting in the deprotonation of more acid molecules present in the medium, but the protons released are not all free; a fraction of them binds to chitosan's amino groups ($R - NH_2 + H^+ \rightleftharpoons R - NH_3^+$). In Fig. 1 – B, for systems containing chitosan, an analogous effect of the acid concentration was observed: as the acid concentration increased from 10 to 50 $mmol \cdot L^{-1}$, a raise in electrical conductivity values of aqueous media with chitosan was found (210.3 to 355.3 $\mu S \cdot cm^{-1}$ in systems containing AA; 355.3 to 1000.7 $\mu S \cdot cm^{-1}$

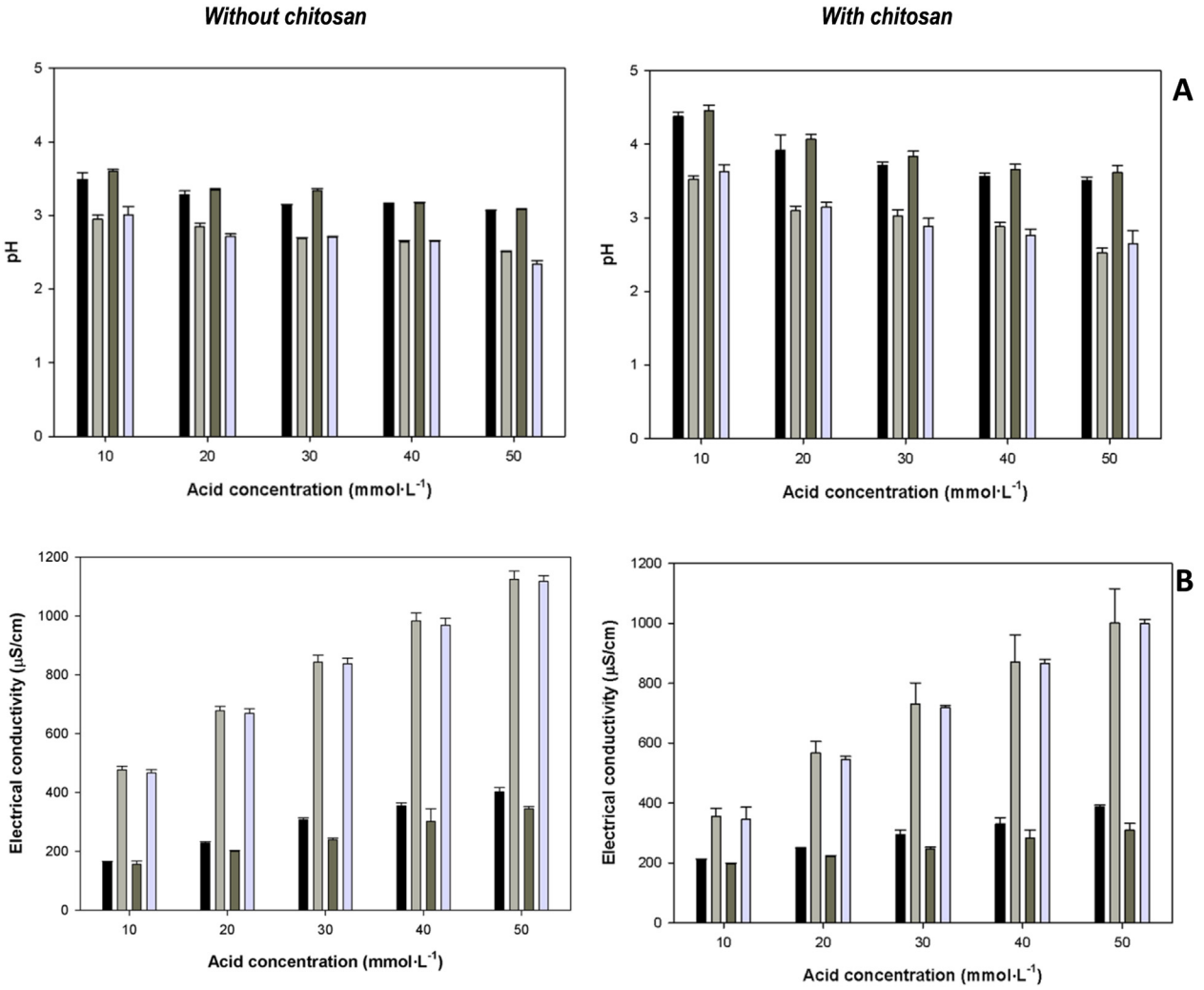

Fig. 1. pH (A) and electrical conductivity (B) of aqueous solutions containing AA (■), GA (▭), PA (▬), or LA (▭), at different concentrations, without or with chitosan [0.1 g·(100 mL)$^{-1}$].

for GA; 196.1 to 309.3 μS·cm^{-1} for PA; and 345.0 to 989.3 μS·cm^{-1} for LA), and higher values for electrical conductivity also can be seen in systems containing GA or LA. However, these values tended to be smaller than those measured for the counterpart systems without chitosan (at the same concentration of acid), which would be expected since the electrical conductivity considers all electrostatically charged chemical species present in aqueous medium. This finding reinforces the previous conclusion that the protonation of chitosan chains during their dispersion reduces the concentration of free protons in the bulk, although it also shifts the equilibrium towards the deprotonation of the acids. Chitosan added to the systems with GA or LA provided a greater deprotonation of the acids (due to the presence of the hydroxyl group in C2), which led to a more pronounced reduction of pH and increased electrical conductivity, when compared to those systems containing AA or PA.

To the best of our knowledge, the literature on the subject reports results of pH and electrical conductivity of chitosan dispersions only for media containing acetic acid [1,8,9], precluding comparisons of our results. On the other hand, the comparisons of pH and electrical conductivity of chitosan dispersions here reported – with four organic acids and five different concentrations each – bring new information about how chitosan chains behave when dispersed in acidic aqueous media, and corroborate that the nature of the acid counter-anion impacts the dispersion of this biopolymer in aqueous media [13,15].

Results for density, hydrodynamic average diameter, ζ potential, and viscosity for chitosan dispersions 0.1 g·(100 mL)$^{-1}$ in aqueous solutions of the four acids studied (from 10 to 50 mmol·L^{-1}) are given in Fig. 2. As shown, regardless the acid used to form the dispersions, ζ potential and viscosity values of the chitosan dispersions decreased, whereas density and hydrodynamic average diameter values increased, when increasing the acid concentration from 10 to 50 mmol·L^{-1}. Indeed, changes in acid concentration can influence the balance of interactions chitosan-water and chitosan-chitosan, and then induce modifications in physical and colloidal properties of this biopolymer [8]. The type of acid also markedly affected the magnitude of each of these physical properties, as described and discussed in the paragraphs thereafter.

According to Fig. 2 – A, dispersions containing 0.1 g·(100 mL)$^{-1}$ chitosan showed a raise in density values as the acid concentration increased from 10 to 50 mmol·L^{-1} (998.0 to 998.4 kg·m^{-3} in systems containing AA; 998.2 to 998.9 kg·m^{-3} for GA; 997.3 to 998.1 kg·m^{-3} for PA; and 997.7 to 998.8 kg·m^{-3} for LA). Chitosan dispersions in aqueous media containing GA or LA showed higher density values, compared to those prepared with AA or PA. This first finding suggests that intermolecular interactions occurring between chitosan and hydroxylated acid counter-anions are different from those formed between the dispersed biopolymer and non-hydroxylated counter-anions. More specifically, the higher electro-polarizability observed in the counter-anions glycollate and lactate could have promoted stronger interactions with the protonated chains of chitosan, which would justify the higher values of density measured in systems containing GA or LA.

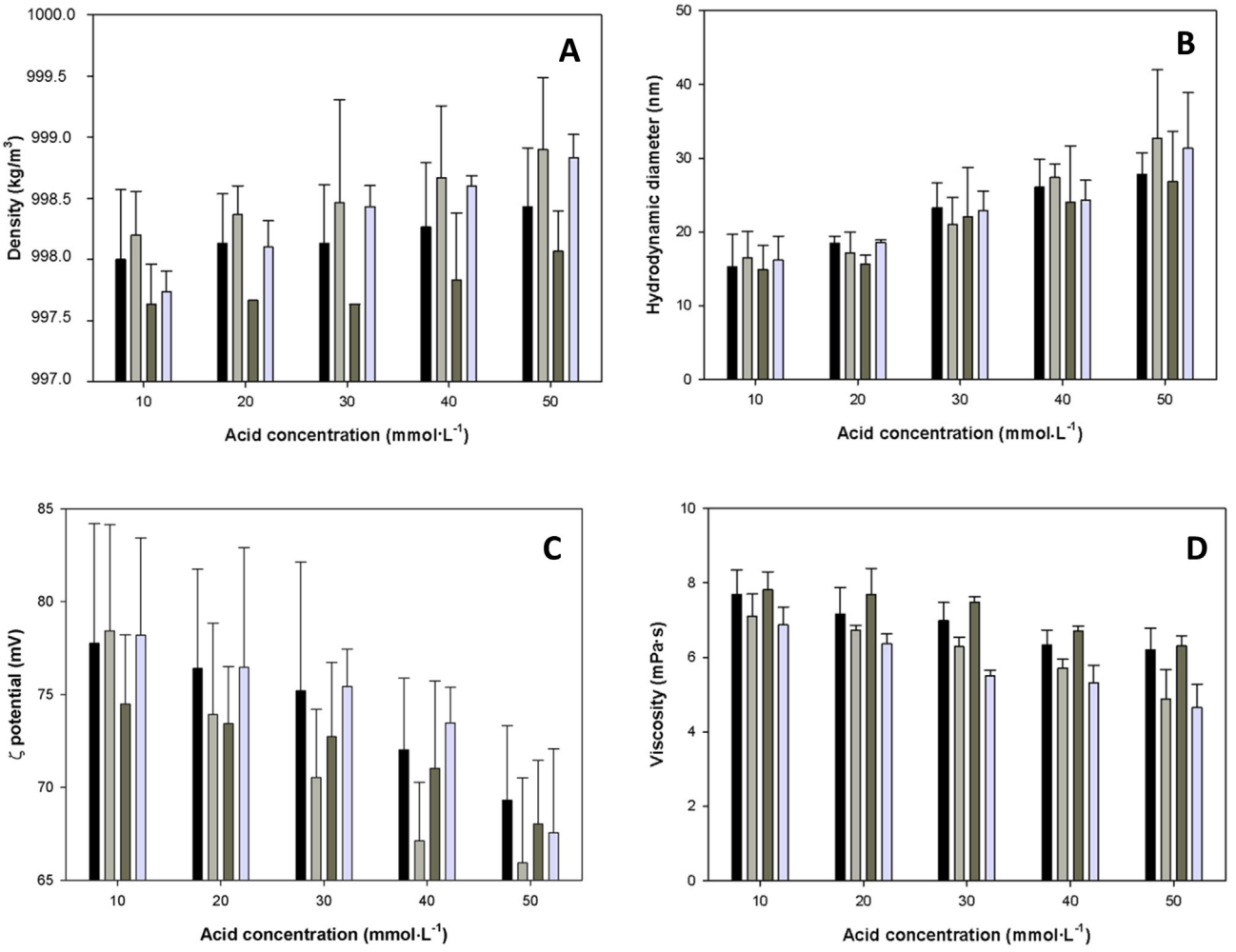

Fig. 2. Density (A), average hydrodynamic diameter of dispersed particles (B), ζ potential of dispersed particles (C), and viscosity (D) of chitosan dispersions [0.1 g·(100 mL)$^{-1}$] in solutions of AA (■), GA (▒), PA (▓), or LA (□), at different concentrations.

In Fig. 2 – B, one can see that the hydrodynamic average diameters (d_h) of dispersed chitosan chains increased as the acid concentration increased from 10 to 50 mmol·L^{-1} (15.30 to 27.76 nm in systems containing AA; 16.54 to 32.71 nm for GA; 14.91 to 26.85 nm for PA; and 16.21 to 31.35 nm for LA). PDI values from d_h were also calculated (for details, see Supplementary material). Their values, between 0.027 and 0.097, are indicative of narrow hydrodynamic average diameter distributions. PDI values ≤0.05 have been correlated to highly monodisperse standards, which are rarely seen. PDI ≤ 0.1 for a given distribution of dispersed particle sizes have been pointed out as indicative of considerable uniformity of sizes within the distribution [28]. Values of d_h were quite similar for dispersions prepared at acid concentration of 10 mmol·L^{-1}. However, in systems containing 50 mmol·L^{-1} of GA and LA, d_h values were sharply smaller compared to those prepared with AA and PA. This suggests different interactions patterns between chitosan and hydroxylated acid counter-anions, and may indicate more elongated chitosan chains, compared to systems in which AA and PA were used. It is noteworthy that this inference is corroborated by the density values above reported.

ζ potential of dispersed chitosan chains were also measured and the corresponding results are represented in Fig. 2 – C. As expected, ζ potential signs were all positive, due to the cationic nature of chitosan. ζ potential values decreased as the acid concentration increased from 10 to 50 mmol·L^{-1} (+77.8 to +69.3 mV in systems containing AA; +78.4 to +65.9 mV for GA; +74.5 to +68.0 mV for PA; and + 78.2 to +67.6 for LA). This decrease in the ζ potential values is likely to reflect changes in the intermolecular interactions between protonated chitosan chains and the counter-anions from organic acids. More specifically, the released counter-anions may form electrostatic interactions with protonated amino groups or ion-dipole interactions with the hydroxyl groups of chitosan, being both attractive interactions. The presence of these counter-anions around the chitosan chains attenuates the density of positive charges on the electrical layer around the dispersed biopolymer chains, leading to smaller ζ potential values. Moreover, lower values of ζ potential were observed in aqueous media containing 50 mmol·L^{-1} GA or LA, and these observations also pointed out to a more intense attractive interaction between chitosan chains and glycollate or lactate counter-anions. Such explanation is also supported by results of density and d_h, which showed greater values according to the increase in acid concentration.

Finally, rheological properties of the chitosan dispersions were analysed. None of them showed hysteresis during rheological analysis, i.e., the three flow curves corresponding to the 1st up-down cycle, and 2nd up cycle were superposed. Therefore, only the 2nd up curves were represented in rheograms (for details, see Supplementary material). Moreover, as these curves were linear with τ_0 approaching zero, the Newtonian model was tested and fitted well to experimental data for $\tau = f(\dot{\gamma})$. In fact, values of $R^2 \geq 0.94$ and MAPE ≤5.3%, indicated the adequacy of the adjusted models to experimental data. Hence, the viscosities of chitosan dispersions containing the different acids were calculated and represented in Fig. 2 – D. Chitosan dispersions had their viscosity diminished as the acid concentration increased from 10 to 50 mmol·L^{-1} (7.68 to

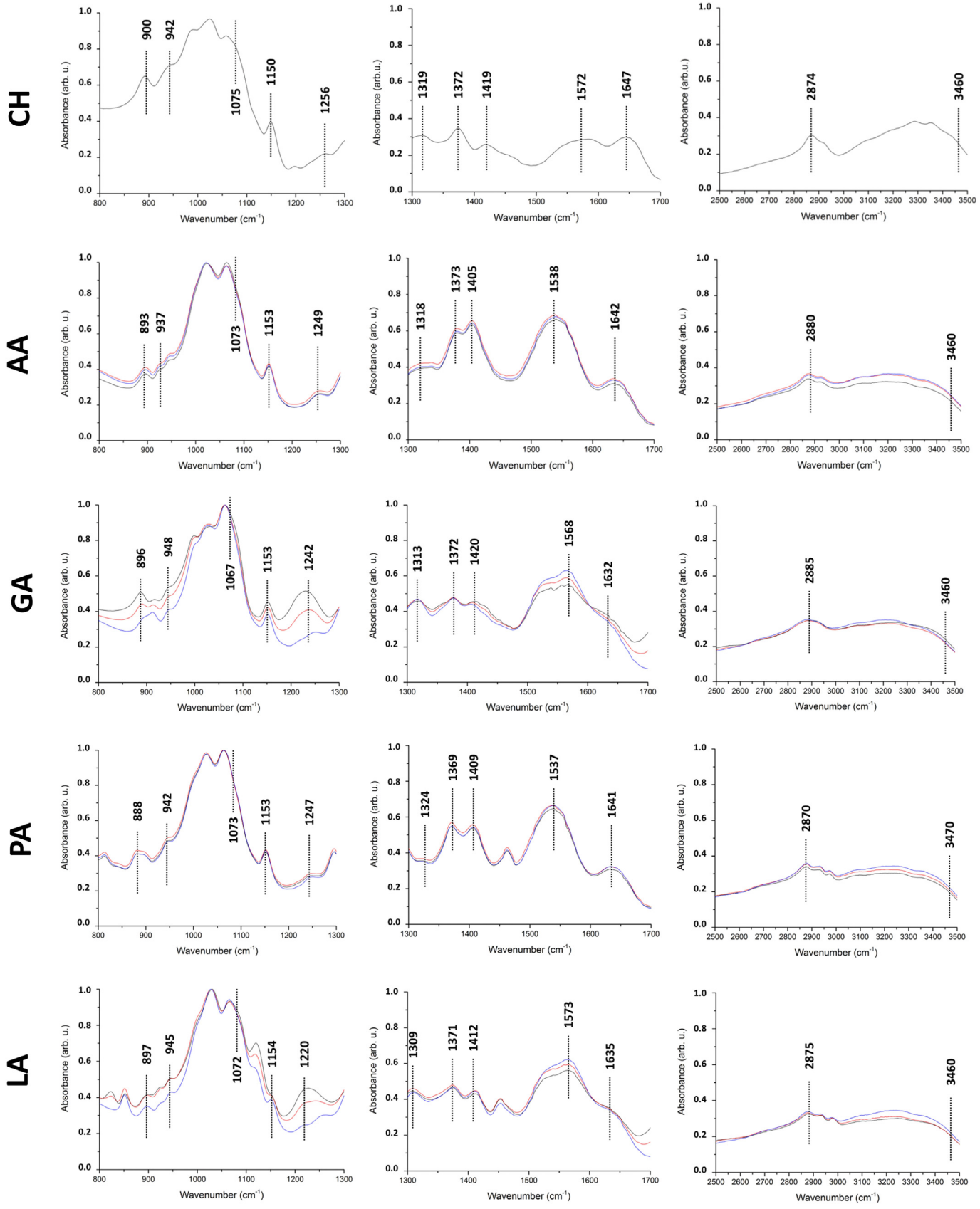

Fig. 3. Three regions (800–1300 cm^{-1}, 1300–1800 cm^{-1}, and 2500–3500 cm^{-1}) of FT-IR spectra obtained from native chitosan (CH), and lyophilized pellets containing chitosan previously dispersed in solutions of acetic (AA), glycolic (GA), propionic (PA), or lactic (LA) acid, at concentrations of 50 mmol·L^{-1} (·), 75 mmol·L^{-1} (·), or 100 mmol·L^{-1} (·).

6.19 mPa·s in systems containing AA; 7.12 to 4.88 mPa·s for GA; 7.74 to 6.30 for PA; and 7.05 to 4.66 for LA). Although noticeable for the entire concentration range, such differences were quite tenuous for chitosan dispersions containing 10 mmol·L^{-1} of acid and became more and more pronounced as the acid concentration increased up to 50 mmol·L^{-1}. This decrease in viscosities values triggered by higher acid concentrations is compatible with inferences made from densities, d_h, and ζ potentials results: as discussed, the increasing counter-ion concentration caused stronger attractive interactions of them with the protonated chitosan chains, which led to a reduction in chains compaction and attenuation of their electrical charges density. Then, these results indicated elevation of the intra-chain electrostatic repulsion, resulting in increased d_h of the dispersed chitosan chains. Conversely, higher acid concentrations seem to have hampered chitosan-water interactions in aqueous media containing all different acids, affording lower viscosity values in these systems. Once again, glycollate and lactate counter-anions had a more strong effect in relation to acetate and propionate (at the same acid concentration), since they led to systems with smaller viscosities.

Based on this ensemble of results, the effects of different organic acid counter-anions on physicochemical properties (pH, electrical conductivity, density, d_h, ζ potential, and viscosity) of aqueous chitosan dispersions was evidenced. In particular, these results demonstrated that such properties were dependent not only on the acid concentration in the aqueous media, but also on the molecular structure of the acid. Acids generating counter-anions with greater electro-polarizability (i.e., those with a hydroxyl group at C2) clearly exerted stronger effects on the variations of the above mentioned physicochemical properties, compared to their non-hydroxylated counterparts. However, the specific intermolecular interactions behind such effects could not be inferred from the results presented and discussed so far. This is why additional spectroscopic analyses were undertaken, and corresponding results are discussed in the next section.

3.3. Intermolecular interactions between chitosan and the organic acids counter-anions

Firstly, a comparison between absorbances of chitosan powder (CH) and lyophilized dispersions containing variable chitosan concentrations [0.5, 1.0, and 1.5 g·(100 mL)$^{-1}$] in 100 mmol·L^{-1} acid solutions (AA, GA, PA, or LA) was performed (see spectra in Supplementary material). Eleven characteristic peaks of chitosan were observed in the region of 450–3750 cm^{-1}: 900 cm^{-1}, 942 cm^{-1}, 1075, 1150, and 1256 cm^{-1} (C—O stretching), 1319 cm^{-1} (amide bending), 1372 cm^{-1} (C—H bending), 1419 cm^{-1} (OH and CH bending), 1572 cm^{-1} (NH_2 bending), 1647 cm^{-1} (C═O stretching vibration of amide I), 2874 cm^{-1} (CH stretching), and 3360 cm^{-1} (OH stretching), based on assignment of absorption bands in accordance with literature data [11,12,29], and also on small variations of peak absorbance among dispersions containing different concentrations of chitosan. Secondly, absorbances of CH were compared with lyophilized chitosan dispersions [1.0 g·(100 mL)$^{-1}$] at variable concentrations of AA, GA, PA, and LA (50, 75, and 100 mmol·L^{-1}). Three regions of each spectrum (800–1300 cm^{-1}, 1300–1800 cm^{-1}, and 2500–3500 cm^{-1}) that were considered strategic, due to changes in characteristic peaks, were expanded and presented in Fig. 3. Chitosan [1.0 g·(100 mL)$^{-1}$] dispersed in solutions containing 50, 75, or 100 mmol·L^{-1} of acid did not present substantial differences between their characteristic peaks absorbances (calculated through deconvolution in Lorentzian components), for the same organic acid (for details, see Supplementary material). Moreover, no substantial changes were observed in absorbances of peaks corresponding to 1075 cm^{-1}, 1150 cm^{-1}, 1256 cm^{-1}, 1319 cm^{-1}, 1372 cm^{-1}, 1647 cm^{-1}, 2874 cm^{-1}, and 3360 cm^{-1}, comparing CH and lyophilized dispersions. The absence of interactions in 1319 and 1650 cm^{-1} bands was not surprising, because it has been pointed out as unusual interactions of organic molecules with the acetamide groups [19]. Tenuous variations in the 3360 cm^{-1} peak would be expected, considering the small water content in all samples [30]. In summary, this set of peaks did not allow inferring any specific interaction between chitosan and organic acids in lyophilized dispersions.

Differences in absorbance values were observed between CH and all the other systems for peaks at 900 cm^{-1} and 942 cm^{-1}, indicating intra-chain conformational changes [23,31], which can be justified from the previous dispersion of chitosan powder and subsequent lyophilization. Absorbance values were increased in lyophilized dispersions compared to CH peaks at 1419 cm^{-1}, suggesting the existence of molecular interactions involving hydroxyl groups of chitosan (hydrogen bonds, dipole-dipole, and ion-dipole interactions, for instance). Higher absorbance values were also found in dispersions containing AA and PA for the peak at 1572 cm^{-1}, while dispersions prepared with GA and LA showed a more subtle increase for this same peak. In fact, the spectral region between 1500 and 1800 cm^{-1} is a rich data source due to amine and amide absorption bands [29], which are widely used to characterize modifications in the molecular structure of chitosan. Moreover, new peaks at 1524 cm^{-1} in GA dispersions, and at 1527 cm^{-1} in LA can be identified, which indicates a peak unfolding and its shifting to smaller wavenumbers. These differences could be explained from two aspects: *i)* vibration energy of NH_3^+/glycollate and NH_3^+/lactate are greater than NH_3^+/acetate and NH_3^+/propionate, causing a displacement of these peaks towards smaller wavenumbers, which is related to complexes formed between these two chemical species [31]; *ii)* glycollate and lactate counter-anions have a different dipole moment, as discussed in previously, compared to acetate or propionate [26]. These results led us to believe that glycollate and lactate counter-anions interact more strongly with the chitosan chains, promoting a more expressive reduction of pH, ζ potential, and viscosity of the dispersions, along with a greater increase of electrical conductivity, density, and d_h, compared to dispersions containing acetic or propionic acids.

4. Conclusions

Chitosan dispersions in aqueous solutions of AA, PA, GA, or LA showed slight differences of their physicochemical, which depended on both nature and concentration of the acid. The increase of acid concentration from 10 to 50 mmol·L^{-1} triggered the reduction of the values of pH, |ζ potential|, and viscosity, while increasing the values of electrical conductivity, density, and hydrodynamic diameter of dispersed chitosan particles. All of these changes were more pronounced for systems containing hydroxylated acids (GA ans LA), compared to those formed with non-hydroxylated acids (AA or PA), at the same concentration. Moreover, spectrophotometric analyses (FT-IR) pointed out to more intense attractive interactions of chitosan chains with glycolate and lactate anions, than with acetate and propionate. Chitosan chains seemed to interact more strongly with hydroxylated acids counter-anions (glycolate and lactate) than with their non-hydroxylated counterparts (acetate and propionate), which led to slight quantitative changes of physicochemical properties of these systems. Therefore, at least in physicochemical terms, GA, LA or PA are suitable to replace AA when preparing aqueous dispersions of chitosan for technological purposes.

Acknowledgements

The authors are thankful to: Brazilian research agencies CAPES (Code 001) and FAPEMIG, for their financial support; *D. Sc.* Eber A. A. Medeiros, Prof. Nilda de Fátima F. Soares, and Prof. Luis A. Minim (DTA-UFV), who allowed us using some facilities in the laboratories coordinated by them; Mr. Márcio Alvarenga, for his technical support in performing FT-IR analyses; Mr. Gustavo Leite Milião, for his kind help in revising the English.

Appendix A. Supplementary data

Supplementary data to this article can be found online at https://doi.org/10.1016/j.ijbiomac.2019.01.106.

References

[1] I. Hamed, F. Ozogul, J.M. Regenstein, Industrial applications of crustacean by-products (chitin, chitosan, and chitooligosaccharides): a review, Trends Food Sci. Technol. 48 (2016) 40–50.

[2] S. Islam, M.A. Bhuiyan, M.N. Islam, Chitin and chitosan: structure, properties and applications in biomedical engineering, J. Polym. Environ. 25 (2017) 854–866.

[3] I. Bano, M. Arshad, T. Yasin, M. Afzal, M. Younus, Chitosan: a potential biopolymer for wound management, Int. J. Biol. Macromol. 102 (2017) 380–383.

[4] A. Oryan, S. Sahvieh, International journal of biological macromolecules effectiveness of chitosan scaffold in skin, bone and cartilage healing, Int. J. Biol. Macromol. 104 (2017) 1003–1011.

[5] F. Garavand, M. Rouhi, S. Hadi, I. Cacciotti, Improving the integrity of natural biopolymer films used in food packaging by crosslinking approach: a review, Int. J. Biol. Macromol. 104 ((2017) 687–707.

[6] S. Dehghani, S. Vali, J.M. Regenstein, Edible films and coatings in seafood preservation: a review, Food Chem. 240 (2018) 505–513.

[7] V. Tolstoguzov, Some thermodynamic considerations in food formulation, Food Hydrocoll. 17 (2003) 1–23.

[8] M. Rinaudo, Chitin and chitosan: properties and applications, Prog. Polym. Sci. 31 (2006) 603–632.

[9] I. Younes, M. Rinaudo, Chitin and chitosan preparation from marine sources. Structure, properties and applications, Mar. Drugs 13 (2015) 1133–1174.

[10] CODEX STAN 192-1995, Codex General Standard for Food Additives, 2018 1–419, Avaible from: http://www.fao.org/gsfaonline/docs/CXS_192e.pdf, Accessed date: 29 June 2018.

[11] M.R. Kasaai, A review of several reported procedures to determine the degree of N-acetylation for chitin and chitosan using infrared spectroscopy, Carbohydr. Polym. 71 (2008) 497–508.

[12] J. Brugnerotto, J. Lizardi, F.M. Goycoolea, W. Argülles-Monal, J. Desbrières, M. Rinaudo, An infrared investigation in relation with chitin and chitosan characterization, Polym. 42 (2001) 3569–3580.

[13] M.L. Amorim, G.M.D. Ferreira, L.S. Soares, W.A.S. Soares, A.M. Ramos, J.S.R. Coimbra, L.H.M. Silva, E.B. Oliveira, Physicochemical aspects of chitosan dispersibility in acidic aqueous media: effects of the food acid counter-anion, Food Biophys. 11 (2016) 388–399.

[14] Z.R. Nieto Galván, L.S. Soares, A.E.A. Medeiros, N.F.F. Soares, A.M. Ramos, J.S.R. Coimbra, E.B. Oliveira, Rheological properties of aqueous dispersions of xanthan gum containing different chloride salts are impacted by both sizes and net electric charges of the cations, Food Biophys. 13 (2018) 186–197.

[15] L.S. Soares, J.T. Faria, M.L. Amorim, J.M. Araújo, L.A. Minim, J.S.R. Coimbra, A.V.N.C. Teixeira, E.B. Oliveira, Rheological and physicochemical studies on emulsions formulated with chitosan previously dispersed in aqueous solutions of lactic acid, Food Biophys. 12 (2017) 109–118.

[16] C. Tanford, Physical Chemistry of Macromolecules, 1st ed. John Wiley & Sons, Inc., New York, 1961.

[17] W. Brown, Dynamic Light Scattering: The Method and Some Applications, 1st ed. Clarendon Press, Oxford, 1993.

[18] M. Hosseinnejad, S.M. Jafari, Evaluation of different factors affecting antimicrobial properties of chitosan, Int. J. Biol. Macromol. 85 (2016) 467–475.

[19] S. Kumari, S. Hari, K. Annamareddy, S. Abanti, P.K. Rath, Physicochemical properties and characterization of chitosan synthesized from fish scales, crab and shrimp shells, Int. J. Biol. Macromol. 104 ((2017) 1697–1705.

[20] M.R. Kasaai, Calculation of Mark–Houwink–Sakurada (MHS) equation viscometric constants for chitosan in any solvent – temperature system using experimental reported viscometric constants data, Carbohydr. Polym. 68 (2007) 477–488.

[21] S.F. Sun, Physical Chemistry of Macromolecules, 2nd ed. John Wiley & Sons, Inc., New York, 2004.

[22] R.G. Jones, J. Kahovec, R. Stepto, E.S. Wilks, M. Hess, T. Kitayama, W.V. Metanomski, Compendium of Polymer Terminology and Nomenclature, 1st ed. RSC Publiching, Cambridge, 2008.

[23] E. Buhler, M. Rinaudo, Structural and dynamical properties of semirigid polyelectrolyte solutions: a light-scattering study, Macromolecules 33 (2000) 2098–2106.

[24] Siggel, T.D. Thomas, Why are organic acids stronger acids than organic alcohols? J. Am. Chem. Soc. 1 (1986) 4360–4363.

[25] Siggel, A. Streitwieser, T.D. Thomas, The role of resonance and inductive effects in the acidity of carboxylic acids, J. Am. Chem. Soc. 1 (1988) 8022–8028.

[26] T.W.G. Solomons, C.B. Fryhle, Organic Chemistry, 7th ed. John Wiley & Sons, Inc., New York, 2000.

[27] S.K. Shukla, A.K. Mishra, O.A. Arotiba, B.B. Mamba, Chitosan-based nanomaterials: a state-of-the-art review, Int. J. Biol. Macromol. 59 (2013) 46–58.

[28] M. Kaszuba, M.T. Connah, F.K. McNeil-Watson, U. Nobbmann, Resolving concentrated particle size mixtures using dynamic light scattering, Part. Part. Syst. Charact. 1 (2007) 159–162.

[29] I.K.D. Dimzon, T.P. Knepper, Degree of deacetylation of chitosan by infrared spectroscopy and partial least squares, Int. J. Biol. Macromol. 72 (2015) 939–945.

[30] C. Berthomieu, R. Hienerwadel, Fourier transform infrared (FTIR) spectroscopy, Photosynth. Res. 101 (2009) 157–170.

[31] J.S. Gaffney, N.A. Marley, E.J. Darin, Fourier transform infrared (FTIR) spectroscopy, Characterization of Materials, 2nd ed.John Wiley & Sons, Inc., New York, 2012.

Capítulo III

Chitosan dispersed in aqueous solutions of acetic, glycolic, propionic or lactic acid as a thickener/stabilizer agent of O/W emulsions produced by ultrasonic homogenization

Abbreviations and symbols

CSD	chitosan stock-dispersions
CI	creaming index (%)
d*P*	Laplace pressure gradient (Pa)
d*r*	infinitesimal radius variation (nm)
DA	degree of acetylation (%)
DD	degree of deacetylation (%)
d_h	hydrodynamic average diameter (nm)
K	consistency index ($Pa \cdot s^n$)
G'	storage modulus (Pa)
G''	loss modulus (Pa)
MAPE	mean absolute percentage error (%)
$\bar{M}_V$	viscometric-average molar mass (kDa)
n	flow behavior index (dimensionless)
n_i	the number of predicted/experimental score pairs
PDI	polydispersity index (dimensionless)
r	droplet radius (nm)
R^2	coefficient of determination
SD	standard deviation of average hydrodynamic diameter (nm)
V_I	initial volume of the emulsion placed in the conical centrifuge tubes (mL)
V_C	creamed oil volume formed at the top of the tubes (mL)
Y_i	the i^{th} experimental score applying the adjusted model
$\hat{Y}_i$	the i^{th} score predicted applying the adjusted model
z-ave	z-average or cumulants average diameter (nm)
Δ*G*	Gibbs free energy change caused by emulsification process
ΔA_{int}	interfacial area change during the emulsification process
ΔP_L	Laplace pressure (Pa)
γ	interfacial tension ($mN\ m^{-1}$)
ζ	zeta potential (mV)
τ	shear stress (Pa)
$\dot{\gamma}$	shear rate (s^{-1})
$\vec{E}$	electric field ($N \cdot C^{-1}$)
$[\eta]_H$	Huggins intrinsic viscosity ($dL \cdot g^{-1}$)
$[\eta]_K$	Kraemer intrinsic viscosity ($dL \cdot g^{-1}$)
$[\bar{\eta}]$	average intrinsic viscosity ($dL \cdot g^{-1}$)

Abstract

Chitosan is a derivate from chitin, which is a polysaccharide obtained of crustaceans processed by seafood industries. This biopolymer has been used in several biotechnological applications, but its presence in food products as an ingredient or additive is not common. In this study, 0.125; 0.250; 0.500; 0.750 and 1.000 $g \cdot (100\ g)^{-1}$ chitosan were dispersed in acid aqueous media (50 $mmol \cdot L^{-1}$) containing acetic, glycolic, propionic or lactic acids. Chitosan dispersions containing 2.000 $g \cdot (100\ g)^{-1}$ Tween 20 (75% m/m) were added to sunflower oil (25% m/m), in order to prepare O/W emulsions through ultrasonic homogenizer (20 kHz, 500 W, 4 min). Small oil droplets (< 600 nm) were produced in the emulsions with different chitosan concentrations. Emulsions containing > 0.500 $g \cdot (100\ g)^{-1}$ chitosan presented a lower increase in hydrodynamic average diameter and PDI of oil droplets between t = 0 d and t = 28 d, and showed no phase separation when exposed to centrifugation, freeze-thawing, and freeze-thaw-heating cycles,

which indicated the stabilizer action of this biopolymer. Furthermore, the increase in chitosan concentration promoted the augment in consistency indexes and storage moduli of emulsions, demostrating its thickening action. Thus, chitosan may be a suitable new alternative as thickener/stabilizer agent to acid emulsions, being its performance influenced by the biopolymer concentration and not by the acid type.

1. Introduction

Emulsions are colloidal systems in which at least one immiscible liquid is dispersed within another liquid as micrometric or nanometric droplets [42]. Emulsification process causes an augment in ΔG of that system, due to the fact that there is an increase of the interfacial area (ΔA_{int}) during the droplets formation, according to Equation 1.

$$\Delta G = \gamma \cdot \Delta A_{int} \quad (1)$$

In Eq. 1, ΔG is the Gibbs free energy change, γ is the interfacial tension, and ΔA_{int} is the interfacial area change during the emulsification process.

As a consequence, a high energy input is necessary to produce emulsions, and shear mixers, colloid mills, high pressure homogenizers, and microfluidizers are the most common devices used to promote droplet disruption [42]. However, emergent approaches include the use of membranes, microchannels and ultrasonic homogenizers to input high energy rates to disperse one liquid into small droplets [68]. The use of ultrasound devices to produce formulations containing oil and aqueous media as ingredients in pharmaceutical and cosmetic industries has been explored due to its safety and non-toxicity characteristics [69,70]. On the other hand, this technology is still considered as emergent to food applications, being used only in laboratory scale for enzymes inactivation, bioactive compounds extraction, and emulsions production [68,70]. Indeed, high-intensity ultrasonic waves act in the droplets disruption mainly due to cavitation phenomena, which is caused by rarefaction and condensation cycles of ultrasound waves [42,71]. The former occurs when the instantaneous pressure that a fluid experiences falls down below a critical value, which is a variable value, dependent on the energy content required to promote the droplets formation with smaller diameters when compared to their diameters immediately before this cycle. It grows accordingly as the fluid continues expanding, and some of the surrounding liquid evaporates and moves within it in the form of bubbles. On the other hand, during the condensation event these bubbles collapse, generating an intense shock wave that propagates and causes droplets (in its vicinity) to be deformed until disruption. The efficiency of ultrasonic homogenizers is determined by the amplitude, frequency, and duration of ultrasonic waves. Moreover, some characteristics of the sample to be sonicated can influence the ultrasonic homogenization efficiency; for instance, its viscosity could reduce the ultrasonic waves propagation [72].

In addition, Eq. 1 show that reducing γ seems to be a strategy to facilitate emulsification, and this can be achieved with the addition of surfactants (surface-active agents) into the system. Surfactants are amphiphilic molecules that are capable of lowering the

interfacial tension of colloidal systems, enabling the production of kinetically stable emulsions [45,73]. Hydrophilic and hydrophobic regions present in the molecular structure of surfactants will interact with immiscible liquids, reducing the energetically unfavorable contact between them (consequently, Δ*G* becomes less positive) [43].

During the emulsions preparation, the immiscible liquids (separated in at least two phases) are mixed together and the surfactant molecules, previously added into one of them, adsorb on the interface. Thus, the interactions between the phases is favored and, hence, the oil droplets formation is facilitated. The energy input necessary to form the droplets during the emulsifying process must be higher than Laplace pressure gradient (d*P*/d*r*) (Eq. 2). Moreover, Eq. 2 presents the resolution of Equation (3), and the change in the Laplace pressure (ΔP_L) term can be observed.

$$\frac{dP}{dr} = \frac{2\gamma}{r^2} \tag{2}$$

$$\Delta P_L = \frac{2\gamma}{r} \tag{3}$$

In Eq. 2 and 3, *r* is the droplet radius, and *γ* is the interfacial tension between two liquids.

According to Eq. 3, ΔP_L is responsible for maintaining the spherical shape of the droplet, and its value tends to increase with a decrease in droplet diameter, *i.e*., higher energy input should be used to form smaller droplets. Discussions up to this point demonstrate the importance of the energy input and a judicious choice of surfactants for obtaining emulsions.

Apart from the contribution of surfactants to emulsion formation, ionic surfactants can favor their kinetic stabilization, since they contain charged groups that contribute to electrostatic and steric repulsion among droplets [45,46,73]. Surfactants used to prepare emulsions are commonly called emulsifiers [74]. Another way to confer additional kinetic stability to emulsions is through the addition of thickening agents [47]. Conventional polysaccharides (xantana gum, modified celluloses, galactomannans, and others) are broadly used as emulsion thickeners/stabilizers due to their ability to increase the consistency of the emulsions' continuous phase [48,75], which reduces the frequency and intensity of collisions among dispersed droplets that experiment constant Brownian movement.

Reports have shown that some polysaccharides underused in the food industries, such as chitosan, present textural and/or processual advantages compared to those conventionally used as thickeners of emulsions. Chitosan is an N-deacetylate derivate of chitin [poly-β-(1→4)-N-acetyl-D-glucosamine], which is a polysaccharide obtained mostly from seashell skeleton of animals processed by seafood industries [76]. Chitosan is a biodegradable, biocompatible, and non-toxic material with a variety of applications [19,20,77–80]. Moreover, numerous studies in humans have been reporting that the oral intake of chitosan (with doses varying from 3 g to 6 g, daily) can promote its hypolipidemic activity. Chitosan cannot be dispersed in pure water, and dilute acid solutions have been used with this purpose, since NH_2 groups become protonated by H^+ cations present in these aqueous media. Therefore, intra and inter-chain electrostatic repulsions of chitosan molecules are allowed, thereby favoring their hydration [18]. Once dispersed, chitosan acts as thickener by changing the rheology (*i.e.* mechanical and flow

properties of the dispersion) and/or textural properties of aqueous media containing this biopolymer [2,14]. Studies have also evaluated the role of chitosan in the formation and stabilization of oil-in-water (O/W) emulsions, containing emulsifiers of low molar mass or proteins as interfacial agents [13]. For instance, Klinkesorn and Namatsila [51] investigated the formation of O/W emulsions containing 5.0 g·(100 g)$^{-1}$ tuna oil, 0.2 g·(100 g)$^{-1}$ Tween 80 as emulsifier, and 0.0 to 10.0 g·(100 g)$^{-1}$ chitosan dispersed in 10 mmol·L^{-1} acetic acid, at pH 6.0. Emulsions were mixed in high-speed homogenizer and passed through a two-stage high-pressure valve homogenizer (34.5 MPa). Oil droplets showed ζ potential values varying from -13 mV to +10 mV (0.0 - 10.0 g·(100 g)$^{-1}$ chitosan) and z-ave diameters between 300 nm and 550 nm (0.0 to 10.0 g·(100 g)$^{-1}$ chitosan), indicating a molecular interaction between chitosan and Tween 80 adsorbed on the interface of the droplets. O/W emulsions containing more than 4.0 g·(100 g)$^{-1}$ chitosan presented highly flocculated droplets when analysed by optical microscopy. However, the serum volume fraction was reduced from 90% to 0% with the increase of chitosan concentration (from 0.0 to 10.0 g·(100 g)$^{-1}$), after 180 h. These results demonstrate the importance of chitosan concentration to produce kinetically stable O/W emulsions. Kaasgaard & Keller [52] studied emulsions prepared with 5.0 g·(100 g)$^{-1}$ carvone as dispersed phase, 1.0 mL·(100 g)$^{-1}$ negatively charged citric acid ester small-molecule (CITREM LR10) as emulsifier, and different chitosan concentrations from 0.00 to 1.00 g·(100 g)$^{-1}$ dispersed in acetate buffer (pH 4.0) as a continuous phase. The authors observed oil droplets diameters of 100 nm in emulsions prepared without chitosan, at one-day storage period, and this result was attributed to the oil:surfactant ratio and to the emulsification process (6 passes through high pressure homogenizer, 69 MPa). Moreover, O/W emulsions containing chitosan (from 0.15 to 1.00 g·(100 g)$^{-1}$) presented oil droplets diameters of 250 nm at one-day storage period. The studies performed by Klinkesorn & Namatsila [51], Kaasgaard & Keller [52], and other reports have used acetic acid or acetate buffer solutions to disperse chitosan [8,13,51,81], which can be a drawback for cosmetic or food applications due to its unpleasant taste. Therefore, techno-functional exploration of this biopolymer in emulsions seems to be conditioned to its dispersion in aqueous media containing acids other than acetic. To the best of our knowledge, only one study focused on evaluating O/W emulsions prepared with chitosan dispersions in aqueous media containing different organic acids as continuous phase. Soares et al. [38] prepared O/W emulsions containing chitosan (0.1 g·(100 mL)$^{-1}$) dispersed in lactic acid aqueous solutions (pH 3.0, 3.5, or 4.0), and 1.0 mL·(100 mL)$^{-1}$ Tween 20 emulsifier as the continuous phase. Then, sunflower oil [10.0 mL·(100 mL)$^{-1}$] and the continuous phase [90.0 mL·(100 mL)$^{-1}$] were mixed in high-speed homogenizer (24,000 r/min, 1 min) and passed repeatedly 6 times through a high-pressure homogenizer (69 MPa). O/W emulsions containing chitosan presented oil droplets with similar ζ potential (next to +50 mV) and hydrodynamic average diameter (two populations of diameters: 45 nm and 360 nm), as well as viscosities (about 3 times higher than those prepared without chitosan). These results showed that lactic acid may be used to prepare chitosan dispersions to be used as continuous phase to produce kinetically stable O/W emulsions, during 7 d. Later, these authors have examined the use of

other organic acids to obtain aqueous chitosan dispersions [39]. They studied the physicochemical properties of 0.1 g·(100 mL)$^{-1}$ chitosan dispersions prepared in aqueous media containing acetic, glycolic, propionic, or lactic, at 10, 20, 30, 40, or 50 mmol·L^{-1}. Thus, glycolic, propionic or lactic acid are suitable to replace acetic acid to prepare chitosan dispersions for technological purposes. However, higher chitosan concentrations may be required for it to act as thickener in cosmetics or food formulations.

Therefore, the formulation of O/W emulsions containing chitosan dispersed in aqueous solutions prepared with acetic, glycolic, propionic, and lactic acids is a relevant proposal to enable future industrial applications of this biopolymer mainly in the food field. Thus, in order to understand if chitosan can be used as a thickener and/or stabilizer agent for O/W emulsions, the purposes of this paper are to: *i*) prepare chitosan dispersions in aqueous media containing acetic, glycolic, propionic or lactic acid; *ii*) produce O/W emulsions, containing chitosan dispersions and Tween 20 emulsifier as a continuous phase, using an ultrasound device to disrupt the oil phase (sunflower oil colored with Sudan III red dye); *iii*) characterize O/W emulsions in terms of rheological measurements, microstructure, hydrodynamic average diameter, PDI, and ζ potential of oil droplets; and *iv*) evaluate the kinetic stability and the destabilization of O/W emulsions exposed to stress conditions.

2. Materials and methods

2.1 Materials

Chitosan (Medium Molecular Weight, Sigma-Aldrich Corporation, USA; Product ID = 448877; Batch number = #STBF8484V) from seashell skeleton was used in all the experiments. Other chemicals were of analytical grade and used without any purification process: glacial acetic acid (Vetec, Brazil; purity = 99.7%), glycolic acid (Vetec, Brazil; purity ≥ 98.0%), lactic acid (Impex Quimica, Spain; purity = 85%), propionic acid (Sigma-Aldrich Corporation, USA; purity ≥ 99.5%), Tween 20 (Sigma-Aldrich Corporation, USA; Product ID = P1379), and Sudan III red dye (Sigma-Aldrich Corporation, USA; purity ≥ 80%). Sunflower oil (Bunge Alimentos, Brazil) was of food grade. Deionized water was obtained from a Mili-Q system (≈ 18.2 MΩ·cm^{-1}, 25 ^{o}C; Reference A+, Millipore, Italy).

2.1.1 Chitosan characterization

Before use, chitosan was washed three times with deionized water, in order to reduce water-soluble chitooligosaccharides content and salts residues [39]. Washed chitosan was recovered using a vacuum filtration system, and qualitative paper (Cat No 1004 125, Whatman). Then, the remaining solid chitosan was frozen, lyophilized (Terroni, LS 3000, Brazil), and stored at 7 ± 2 °C (Consul, Pratice 410, Brazil). Chitosan powder was analysed using a FT-IR spectrophotometer (600-IR, Varian, USA) equipped with an attenuated reflectance accessory (GladiATR, PIKE Technologies, USA). Next, the degree of acetylation (DA) was estimated from the empirical relationship between normalized absorbances of the peaks at wavenumbers 1320

and 1420 cm^{-1} [82,83]. Degree of deacetylation (DD) was obtained by simple difference [DD(%) = 100% - DA(%)], and DD value of the chitosan used in the present study was estimated as 72.5%. In order to obtain the average intrinsic viscosity ($[\bar{\eta}]$), chitosan [0.02, 0.04, 0.06, 0.08, and 0.10 $g\cdot(100\ g)^{-1}$] was dispersed in acetic acid-sodium acetate buffer [84], and flow times of each dispersion were measured in a Cannon-Fenske viscometer (model 513 20, Schott, Germany). Then, viscometric-average molar mass ($\bar{M}_V$) of chitosan was calculated as 430 ± 30 kDa using the Mark-Houwink-Sakurada (MHS) relationship [84,85].

2.2 Experimental design

A factorial design 6 x 4 (totaling 24 systems) was adopted to understand the effect of two independent variables (chitosan concentration and the type of organic acid used to disperse this biopolymer) on the formation and the destabilization of O/W emulsions. Six chitosan concentrations were 0.000 $g\cdot(100\ g)^{-1}$, 0.125 $g\cdot(100\ g)^{-1}$, 0.250 $g\cdot(100\ g)^{-1}$, 0.500 $g\cdot(100\ g)^{-1}$, 0.750 $g\cdot(100\ g)^{-1}$, and 1.000 $g\cdot(100\ g)^{-1}$; and four organic acids were acetic, glycolic, propionic, or lactic acid (50 $mmol\cdot L^{-1}$). Treatments were repeated three times, and results were presented as average ± standard deviation.

2.3 Preparation of chitosan dispersions

Previously, a 50 $mmol\cdot L^{-1}$ solution was prepared for each acid (acetic, glycolic, propionic or lactic). Then, 1.000 $g\cdot(100\ g)^{-1}$ chitosan was added to appropriate amounts of these solutions (AUY220, Shimadzu, Japan), in order to obtain four chitosan stock-dispersions (CSD). Resulting systems were stirred during 4 h using a mechanical agitator (MA-039, Marconi, Brazil) equipped with a helical propeller (270 r/min), within a thermostatic bath (TE-184, Tecnal, Brazil), at 25.0 ± 0.1 °C. Subsequently, CSD were centrifuged (7830 r/min; 5430, Eppendorf, Germany) during 20 min, in order to remove insoluble impurities.

CSD were transferred to amber bottles and stored at 7 ± 2 °C. Chitosan diluted-dispersions were prepared by CDS dilution to 0.125 $g\cdot(100\ g)^{-1}$, 0.250 $g\cdot(100\ g)^{-1}$, 0.500 $g\cdot(100\ g)^{-1}$, and 0.750 $g\cdot(100\ g)^{-1}$ using the same solution for each acid (50 $mmol\cdot L^{-1}$) as a diluent.

2.4 Preparation of O/W emulsions

2.0 $g\cdot(100\ g)^{-1}$ Tween 20 emulsifier was added to chitosan dispersions containing acetic, glycolic, propionic, or lactic acid, and the resulting mixtures were used as continuous phases for preparing oil-in-water (O/W) emulsions. Additionally, control systems, without chitosan (0.000 $g\cdot(100\ g)^{-1}$) were prepared to each one of organic acid. 0.02 $g\cdot(100\ g)^{-1}$ Sudan III red dye was used to color sunflower oil (oily phase of the O/W emulsions). Then, emulsions were prepared with 18.75 g of aqueous phase and 6.25 g oil phase (totaling 25.00 g). The emulsification process was performed in two steps: *i*) the two phases were mixed using a vortex stirrer (Phoenix, Tecnal, Brazil) during 20 s; and *ii*) O/W emulsions were obtained by an ultrasonic homogenizer (Vibra Cell, Sonics and Materials, Inc., USA), operating at 20 kHz with a power output of 500 W for 4 min. In order to control systems temperature (≤ 40 °C) during the

droplets formation, the tubes containing the emulsions were immersed in an ice bath during the sonication process [86]. 10 mL of O/W emulsions were transferred to Falcon 15 mL conical centrifuge tubes and identified. Then, they were stored at room temperature (25 ± 1 ^{o}C) in a dark environment to avoid light and oxygen pro-oxidative effects.

2.5. Characterization of O/W emulsions

Emulsions containing different concentrations of chitosan (0.000 g·(100 g)$^{-1}$, 0.125 g·(100 g)$^{-1}$, 0.250 g·(100 g)$^{-1}$, 0.500 g·(100 g)$^{-1}$, 0.750 g·(100 g)$^{-1}$, and 1.000 g·(100 g)$^{-1}$) prepared with acetic, glycolic, propionic, or lactic acid solutions were characterized in terms of flow behavior, viscoelasticity, microstructure, and visual appearance, apart from hydrodynamic average diameter, PDI, and ζ potential of oil droplets, after preparation of the emulsions (t = 0 d).

2.5.1. Rheological analyses

Rheological measurements of emulsions were performed, at 25.0 ± 0.1 ^{o}C, using a rotational rheometer (Discovery Hybrid Rheometer 1 (DHR-1), TA Instruments, USA), equipped with a stainless steel parallel plate sensor (diameter = 25 mm; gap = 1 mm).

Flow curves were determined by progressively varying the shear rate ($\dot{\gamma}$) from 0.1 to 200.0 s^{-1} in three flow curves (1st up-down cycle, and 2nd up cycle; 300 s each cycle), and measuring the corresponding shear stresses (τ). Ostwald de Waele model (Equation 4) was fitted to $\tau = f(\dot{\gamma})$ data using the SAS software (SAS Institute Inc., North Carolina, USA).

$$\tau = K \cdot (\dot{\gamma})^n \quad (4)$$

In Eq. 4, *K* is the consistency index and *n* is the flow behavior index.

Coefficient of determination (R^2) and mean absolute percentage error (MAPE) (Equation 5) were used to evaluate the adequacy of fitting in all cases.

$$\text{MAPE } (\%) = \frac{1}{n_i}\sum_{i=1}^{n}\left|\frac{(Y_i - \hat{Y}_i)}{Y_i}\right| \text{x } 100\% \quad (5)$$

In Eq. 5, Y_i is the i^{th} experimental score, $\hat{Y}_i$ is the i^{th} score predicted by applying the adjusted model, and n_i is the number of predicted/experimental score pairs. In this paper, experimental data are considered well-fitted when models present R^2 values ≥ 0.9 and *MAPE* values ≤ 10%.

The viscoelasticity of emulsions was studied in dynamic oscillatory assays. Firstly, the linear viscoelastic range of the emulsions was determined upon performing a strain sweep (0.01 to 2.5%), at a constant frequency of 1 Hz. After that, the frequency sweep was carried out from 0.1 to 10 Hz, at constant strain amplitude of 0.125% (according to the determined linear viscoelastic range). Results were presented in terms of the storage modulus (*G'*) and loss modulus (*G''*) as a function of the frequency.

2.5.2. Microstructure

The microstructure of the emulsions was studied using an optical microscope (CX40, Olympus, USA). Emulsion aliquots (3 µL) were sampled at 0.5 - 1.0 cm below the surface and

poured onto microscope slides. Then, the microscope slides were covered with glass cover slips and observed at a magnification of x100. Images were taken using a digital camera, and at least 10 images were taken for each emulsion.

2.5.3. Hydrodynamic average diameter, PDI, and ζ potential of oil droplets

Hydrodynamic average diameter, PDI, and ζ potential of the oil droplets were evaluated by dynamic light scattering (DLS) (Zetasizer Nano-ZS, Malvern Instruments, United Kingdom), at 25.0 ± 0.1 °C. Emulsions were sampled at 0.5 - 1.0 cm below the surface and then diluted (1:250) to prevent multiple scattering effects, using as diluent the same acid solution (used to disperse chitosan in the continuous phase) added to 2.0 g·(100 g)$^{-1}$ Tween 20 emulsifier. Diluted emulsions were placed in a cuvette for carrying out the instrumental analyses. Diameters distributions were obtained by means of the amplitude of the decay rate, which is obtained by fitting the normalized temporal intensity correlation functions, by Non-Negative Least Square algorithm (NNLS) [38,39,87]. PDI also was calculated. This index is usually a number calculated from of the correlation data (the cumulants analysis), considering all peaks present. However, in this study PDI was estimated from hydrodynamic average diameter (d_h) and standard deviation (SD) relationship (Equation 6) for each oil droplet distributions [88].

$$\mathrm{PDI} = \left(\frac{\mathrm{SD}}{d_h}\right)^2 \tag{6}$$

ζ potential of oil droplets was estimated from the electrophoretic mobility phenomena. Emulsions diluted within the cuvette were subjected to a controlled electric field. Then, electrophoretic mobility was estimated from the speed and the direction of the particle movement due to this electric field, and ζ potential values were calculated considering the Smoluchowski model for the double electrical layer.

2.6. Destabilization of O/W emulsion

Destabilization of the emulsions because of flocculation/creaming was evaluated by visually monitoring the development of an upper phase during twenty eight-day storage period at room temperature (25 ± 1 ^{o}C). The extension of the oil creaming was quantified in terms of creaming index (CI %) according to Equation 7.

$$\mathrm{CI}\ (\%) = \left(\frac{\mathrm{V_C}}{\mathrm{V_I}}\right) \times 100\% \tag{7}$$

In Eq. 7, V_I represents the initial volume of the emulsion placed in the conical centrifuge tubes and V_C is the creamed oil volume formed at the top of the tubes measured in each time after emulsion preparation.

Results of CI (%) were presented as a function of time. Hydrodynamic average diameter, and PDI from hydrodynamic diameter distribution of oil droplets were also evaluated at fourteen (t = 14 d) and at twenty eight-day storage period (t = 28 d), in order to compare their values with those observed at t = 0 d and to identify the destabilization process that might occur during storage time.

Emulsions were exposed to three stress conditions for the purpose of studying their destabilization: *i*) emulsions were frozen at – 18 ± 1 °C (2800, Metalfrio, Brazil) during 24 h, and evaluated after 24 h; *ii*) freeze-thawed emulsions (24 h each step) were heated at 100 ± 5 °C (MA 032, Marconi, Brazil) during 1 h, and cooled to room temperature (25 ± 1 °C); and *iii*) emulsions were centrifuged (7830 r/min) during 10 min, and evaluated after 24 h. Results were presented in terms of hydrodynamic average diameter, PDI from hydrodynamic diameter distribution of oil droplets, and CI (%) values.

3. Results

3.1. Rheological analyses

3.1.1. Flow behavior of O/W emulsions

Rheograms of O/W emulsions show that none of the emulsions had hysteresis during rheological analyses, *i. e*. the three flow curves corresponding to the 1st up-down cycle, and 2nd up cycle were superposed. Then, 2nd up curves were used to mathematical fitting. Experimental data for $\tau = f(\dot{\gamma})$ were inspected visually, and flow behavior curves of O/W emulsions showed a pseudoplastic behavior (rheograms of 2nd up curves can be seen in Figure SM3, Appendix II). Upon testing some rheological models, Ostwald de Waele model was well fitted to $\tau = f(\dot{\gamma})$ values, resulting in $R^2 \geq 0.991$ and MAPE $\leq$ 6.1% according to Table 1. R^2 and MAPE values indicated the good adequacy of the fitted models. Rheological parameters of the Ostwald de Waele model adjusted to chitosan emulsions prepared with acetic, glycolic, propionic or lactic acid are also presented in Table 1.

Table 1 - Rheological parameters (*K* and *n*) and adequacy fitting of the Ostwald de Waele model adjusted to O/W emulsions containing different chitosan concentrations dispersed in acid continuous phase prepared with acetic, glycolic, propionic or lactic acid.

Chitosan concentration g·(100 g)$^{-1}$	Type of acid															
	AA				GA				PA				LA			
	Parameters		Adequacy of fitting		Parameters		Adequacy of fitting		Parameters		Adequacy of fitting		Parameters		Adequacy of fitting	
			R^2	MAPE (%)			R^2	MAPE (%)			R^2	MAPE (%)			R^2	MAPE (%)
0.000	*K* (Pa·s^n)	0.30 ± 0.02	0.911	4.5	*K* (Pa·s^n)	0.46 ± 0.01	0.949	2.2	*K* (Pa·s^n)	0.20 ± 0.02	0.911	5.8	*K* (Pa·s^n)	0.34 ± 0.02	0.890	3.7
	n	0.20 ± 0.01			*n*	0.14 ± 0.01			*n*	0.30 ± 0.02			*n*	0.15 ± 0.01		
0.125	*K* (Pa·s^n)	0.26 ± 0.02	0.948	6.1	*K* (Pa·s^n)	0.38 ± 0.02	0.947	5.3	*K* (Pa·s^n)	0.28 ± 0.03	0.930	6.0	*K* (Pa·s^n)	0.31 ± 0.02	0.969	4.7
	n	0.35 ± 0.01			*n*	0.28 ± 0.01			*n*	0.36 ± 0.02			*n*	0.34 ± 0.01		
0.250	*K* (Pa·s^n)	0.25 ± 0.02	0,971	4.9	*K* (Pa·s^n)	0.28 ± 0.02	0.959	5.3	*K* (Pa·s^n)	0.31 ± 0.03	0.966	5.0	*K* (Pa·s^n)	0.22 ± 0.02	0.969	4.8
	n	0.48 ± 0.02			*n*	0.39 ± 0.02			*n*	0.41 ± 0.02			*n*	0.45 ± 0.02		
0.500	*K* (Pa·s^n)	0.37 ± 0.02	0.986	4.4	*K* (Pa·s^n)	0.49 ± 0.03	0.976	4.7	*K* (Pa·s^n)	0.38 ± 0.02	0.991	5.0	*K* (Pa·s^n)	0.41 ± 0.02	0.992	4.6
	n	0.49 ± 0.01			*n*	0.40 ± 0.01			*n*	0.50 ± 0.01			*n*	0.53 ± 0.01		
0.750	*K* (Pa·s^n)	0.45 ± 0.02	0.995	4.4	*K* (Pa·s^n)	0.70 ± 0.05	0.979	0.9	*K* (Pa·s^n)	0.64 ± 0.02	0.997	2.1	*K* (Pa·s^n)	0.48 ± 0.01	0.998	0.8
	n	0.56 ± 0.01			*n*	0.44 ± 0.01			*n*	0.43 ± 0.01			*n*	0.58 ± 0.01		
1.000	*K* (Pa·s^n)	0.78 ± 0.03	0.997	3.1	*K* (Pa·s^n)	0.95 ± 0.04	0.996	3.3	*K* (Pa·s^n)	0.86 ± 0.03	0.997	2.3	*K* (Pa·s^n)	1.11 ± 0.04	0.998	
	n	0.57 ± 0.01			*n*	0.50 ± 0.01			*n*	0.53 ± 0.01			*n*	0.53 ± 0.01		0.9

O/W emulsions prepared without chitosan showed *K* values from 0.20 Pa to 0.46 Pa·s^n and *n* values from 0.14 to 0.30. *K* values from 0.26 Pa to 0.38 Pa·s^n and *n* values from 0.28 to 0.36 were observed in O/W emulsions containing 0.125 g·(100 g)$^{-1}$ chitosan in the continuous phase, and *K* values from 0.22 Pa to 0.31 Pa·s^n and *n* values from 0.39 to 0.48 in those prepared with 0.250 g·(100 g)$^{-1}$. Emulsions prepared with continuous phases containing lower concentrations, (0.125 g·(100 g)$^{-1}$ and 0.250 g·(100 g)$^{-1}$), or without chitosan may have been more influenced by the experimental error and variations in the oil droplets diameters. Moreover, droplet-droplet and droplet-continuous-phase interactions can influence the system structure, complicating the experimental elucidation of emulsions behavior.

O/W emulsions containing higher chitosan concentrations in their continuous phase showed: *K* values from 0.37 Pa·s^n to 0.49 Pa·s^n and *n* values from 0.40 to 0.53 for 0.500 g·(100 g)$^{-1}$; *K* values from 0.45 Pa·s^n to 0.70 Pa·s^n and *n* values from 0.43 to 0.58 for 0.750 g·(100 g)$^{-1}$; and *K* values from 0.78 Pa·s^n to 1.11 Pa·s^n and *n* values from 0.50 to 0.57 for 1.000 g·(100 g)$^{-1}$. Emulsions containing 0.500 g·(100 g)$^{-1}$; 0.750 g·(100 g)$^{-1}$ and 1.000 g·(100 g)$^{-1}$ chitosan in acetic, glycolic, propionic or lactic acid in the continuous phase showed a raise in *K* values with increasing biopolymer concentration. Moreover, the type of acid used to disperse chitosan in the continuous phase of emulsions did not influence the values of *K* e *n*, at a given chitosan concentration. These results pointed out that chitosan added in O/W emulsions promoted a thickening effect, contributing to reduce the emulsions destabilization. In addition, a similar behavior was seen for the *n* values of these emulsions, which indicates that the shear rate range values were not greatly affected by the increase in the chitosan concentrations.

3.1.2. Viscoelasticity of O/W emulsions

Frequency sweeps were performed to evaluate the viscoelasticity of O/W emulsions. The curves of *G'* and *G''* observed from 0.1 to 10 Hz are presented in Figure 1.

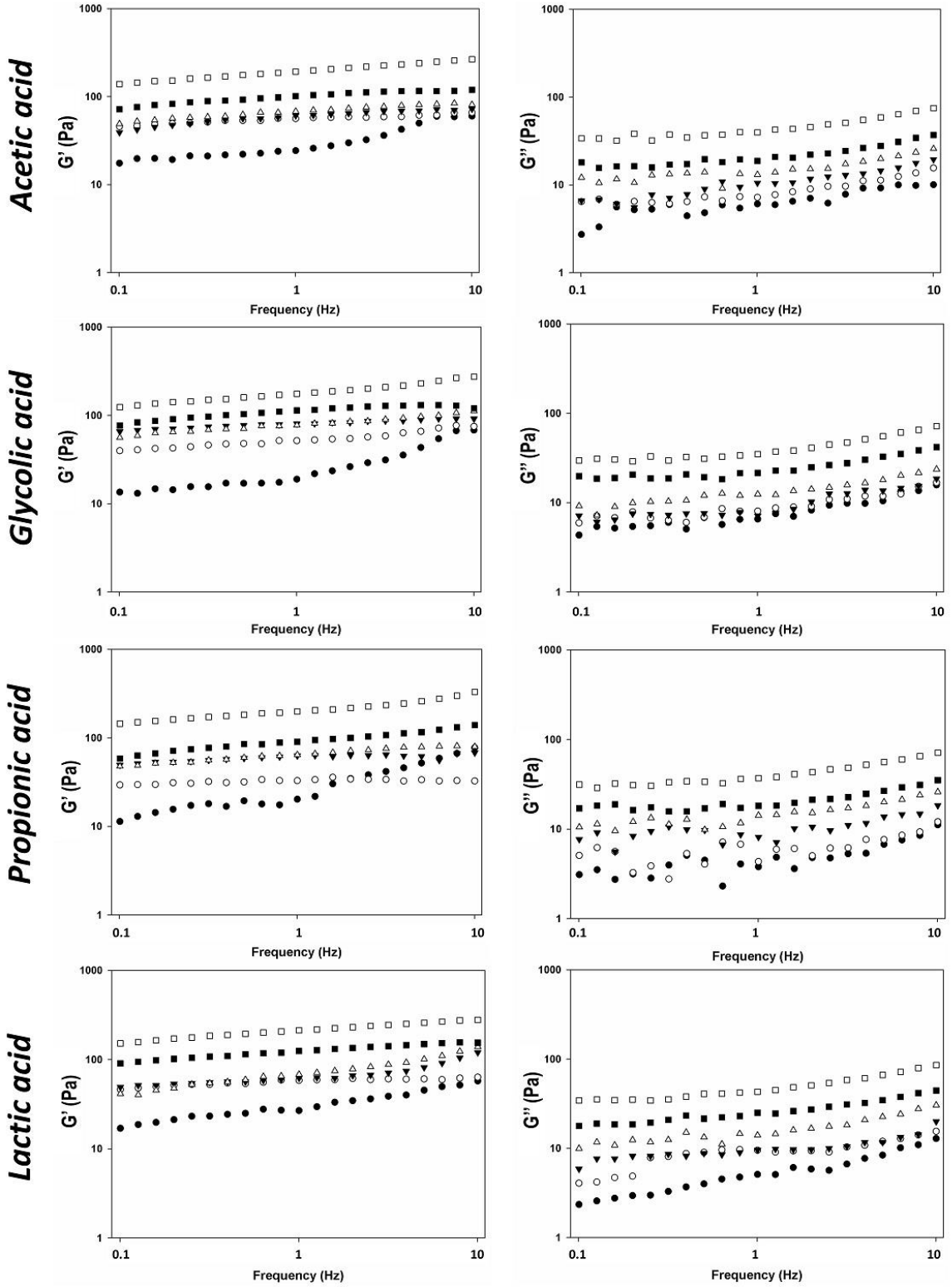

Figure 1 - *G'* and *G''* in frequency sweeps (from 0.1 to 10 Hz) of O/W emulsions containing chitosan dispersed in different acid continuous phase. (●) 0.000 g·(100 g)$^{-1}$, (○) 0.125 g·(100 g)$^{-1}$, (▼) 0.250 g·(100 g)$^{-1}$, (Δ) 0.500 g·(100 g)$^{-1}$, (■) 0.750 g·(100 g)$^{-1}$, and (□) 1.000 g·(100 g)$^{-1}$ of chitosan.

O/W emulsions prepared without chitosan showed similar *G'* and *G''* from 0.1 to 10 Hz, independent of the type of organic acid used to prepare the continuous phase. *G'* presented values of $1 \cdot 10^1$ Pa which increased over the frequency range until reaching $6 \cdot 10^1$ Pa, whereas *G''* values were raised from $2 \cdot 10^0$ Pa to $10 \cdot 10^0$ Pa. O/W emulsions containing chitosan presented an increase in the initial and final values of *G'* and *G''* as the biopolymer concentration was incremented. In addition, the type of acid used to disperse chitosan in the continuous phase of emulsions did not influence the behavior of *G'* and *G''*. Emulsions prepared with higher chitosan concentrations (1.000 g·(100 g)$^{-1}$) presented *G'* values of $1 \cdot 10^2$ Pa at 0.1 Hz increasing to $3 \cdot 10^2$ Pa at 10 Hz, and *G'* values grew from $3.0 \cdot 10^1$ Pa to $8.0 \cdot 10^1$ Pa within the same shear frequency range. The increase of chitosan concentration in O/W emulsions contributed to a lower increase of *G'* and *G''* values, at frequencies from 0.1 to 10 Hz.

3.2. Microstructure of O/W emulsions

Microphotographs observed at a magnification x100 revealed different behaviors between O/W emulsions prepared without chitosan and those containing chitosan dispersed in their continuous phase. Microstructures of O/W emulsions containing different chitosan concentrations and 2.0 g·(100 g)$^{-1}$ Tween 20 in the continuous phase are shown in Figure 2.

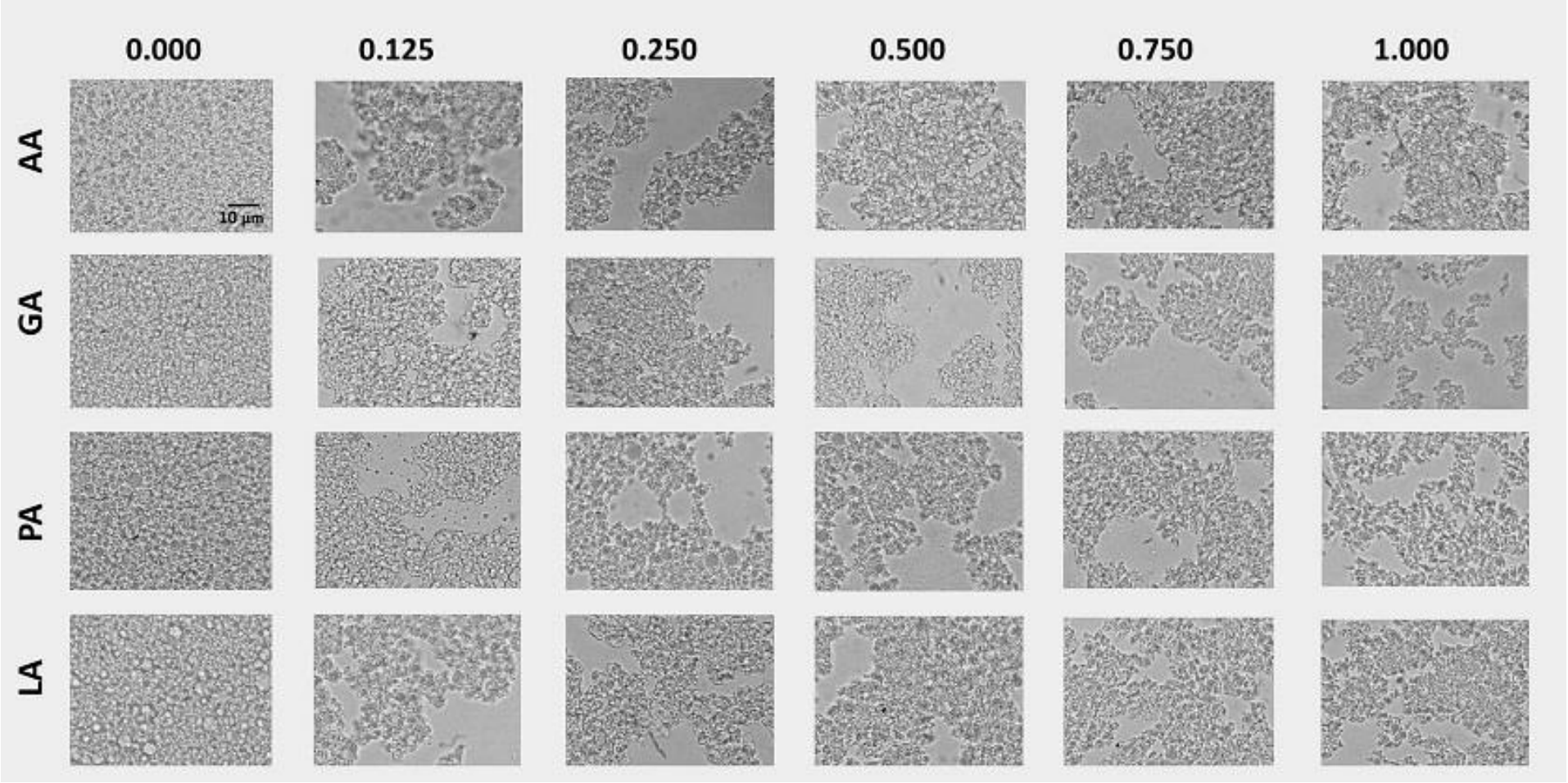

Figure 2 – Optical micrographs of O/W emulsions containing different chitosan concentrations (0.000 g·(100 g)$^{-1}$ to 1.000 g·(100 g)$^{-1}$) dispersed in acid continuous phase prepared with acetic (AA), glycolic (GA), propionic (PA) or lactic (LA) acid.

No evidence of droplet aggregation was observed in emulsions prepared without chitosan analysed by optical microscopy. O/W emulsions containing chitosan (0.125, 0.250, 0.500, 0.750, and 1.000 g·(100 g)$^{-1}$) presented aggregates, which can be attributed to a three-dimensional network containing oil droplets and dispersed chitosan chains. However, it was not possible to establish any relationship between chitosan concentration in the emulsions and the appearance of the aggregates from micrographs presented in Figure 2. Mechanisms such as bridging flocculation of oil droplets could have led to their aggregation with chitosan chains. Furthermore, oil droplets flocculation did not necessarily cause phase separation of O/W emulsions. Differences were not noticed between O/W emulsions, whose continuous phase contained acetic, glycolic, propionic or lactic acid.

3.3. Hydrodynamic average diameter, PDI, and ζ potential of oil droplets

Hydrodynamic average diameter, PDI from hydrodynamic diameter distribution, and ζ potential of oil droplets emulsions were analysed after O/W emulsions preparation (t = 0 d), and the results are presented in Figure 3.

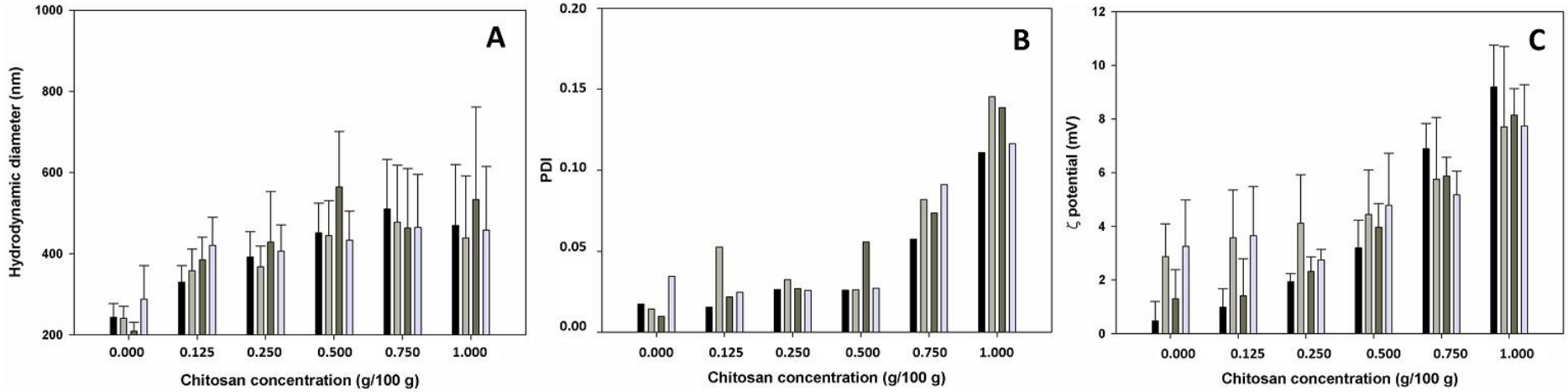

Figure 3 - Hydrodynamic average diameter (A), PDI from hydrodynamic diameter distribution (B), and ζ potential (C) of oil droplets present in O/W emulsions containing different chitosan concentrations in the continuous phase prepared with acetic (▬), glycolic (▭), propionic (▬), or lactic (▭) acid. Error bars in Figure 3 (A, B and C) represent the standard deviation.

Hydrodynamic average diameter, PDI from hydrodynamic diameter distribution, and ζ potential of oil droplets showed similar values to each chitosan concentration in the continuous phase of O/W emulsions containing acetic, glycolic, propionic or lactic acid. As depicted in Figure 3 – A, the hydrodynamic average diameters of oil droplets increased as the chitosan concentration was raised in the continuous phase of emulsions (from 210 nm to 290 nm for continuous phase containing 0.000 g·(100 g)$^{-1}$ chitosan; 330 nm to 420 nm for 0.125 g·(100 g)$^{-1}$; 370 nm to 430 nm for 0.250 g·(100 g)$^{-1}$; and 430 nm to 560 nm for 0.500 g·(100 g)$^{-1}$; 460 nm to 510 nm for 0.750 g·(100 g)$^{-1}$; and 440 nm to 530 nm for 1.000 g·(100 g)$^{-1}$ chitosan). The PDI calculated from hydrodynamic diameter distribution of oil droplets presented small values to O/W emulsions containing between 0.000 and 0.500 g·(100 g)$^{-1}$ chitosan (from 0.01 to 0.04 for continuous phase containing 0.000 g·(100 g)$^{-1}$ chitosan; 0.02 to 0.05 for 0.125 g·(100 g)$^{-1}$; 0.02 to 0.03 for 0.250 g·(100 g)$^{-1}$; and 0.03 to 0.05 nm for 0.500 g·(100 g)$^{-1}$). PDI values of oil droplets in the O/W emulsions prepared with a continuous phase containing 0.750 g·(100 g)$^{-1}$ and 1.000 g·(100 g)$^{-1}$ chitosan showed higher values than the other emulsions (from 0.06 to 0.09 for continuous phase containing 0.750 g·(100 g)$^{-1}$, and 0.11 to 0.15 for 1.000 g·(100 g)$^{-1}$ chitosan).

ζ potential values of oil droplets in the O/W emulsions were also measured and the corresponding results are represented in Figure 3 – C. ζ potential values of oil droplets values were raised as the chitosan concentration was increased in the continuous phase of O/W emulsions (from 0.5 mV to 3.2 mV for continuous phase containing 0.000 g·(100 g)$^{-1}$ chitosan; 0.9 mV to 3.6 mV for 0.125 g·(100 g)$^{-1}$; 1.9 mV to 4.1 mV for 0.250 g·(100 g)$^{-1}$; 3.2 mV to 4.8 mV for 0.500 g·(100 g)$^{-1}$; 5.2 mV to 6.9 mV for 0.750 g·(100 g)$^{-1}$; and 7.7 mV to 9.2 mV for 1.000 g·(100 g)$^{-1}$ chitosan). ζ potential values are pointing out a progressive raise in the density of positive charges according to chitosan concentration increment in the continuous phase of emulsions between 0.000 and 1.000 g·(100 g)$^{-1}$, indicating the existence of intermolecular interactions between protonated chitosan chains and the O/W interface covered with Tween 20 [13,38,51].

3.4. Destabilization of O/W emulsions

3.4.1. Destabilization kinetics

Creaming extension of O/W emulsions containing different chitosan concentrations and 2.0 g·(100 g)$^{-1}$ Tween 20 in the continuous phase was evaluated through creaming index (CI %). Then, CI (%) kinetics curves were presented as a function of time in Figure 4.

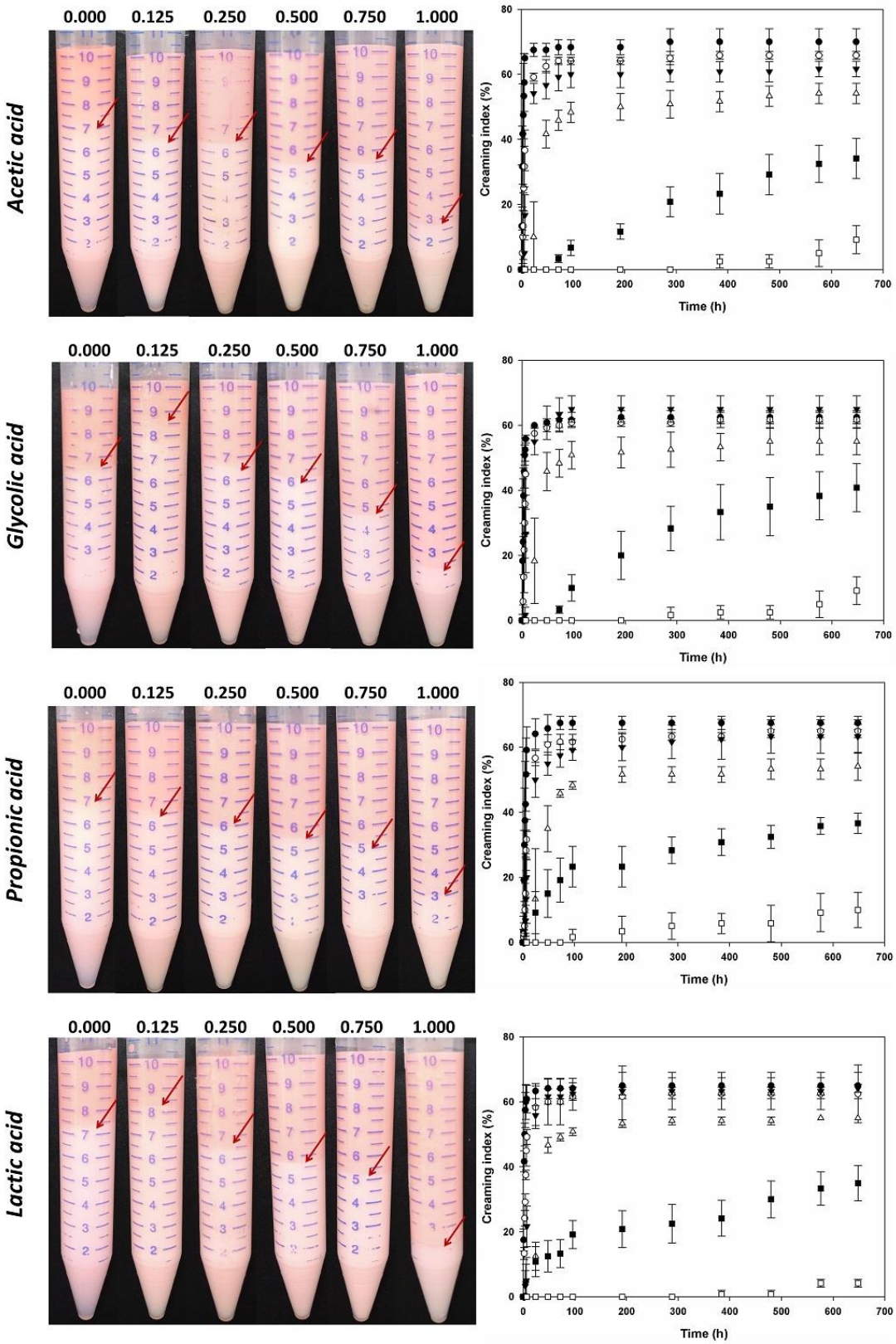

Figure 4 - Visual appearance of O/W emulsions (2nd repetition) after 28 d storage period (on the left) and CI (%) as a function of time for O/W emulsion containing chitosan dispersed in different acid continuous phase (on the right). (●) 0.000 g·(100 g)$^{-1}$, (○) 0.125 g·(100 g)$^{-1}$, (▼) 0.250 g·(100 g)$^{-1}$, (Δ) 0.500 g·(100 g)$^{-1}$, (■) 0.750 g·(100 g)$^{-1}$, and (□) 1.000 g·(100 g)$^{-1}$ of chitosan. Error bars in Figure 3 (A, B and C) represent the standard deviation.

Emulsions destabilization was evaluated by visually monitoring the development of an upper phase during twenty eight-day storage period at room temperature (25 ± 1 ^{o}C) and a similar behavior can be seen in the kinetics curves of O/W emulsions prepared with the same chitosan concentration. CI (%) equilibrium occurred after short times (≤ 96 h) for emulsions prepared with 0.000 g·(100 g)$^{-1}$, 0.125 g·(100 g)$^{-1}$ and 0.250 g·(100 g)$^{-1}$ chitosan in the continuous phase containing acetic, glycolic, propionic or lactic acid. O/W emulsions prepared with 0.500 g·(100 g)$^{-1}$ chitosan in their continuous phase containing the four organic acids reached an equilibrium in the CI (%) value at 192 h. However, emulsions prepared with 0.750 g·(100 g)$^{-1}$ and 1.000 g·(100 g)$^{-1}$ chitosan in the continuous phase containing acetic, glycolic, propionic or lactic acid did not seem to have achieved the equilibrium in CI (%) after 672 h and, therefore, were considered as more kinetically stable emulsions.

The destabilization kinetics was also evaluated in terms of hydrodynamic average diameter, PDI from hydrodynamic diameter distribution of oil droplets, and CI (%) values at fourteen-day (t = 14 d) or at twenty eight-day storage period (t = 28 d) are presented in Figure 5.

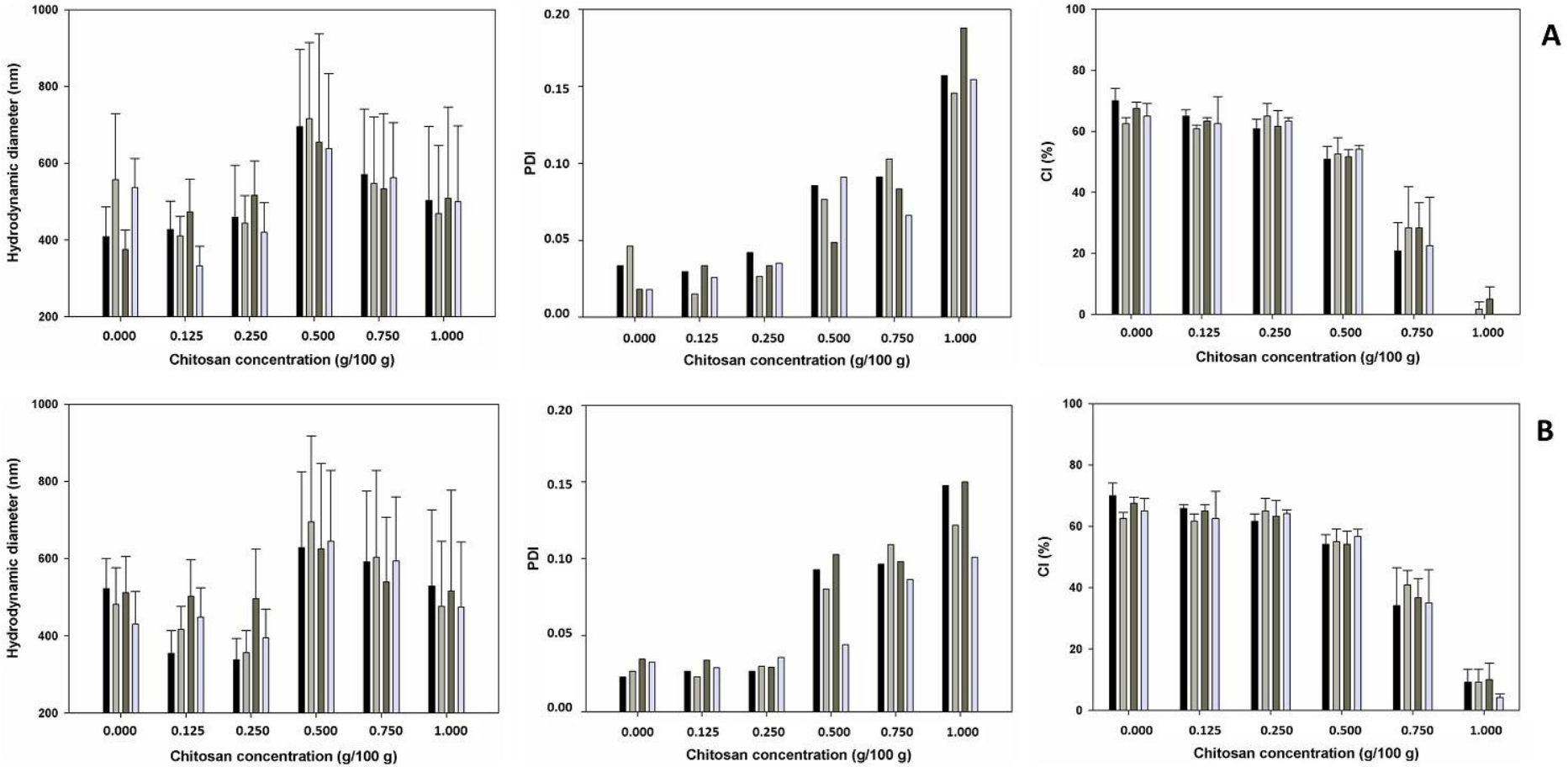

Figure 5 - Hydrodynamic average diameter of oil droplets, PDI from oil droplets hydrodynamic diameter distribution, and CI (%) of O/W emulsions containing different chitosan concentrations in the continuous phase prepared with acetic (■), glycolic (▭), propionic (▭), or lactic (▭) acid, at t = 14 d (A) and at t = 28 d (B). Error bars in Figure 3 (A, B and C) represent the standard deviation.

Hydrodynamic average diameter, PDI from hydrodynamic diameter distribution of oil droplets and CI (%) of O/W emulsions presented similar values to each chitosan concentration in the continuous phase of O/W emulsions containing acetic, glycolic, propionic or lactic acid, at t = 14 d or at t = 28 d. Figure 5 – A shows an increase in hydrodynamic average diameters of oil droplets at t = 14 d when compared with values obtained at t = 0 for all emulsions (from 370 nm to 560 nm for continuous phase without chitosan; 330 nm to 470 nm for 0.125 g·(100 g)$^{-1}$; 420 nm to 520 nm for 0.250 g·(100 g)$^{-1}$; 640 nm to 720 nm for 0.500 g·(100 g)$^{-1}$; 530 nm to 570 nm for 0.750 g·(100 g)$^{-1}$; and 470 nm to 510 nm for 1.000 g·(100 g)$^{-1}$). Hydrodynamic average diameters of oil droplets presented a more expressive increase in O/W emulsions without (0.000 g·(100 g)$^{-1}$) and with 0.500 g·(100 g)$^{-1}$ chitosan, and their PDI values were raised between t = 14 d and t = 0 d (from 0.02 to 0.05 for continuous phase containing 0.000 g·(100 g)$^{-1}$ chitosan; and 0.05 to 0.09 for 0.500 g·(100 g)$^{-1}$). PDI obtained from hydrodynamic diameter distribution of oil droplets showed similar values for the other emulsions between t = 14 d and t = 0 d (from 0.02 to 0.03 for continuous phase containing 0.125 g·(100 g)$^{-1}$ chitosan; 0.03 to 0.04 for 0.250 g·(100 g)$^{-1}$; 0.07 to 0.10 for 0.750 g·(100 g)$^{-1}$; and 0.15 to 0.19 for 1.000 g·(100 g)$^{-1}$). CI (%) values were reduced as chitosan concentration was increased in the continuous phase of all emulsions (from 63% to 70% for continuous phase containing 0.000 g·(100 g)$^{-1}$ chitosan; 61% to 65% for 0.125 g·(100 g)$^{-1}$; 61% to 65% for 0.250 g·(100 g)$^{-1}$; 51% to 54% for 0.500 g·(100 g)$^{-1}$; 21% to 28% for 0.750 g·(100 g)$^{-1}$; and 0% to 5% for 1.000 g·(100 g)$^{-1}$).

As it can be seen in Figure 5 – B, hydrodynamic average diameters of oil droplets at t = 28 d is showing similar values comparing with those obtained at t = 14 d for all emulsions (from 430 nm to 520 nm for continuous phase containing 0.000 g·(100 g)$^{-1}$ chitosan; 350 nm to 500 nm for 0.125 g·(100 g)$^{-1}$; 340 nm to 500 nm for 0.250 g·(100 g)$^{-1}$; 630 nm to 700 nm for 0.500 g·(100 g)$^{-1}$; 540 nm to 600 nm for 0.750 g·(100 g)$^{-1}$; and 480 nm to 530 nm for 1.000 g·(100 g)$^{-1}$). Similar PDI values of oil droplets distribution can be noticed between O/W emulsions, comparing t = 14 d and t = 28 d, (from 0.02 to 0.03 for continuous phase containing 0.000 g·(100 g)$^{-1}$ chitosan; 0.02 to 0.03 for 0.125 g·(100 g)$^{-1}$; 0.03 to 0.04 for 0.250 g·(100 g)$^{-1}$; 0.04 to 0.10 for 0.500 g·(100 g)$^{-1}$; 0.09 to 0.11 for 0.750 g·(100 g)$^{-1}$; and 0.10 to 0.15 for 1.000 g·(100 g)$^{-1}$). O/W prepared without chitosan or 0.125 g·(100 g)$^{-1}$ and 0.250 g·(100 g)$^{-1}$ chitosan presented similar CI (%) values between t = 14 d and t = 28 d, and this observation is due to the fact that the creaming phenomenon had already reached up an equilibrium state at t = 14 d. CI (%) values for the other O/W emulsions were increased from t = 14 d to t = 28 d (between 54% and 57% for continuous phase containing 0.500 g·(100 g)$^{-1}$ chitosan; 34% and 40% for 0.750 g·(100 g)$^{-1}$; 4% and 10% for 1.000 g·(100 g)$^{-1}$). However, CI (%) values presented the same behavior observed at t = 14 d, *i.e*. there was a reduction in their value according to increase of chitosan concentration in the continuous phase of O/W emulsions. None of the emulsions analysed during t = 28 d showed irreversible phase separation regardless the CI (%) value, which indicates that the increase in average hydrodynamic diameter of oil droplets did not result in the rupture of its interfacial layer.

3.4.2. Destabilization under stress conditions

Destabilization of O/W emulsions was also assessed, when exposed to three stress conditions: *i*) emulsions were frozen and then thawed; *ii*) freeze-thawed emulsions were then heated; and *iii*) emulsions were centrifuged. These systems were analysed in terms of visual appearance (Figure 6) and hydrodynamic average diameter, PDI from hydrodynamic diameter distribution of oil droplets, or CI (%) values of O/W emulsions (Figure 7).

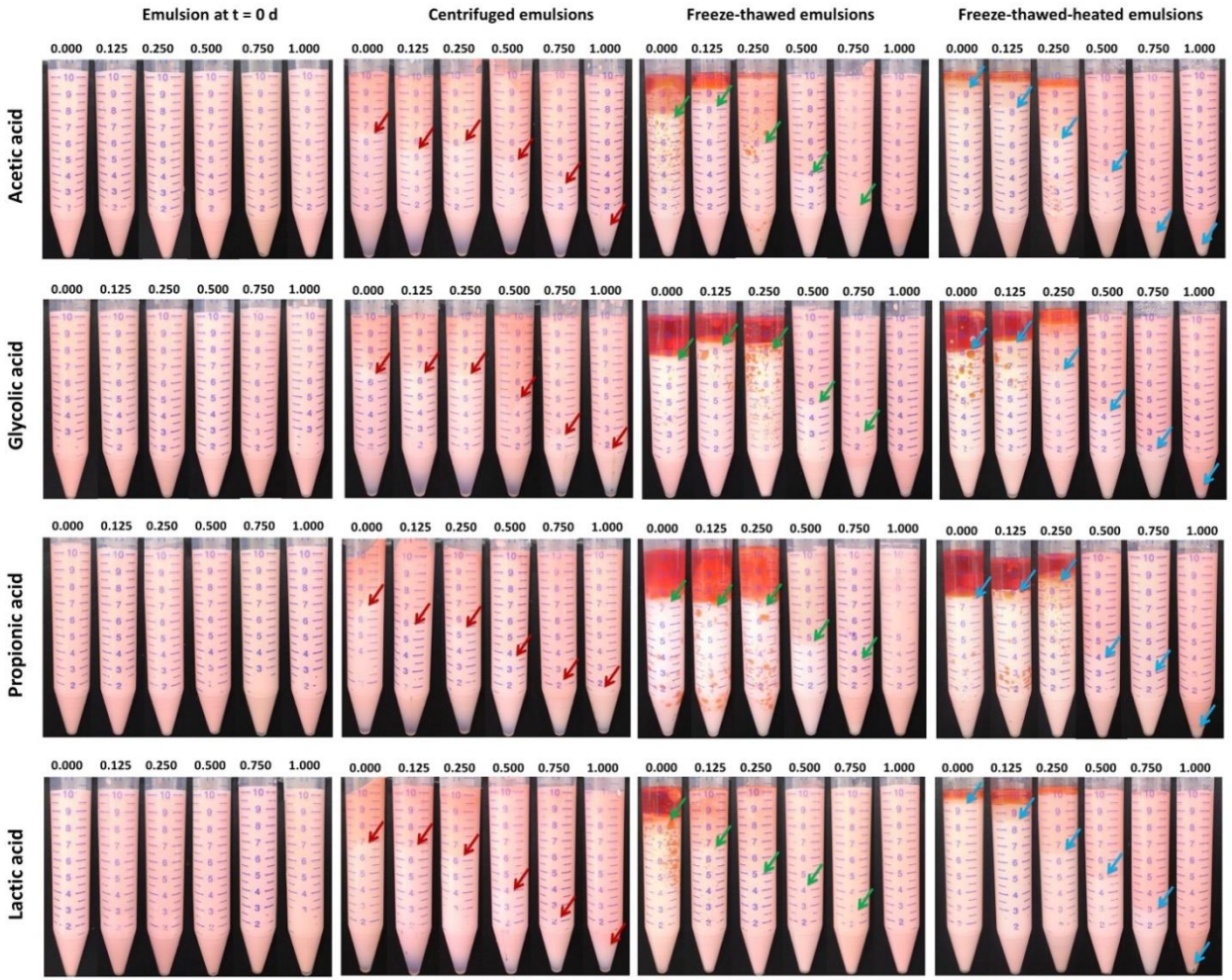

Figure 6 - Visual appearance of O/W emulsions (2nd repetition) at t = 0 d and after: centrifugation, freeze-thawed, and freeze-thawed-heated cycle for systems containing chitosan dispersed in acid continuous phase prepared with acetic, glycolic , propionic or lactic acid.

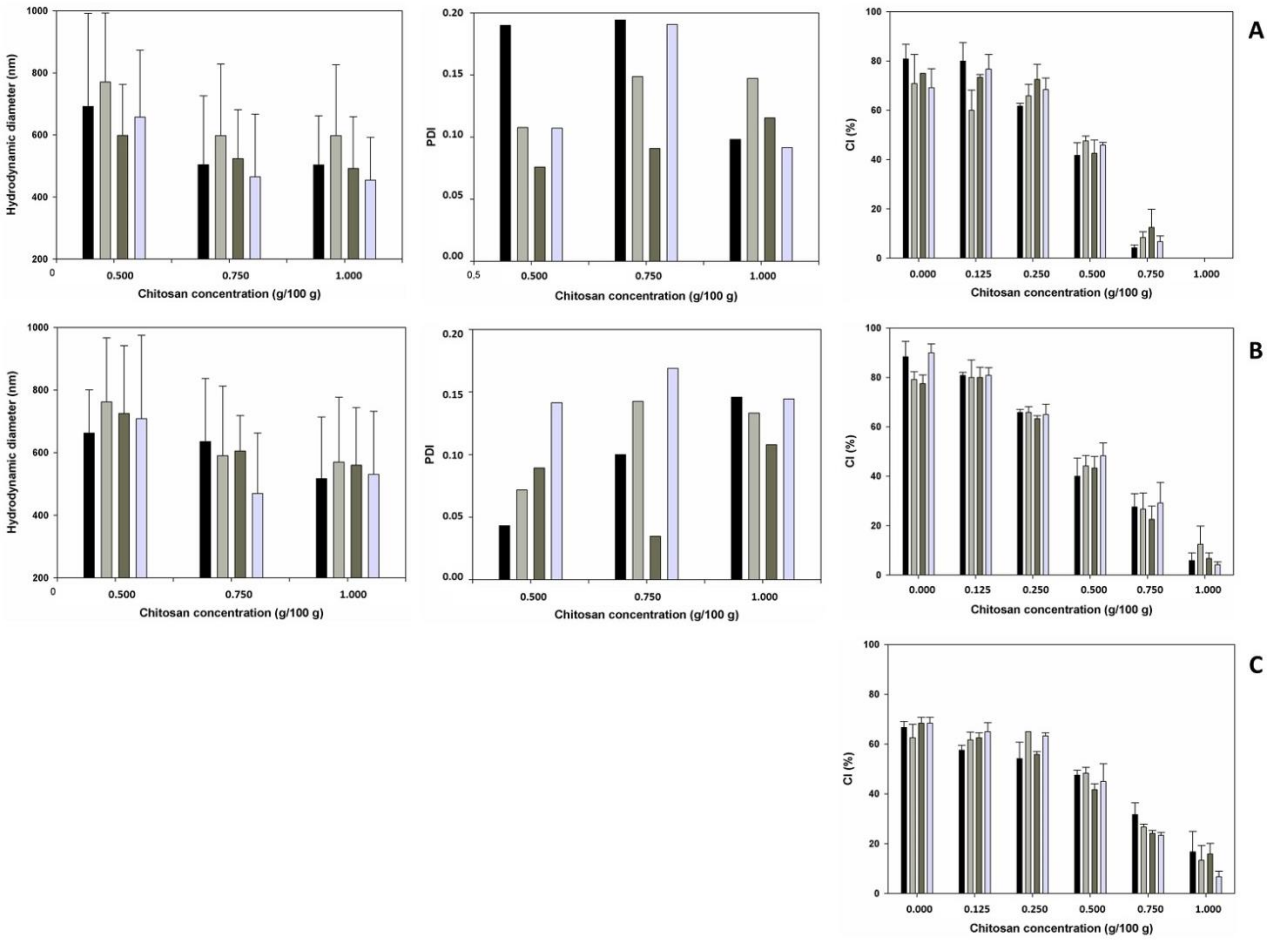

Figure 7 - Hydrodynamic average diameter of oil droplets, PDI from oil droplets hydrodynamic diameter distribution, and CI (%) of O/W emulsions containing different chitosan concentrations in the continuous phase prepared with acetic (▬), glycolic (▭), propionic (▬), or lactic (▭) acid exposed to freeze-thawed cycle (A), freeze-thawed-heated cycle (B), and centrifugation (C). Error bars in Figure 3 (A, B and C) represent the standard deviation.

Hydrodynamic average diameter, PDI from hydrodynamic diameter distribution of oil droplets and CI (%) presented similar values to each chitosan concentration in the continuous phase of O/W emulsions containing acetic, glycolic, propionic or lactic acid, when they were exposed to stress conditions. Emulsions without or containing 0.125 g·(100 g)$^{-1}$, and 0.250 g·(100 g)$^{-1}$ chitosan in the continuous phase presented a phase separation after freeze-thawed and freeze-thawed-heated cycles (Figure S6). As a result, hydrodynamic average diameter values cannot be determined for these O/W emulsions. As illustrated in Figure 7 - A, emulsions exposed to freeze-thawed cycle presented an increase in hydrodynamic average diameters (from 600 nm to 700 nm for continuous phase containing 0.500 g·(100 g)$^{-1}$ chitosan; 464 nm to 598 nm for 0.750 g·(100 g)$^{-1}$; and 504 nm to 597 nm for 1.000 g·(100 g)$^{-1}$), and in PDI values of oil droplets when compared with those at t = 0 d (from 0.08 to 0.19 for continuous phase containing 0.500 g·(100 g)$^{-1}$ chitosan; 0.09 to 0.19 for 0.725 g·(100 g)$^{-1}$; and 0.09 to 0.14 for 1.000 g·(100 g)$^{-1}$). Figure 7 - B, which is related to emulsions that have been freeze-thawed-heated, also show an increase in hydrodynamic average diameters (from 663 nm to 762 nm for continuous phase containing 0.500 g·(100 g)$^{-1}$ chitosan; 470 nm to 635 nm for 0.725 g·(100 g)$^{-1}$; and 517 nm to 570 nm for 1.000 g·(100 g)$^{-1}$), and in PDI values of oil droplets comparing with those at t = 0 d (from 0.04 to 0.14 for continuous phase containing 0.500 g·(100 g)$^{-1}$ chitosan; 0.03 to 0.17 for 0.725 g·(100 g)$^{-1}$; and 0.11 to 0.15 for 1.000 g·(100 g)$^{-1}$), when emulsions were submited to freeze-thawed cycle. These results indicated that destabilization processes in emulsions containing 0.500 g·(100 g)$^{-1}$, 0.750 g·(100 g)$^{-1}$, and 1.000 g·(100 g)$^{-1}$ chitosan in the continuous phase exposed to freeze-thaw and freeze-thaw-heated cycles were accelerated. In addition to phase separation shown by emulsions containing 0.000 g·(100 g)$^{-1}$, 0.125 g·(100 g)$^{-1}$, and 0.250 g·(100 g)$^{-1}$ chitosan, hydrodynamic average diameter and PDI values of emulsions prepared with 0.500 g·(100 g)$^{-1}$ have showed a greater destabilization of oil droplets exposed to both cycles, indicating that the increase in biopolymer concentration can have some effect in the oil droplets maintenance.

CI (%) values of freeze-thawed emulsions were reduced according to increase of chitosan concentration in the continuous phase (from 69% to 81% for continuous phase containing 0.000 g·(100 g)$^{-1}$ chitosan; 60% to 80% for 0.125 g·(100 g)$^{-1}$; 62% to 73% for 0.250 g·(100 g)$^{-1}$; 42% and 48% for 0.500 g·(100 g)$^{-1}$; 4% to 13% for 0.750 g·(100 g)$^{-1}$; and 0% 1.000 g·(100 g)$^{-1}$). Higher CI (%) values were observed (Figure 7 – C) in freeze-thawed-heated emulsions compared to freeze-thawed systems only (from 79% to 90% for continuous phase containing 0.000 g·(100 g)$^{-1}$ chitosan; 80% to 81% for 0.125 g·(100 g)$^{-1}$; 63% to 66% for 0.250 g·(100 g)$^{-1}$; 40% and 48% for 0.500 g·(100 g)$^{-1}$; 23% to 28% for 0.750 g·(100 g)$^{-1}$; and 4% to 13% for 1.000 g·(100 g)$^{-1}$). Summarizing, after being exposed to the stress conditions, CI (%) values observed for freeze-thawed and freeze-thawed-heated O/W emulsions containing 0.000 g·(100 g)$^{-1}$, 0.125 g·(100 g)$^{-1}$, 0.250 g·(100 g)$^{-1}$ chitosan showed phase separation, which is considered the final destabilization event of emulsions since it is irreversible [42].

Hydrodynamic average diameter of oil droplets in O/W emulsions cannot be evaluated after centrifugation due to rough upper layer formation at tubes top, preventing the removal of

the aliquot to be diluted. Thus, centrifuged emulsions were evaluated in terms of CI (%) values, and results are showed in Figure 7 – C. After centrifugation, CI (%) values from O/W emulsions were reduced according to increase of chitosan concentration in the continuous phase (from 63% to 68% for continuous phase containing 0.000 g·(100 g)$^{-1}$ chitosan; 58% to 65% for 0.125 g·(100 g)$^{-1}$; 54% to 65% for 0.250 g·(100 g)$^{-1}$; 42% and 48% for 0.500 g·(100 g)$^{-1}$; 23% to 32% for 0.750 g·(100 g)$^{-1}$; and 7% to 17% for 1.000 g·(100 g)$^{-1}$). These results demonstrate that chitosan acted as a stabilizer, reducing the creaming of emulsions subjected to stress caused by centrifugal force.

4. Discussion

1.000 g·(100 g)$^{-1}$ chitosan added to acidic aqueous media containing acetic, glycolic, propionic or lactic acid (50 mmol·L^{-1}) was fully dispersed when visually assessed, as also occurred with diluted chitosan dispersions (from 0.125 to 0.750 g·(100 g)$^{-1}$). Then, O/W emulsions were produced using chitosan dispersions and Tween 20 as the continuous phase by an ultrasonic homogenizer.

Hydrodynamic average diameters of oil droplets were increased accordingly as chitosan concentration was raised at t = 0 d, and this observation can be related to the efficiency of ultrasonic waves in the different systems. As it was expected, the increase in chitosan concentration in the continuous phase favored the thickening of the systems, which could decrease the propagation of ultrasonic waves and reduce their efficiency to form smaller droplets. Apart from the increase in average diameters at t = 0 d, PDI values obtained from hydrodynamic diameter distribution of oil droplets for emulsion containing 0.000 to 0.500 g·(100 g)$^{-1}$ were ≤ 0.05 pointing out a considerable uniformity of diameters within the distribution [89]. Emulsions containing 0.750 to 1.000 g·(100 g)$^{-1}$ chitosan presented higher PDI values (≤ 0.15), indicating that the increase of chitosan concentration promoted a higher range of oil droplets diameters. Texture and kinetic stability of emulsion are highly influenced by the droplet size distribution, and its evaluation and control are important [42,90]. However, the production of monodispersed emulsions with small droplet size is very difficult, even if an adequate amount of energy and emulsifiers are added to the systems [74]. Results of the present study and the Klinkesorn & Namatsila [51] or Kaasgaard & Keller [52] showed that chitosan addition caused an increase in oil droplets diameters, which could be attributed to a biopolymer layer formed around the oil droplets. In this case, chitosan concentration could influence the layer thickness until a threshold concentration in which its diffusion from emulsion bulk to interfacial region is not energetically favorable anymore. Moreover, hydrodynamic average diameters of oil droplets from different emulsions presented in this study were also similar to those showed by Klinkesorn & Namatsila [51] and Kaasgaard & Keller [52], who used high pressure in the emulsification process. These results demonstrated the efficiency of ultrasonic homogenization when compared to high pressure process for emulsions production, since the ultrasonic waves could promote the oil droplets dispersion in aqueous media with different consistencies.

ζ potential values of oil droplets in O/W emulsions without chitosan or containing 0.125, 0.250 and 0.500 g·(100 g)$^{-1}$ chitosan in their continuous phase were -5.0 mV < ζ potential values < +5.0 mV, which is considered electrostatically neutral. However, oil droplets of emulsions prepared with a continuous phase containing 0.750 g·(100 g)$^{-1}$ and 1.000 g·(100 g)$^{-1}$ chitosan presented low ζ potential values (< +10.0 mV). There was an increase in ζ potential values of oil droplets as chitosan concentration was raised. This trend was also observed in the studies performed by Kaasgaard & Keller (- 55.0 mV for 0.00 g·(100 g)$^{-1}$ up to + 55.0 mV for 1.00 g·(100 g)$^{-1}$) [52], and Klinkesorn & Namatsila (- 13.0 mV for 0.0 g·(100 g)$^{-1}$ up to + 10.0 mV for 10.0 g·(100 g)$^{-1}$) [51]. The increase of positive ζ potential values are related to raise in the density of positive charges, which suggests attractive intermolecular interactions between protonated chitosan chains and the O/W interface covered with Tween 80 [13,38,51]. Moreover, the adsorption of chitosan chains on the O/W interface covered with Tween 80 emulsifier was proven for emulsions containing between 1.0 and 10.0 g·(100 g)$^{-1}$ chitosan by confocal microscopy [51]. An increase in electrostatic repulsion among the oil droplets was expected, since there was a raise on their electric charge [42]. However, our results suggested that electrical charge density at interfaces was not sufficient to cause droplet stabilization by electrostatic mechanisms, since emulsions containing chitosan presented aggregates in their microstructure. In this case, bridging flocculation could have contributed to oil droplets with chitosan aggregation. Klinkesorn & Namatsila [51] also observed aggregates in emulsions containing ≥ 4.0 g·(100 g)$^{-1}$ chitosan in their continuous phase, indicating that the aggregation phenomenon between droplets and chitosan chains is dependent on the concentration of chitosan and the type of acid solvent used to disperse it.

Under process conditions (500 W, 20 kHz, 4 min), after their preparation the emulsions showed a homogeneous aspect, when assessed macroscopically/visually. Then, the systems were evaluated by visually monitoring the development of an upper phase, in order to quantify the extension of oil creaming. O/W emulsions without chitosan or containing 0.125 and 0.250 g·(100 g)$^{-1}$ chitosan in the continuous phase showed a rapid destabilization, that reached an equilibrium of CI (%) values at ≤ 96 h. However, the destabilization that became visible later could have happened microscopically even right after the moment of its preparation, and might have caused variability in the values of consistency and behavior index obtained by the flow curves. Moreover, *K* values were increased as chitosan was raised in O/W emulsions from 0.500 to 1.000 g·(100 g)$^{-1}$. Regarding the frequency sweeps, all emulsions analysed were more elastic than viscous (*G'* ≥ *G''*), and this observation might be related to the ultrasonic homogenization performance in the production of small oil droplets [42]. Both parameters *G'* and *G''* were increased as chitosan concentration was increased, and O/W emulsions containing 1.000 g·(100 g)$^{-1}$ chitosan showed *G'* and *G''* values almost ten times higher than those prepared without chitosan. Observations about the increase in *K*, *G'*, and *G''* values indicate that chitosan can improve emulsions structuration, reducing the frequency and intensity of collisions between oil droplets in Brownian motion and, consequently, improving the kinetic stability [91].

Results discussed up to this point refer to the characterization of emulsions at t = 0 d. These emulsions were prepared with six chitosan concentrations, previously dispersed in organic acid solutions (acetic, glycolic, propionic or lactic acid). Expressive differences were not seen for emulsions containing these acids used to chitosan dispersion, at a given concentration of the biopolymer. Aqueous media containing glycolic, propionic or lactic acids were suitable to replace acetic acid to prepare chitosan dispersions. Thus, emulsions containing chitosan dispersions in acids other than acetic in the continuous phase can be prepared for cosmetic and/or food applications. Chitosan acted as a thickener agent, since biopolymer chains interacted with water molecules (dipole-dipole, hydrogen bonds and/or ion-dipole interactions, for instance) in acid aqueous media, altering emulsions rheological properties. The existence of intermolecular interactions between protonated chitosan chains and the O/W interface covered with Tween 20 could explain the increase of hydrodynamic average diameter and ζ potential of droplets. Then, the electrostatic and/or steric repulsion among droplets could be favored, improving the kinetic stability of emulsions. So far, attention has been given to demonstrate chitosan influence on the oil droplets formation and as a thickener for emulsions. The sections ahead will highlight the chitosan as a potential stabilizer.

Hydrodynamic average diameters of oil droplets were increased at t = 28 d comparing to t = 0 d for all emulsions, but none of them showed visually phase separation. On the other hand, PDI presented similar values at the same time interval, indicating a good kinetic stability of the oil droplets formed. An increase in average hydrodynamic diameters and/or PDI values of oil droplets is related to the existence of some destabilization processes, which will not necessarily lead to phase separation at a short time interval [92]. Similar behavior was observed for emulsions analysed at a fifteen-day storage period by Kaasgaard & Keller [52], who reported oil droplets diameters of 100 nm (without chitosan) and 450 nm (with 0.15 to 1.00 g·(100 g)$^{-1}$). These results show the same values of oil droplets diameters for emulsions without chitosan, while there was an increase in those containing the biopolymer. As previously mentioned, emulsions containing ≤ 0.250 g·(100 g)$^{-1}$ chitosan reached up the creaming equilibrium at t ≤ 96 h. In this case, 0.125 and 0.250 g·(100 g)$^{-1}$ chitosan added to the continuous phase have neither influenced the small droplets formation during emulsification process nor contributed to the increase in the kinetic stability of the emulsions when compared to emulsions without chitosan. As chitosan concentration was raised from 0.500 to 1.000 g·(100 g)$^{-1}$, it was noticeable that there was a reduction in CI (%) as a function of time, and in CI (%) at t = 28 d. However, emulsions prepared with 0.750 g·(100 g)$^{-1}$ did not seem to have achieved the equilibrium in CI (%) after 672 h, and were considered as more kinetically stable emulsions. Klinkesorn & Namatsila [51] also observed a reduction in the creaming index (from 90% to 0%) as chitosan concentration was increased (0.0 to 10.0 g·(100 g)$^{-1}$) for emulsions stored during 172 h. These results are similar to those observed in the present study, *i.e*. emulsions containing 1.000 g·(100 g)$^{-1}$ showed no creaming at t = 172 h. These findings demonstrate that chitosan acted as a stabilizing agent and that its performance was dependent on the concentration added into the emulsions.

Emulsions were exposed to environmental stresses, in order to simulate adverse conditions to their kinetic stability. Centrifugation cycles aimed to accelerate emulsions destabilization, which would naturally occur by the gravitational force. Freeze-thawed and/or freeze-thaw-heated cycles intended to change the temperature systems abruptly, simulating a hypothetical situation that emulsified systems would undergo during storage and transport. Regarding the emulsions exposed to stress conditions, CI (%) values for O/W emulsions were reduced accordingly as chitosan concentration increased (from 63%-68% to 7%-17%), but none of them showed phase separation. CI (%) values after centrifugation were similar to those observed at t = 28 d to each chitosan concentration present in the continuous phase of O/W emulsions. In this case, the centrifugation cycle accelerated the creaming destabilization process, which would naturally occur under the action of gravitational force. Emulsions containing 0.000, 0.125 and 0.250 $g \cdot (100\ g)^{-1}$ chitosan in the continuous phase presented a phase separation after freeze-thawed and freeze-thawed-heated cycles, which also indicated that 0.125 and 0.250 $g \cdot (100\ g)^{-1}$ chitosan added to continuous phase did not affect their stability compared to those without chitosan. O/W emulsion containing 0.500 $g \cdot (100\ g)^{-1}$, 0.750 $g \cdot (100\ g)^{-1}$, and 1.000 $g \cdot (100\ g)^{-1}$ chitosan exposed to freeze-thawed and freeze-thawed-heating cycles presented an increase in hydrodynamic average diameter and PDI of oil droplets values comparing with those values at t = 0; however, they did not present phase separation. Moreover, CI (%) values of freeze-thawed and freeze-thawed-heated emulsions were reduced according to increase of chitosan concentration in the continuous phase. As it is expected, oil droplets were freeze-thawed before the continuous aqueous phase, causing the solid oil droplets to be excluded from the space taken up by the ice. As a result, the droplets are forced to pack with one another during thaw cycle [93]. Consequently, destabilization is expected due to the formation of aggregated droplets that coalesce, suggesting that freezing conditions cause the rupture of O/W interface covered with Tween 20 [93,94]. Chitosan chains interacting with Tween 20 molecules on the O/W interface preclude previously-formed freeze oil droplets coalescence during thawing, and this behavior was chitosan concentration-dependent. In regards to systems that have been heated upon freeze-thaw, the increase in emulsions temperature to values about 100 ^{o}C could have caused the phase separation due to the attainment of the cloud point of Tween 20, which is around 76 ^{o}C, according to Sigma Aldrich [95,96]. Cloud point can be defined as the temperature that promotes a dehydration of the head group of a nonionic surfactant molecule, causing the surfactant insolubility and carrying on to phase separation [97]. In this case, chitosan layer around oil droplets could have attenuated the Tween 20 emulsifier insolubility and reduced the coalescence, foreclosing the phase separation. In addition to the thickening effect in the continuous phase, the aggregation between oil droplets and chitosan could also have contributed to increase the kinetic stability and to reduce destabilization caused by environmental stress in the emulsions. Chitosan did not preclude destabilizing mechanisms, since the hydrodynamic diameters of the oil droplets were increased after freeze-thawed and freeze-thawed-heating cycles. These observations indicate that the stabilizer action of chitosan and its performance was dependent on the concentration, since

emulsions containing 0.500 to 1.000 g·(100 g)$^{-1}$ showed a greater thickening effect, which contributed to prevent the phase separation phenomenon.

5. Conclusions

O/W emulsions were produced using chitosan dispersions and Tween 20 as the continuous phase by an ultrasonic homogenizer. Small oil droplets (< 600 nm) were observed at t = 0 d, which highlighted: *i*) the efficiency of ultrasonic waves to promote the oil droplets disruption in emulsions with different textures; and *ii*) the role of the emulsifier to form the interfacial area. Emulsions containing > 0.500 g·(100 g)$^{-1}$ chitosan presented a lower increase in hydrodynamic average diameter and PDI of oil droplets between t = 0 d and t = 28 d, and showed no phase separation when exposed to centrifugation, freeze-thawing, and freeze-thaw-heating cycles, which indicated the stabilizer action of this biopolymer. Furthermore, the increase in chitosan concentration promoted the augment in consistency indexes and storage moduli of emulsions, demostrating its thickening action. Thus, chitosan may be considered as a potential thickener/stabilizer agent for emulsions, when added in concentrations ≥ 0.500 g·(100 g)$^{-1}$. Furthermore, aqueous media containing glycolic, propionic or lactic acids were suitable to replace acetic acid to prepare chitosan dispersions, considering future industrial applications for this biopolymer.

Capítulo IV

Partial replacement of gelling agents by chitosan: impact on the color, viscoelastic properties, and release of Yellow sunset (INS 110) from carrageenan or starch hydrogels

Abbreviations and symbols

a	first constant of Mark-Houwink-Sakurada relationship (dimensionless)
A_{1320}	normalized absorbance of the peak at wavenumbers 1320 cm^{-1}
A_{1420}	normalized absorbance of the peak at wavenumbers 1420 cm^{-1}
a^*	position between red and green in the CIELab coordinates
b^*	position between Yellow and blue in the CIELab coordinates
C	Yellow sunset (INS 110) concentration ($g\cdot(100\ g)^{-1}$)
C_{Real}	Yellow sunset (INS 110) corrected concentration ($g\cdot(100\ g)^{-1}$)
C_{Total}	Yellow sunset (INS 110) total concentration ($g\cdot(100\ g)^{-1}$)
DA	degree of acetylation (%)
DD	degree of deacetylation (%)
G'	storage modulus (Pa)
G''	loss modulus (Pa)
k	release constant for Yellow sunset (INS 110)
K_{MHS}	second constant of Mark-Houwink-Sakurada relationship (dimensionless)
J	compliance or strain per stress unit in creep-recovery tests (Pa^{-1})
J_0	instantaneous elastic term in creep-recovery tests (Pa^{-1})
J_1	retarded elastic term in creep-recovery tests (Pa^{-1})
MAPE	mean absolute percentage error
n	exponent of release for INS 110 (dimensionless)
R	release of Yellow sunset (INS 110) (%)
R^2	coefficient of determination
t	time (s)
tan δ	tangent of the phase shift (º)
V_E	existing volume in the tube at each time of the diffusivity experiment (mL)
V_T	total solution volume in the tube at the beginning of the diffusivity experiment (mL)
Y_i	the i^{th} experimental score applying the adjusted model
$\hat{Y}_i$	the i^{th} score predicted applying the adjusted model
γ	strain in creep-recovery tests (%)
λ_{ret}	retardation time (s)
μ_0	viscous modulus associated with Newtonian viscosity in creep-recovery test (Pa)
τ_0	decaying stress after the time in stress-relaxation tests (Pa)
τ_{eq}	equilibrium stress in stress-relaxation tests (Pa)
$\bar{M}_V$	viscometric-average molar mass (kDa)
$[\bar{\eta}]$	average intrinsic viscosity ($dL\cdot g^{-1}$)

Abstract

The mixture of biopolymers appears as a strategy to improve techno-functional properties of gels, and the combination of chitosan with other food-grade polysaccharides seems to be an attractive alternative for this purpose. In this study, appearance, color and rheological properties of carrageenan (1.5 $g\cdot(100\ mL)^{-1}$) or starch (10.0 $g\cdot(100\ mL)^{-1}$) hydrogels partially replaced by 5.0%, 7.5% or 10.0% (w/v) chitosan, containing 0.02 $g\cdot(100\ mL)^{-1}$ Yellow sunset (INS 110), were analysed. Additionally, the release of INS 110 from hydrogels to sucrose solution (20.0 $g\cdot(100\ mL)^{-1}$) was evaluated. Hydrogels without or with a partial replacement of carrageenan or starch by chitosan have neither showed significant differences for color parameters nor expressive changes for viscoelastic properties, according to transient tests and frequency sweeps (< 5 Hz). All carrageenan hydrogels presented similar release of INS 110 (about 40%), while hydrogels with a partial replacement of starch by chitosan presented lower INS 110

release (5%, 8%, and 15% for 5.0%. 7.5% and 10.0% w/v, respectively), after 316 h. Thus, our findings pointed out that the replecement of starch by chitosan did not promote major changes on color and viscoelastic characteristics of hydrogels, but altered drastically the INS 110 release to an aqueous phase. Therefore, the replacement of gelling agents by chitosan has demonstrated to be a potential strategy to reduce INS 110 release from starch hydrogels, in which this biopolymer may act simultaneously as a biofunctional and a technico-functional agent.

1. Introduction

Gelation phenomena occur when macromolecules are induced to interact among themselves, and form a tridimensional solid network containing a liquid phase in their interstices [98]. Biomolecules (often proteins and/or polysaccharides) dispersed in aqueous media can be used to produce “hydrogels”, since they will establish either chemical (disulfide bonds) or physical interactions (hydrogen bonds, electrostatic interactions, and hydrophobic interactions, for instance) to create junction zones, in order to hold water molecules inside them [55,99]. Jellies, dairy desserts, yogurts, and processed meat products are some examples of foods with a gel-like structure. Gels play an important role in sensory attributes of foods, modulating texture, color and flavor of the products [100]. Macroscopically, gels are materials that partially recover from physical deformations caused by mechanical stresses. Thus, gels present mechanic characteristics of solids (a partially elastic character) and fluids (a partially viscous character), and frequently are referred as soft semisolid or viscoelastic materials [101].

Beyond their appreciated sensory/texture properties, another essential function of gelled food formulations is to retain or to progressively release vitamins and food additives, at low rates. Food dyes present a particular importance among food additives, since the sensory attribute “color” often indicates the products quality and exerts a great impact on consumers purchase decision [102–104]. Hence, the release or the diffusion of colorants from the gelled matrix to the contacting fluid (a pudding with sugar syrup, for instance) may be undesirable, being accelerated if adequate formulation and/or storage strategies are not adopted. Such strategies should enhance, or at least keep rheological characteristics in food products. Some approaches for this purpose have been proposed in food structure engineering, including the use of protein-polysaccharide complexes [105], protein fibrils or nanorods [47], structurally modified polysaccharides [106], or still the combination of polysaccharides [107].

Hydrogels containing a combination of polysaccharides in their formulation have been reported by some authors. These studies have proposed to evaluate the techno-functionalities of materials, besides their physical characterization (viscoelastic properties, color, swellling, and others). For instance, Thompson et al. (2017) studied rheological and thermal properties of agar (1.0% or 2.0% w/v) and methylcellulose (1.0% or 2.0% w/v) gels, when compared to a mixture between these gelling agents (1.0% (w/v) agar: 1.0% (w/v) methylcellulose). Storage modulus (*G'*) of agar-methylcellulose hydrogel showed a constant behavior ($7.0 \cdot 10^3$ Pa) between 25 ^{o}C

and 85 °C, while *G'* presented an increase in methylcellulose gels ($7{,}0 \cdot 10^0$ Pa to $6.5 \cdot 10^3$ Pa in 1.0% (w/v); $10.0 \cdot 10^0$ Pa to $10.0 \cdot 10^3$ Pa in 2.0% (w/v)) and a decrease in agar gels ($6.0 \cdot 10^3$ Pa to $10.0 \cdot 10^0$ Pa in 1.0% (w/v); $13.0 \cdot 10^3$ Pa to $12.0 \cdot 10^0$ Pa in 2.0% (w/v)), as a function of temperature. Therefore, agar-methylcellulose hydrogel showed an elastic component stable at temperatures from 25 °C to 85 °C, which did not occur with agar or methylcellulose gels [66]. Zhu, Sheng & Tong (2015) analyzed the effect of adding pullulan (PU) in carboxymethyl (CMGe) films, containing 4.0% (w/v) polysaccharide (1:0; 0.75:0.25; 0.5:0.5; and 0:25:0.75 to CMGe:PU ratio). The addition of PU to CMGe decreased values of water vapor permeability ($2.64 \cdot 10^{-6} \cdot (g \cdot m \cdot Pa^{-1} \cdot h^{-1} \cdot m^{-2})$; $1.56 \cdot 10^{-6} \cdot (g \cdot m \cdot Pa^{-1} \cdot h^{-1} \cdot m^{-2})$; $1.37 \cdot 10^{-6} \cdot (g \cdot m \cdot Pa^{-1} \cdot h^{-1} \cdot m^{-2})$, and $1.36 \cdot 10^{-6} \cdot (g \cdot m \cdot Pa^{-1} \cdot h^{-1} \cdot m^{-2})$ respectively to 1:0; 0.75:0.25; 0.5:0.5; and 0:25:0.75 CMGe:PU ratio) leading to an improvement of barrier properties of the films [108]. These last two works exemplify how the mixture of different polysaccharides can be used as a strategy to prepare materials with a techno-functional performance superior than those prepared with the biopolymers separately.

In this context, traditional gelling agents combined with chitosan could be used in food applications to make gel-based products with different techno-functionalities. The polysaccharide known as chitosan is an N-deacetylate derivate of chitin [poly-β-(1→4)-N-acetyl-D-glucosamine], which is the second most abundant natural biopolymer obtained from exoskeletons of crustaceans and also from cell walls of fungi [76]. The monomer of each deacetylated unit (glucosamine) presents an amino group (NH_2), conferring differentiated physicochemical properties to chitosan dispersed in acidic aqueous media [1]. Chitosan has been used in several biotechnological studies, since it is a biofunctional, biocompatible, biodegradable, and non-toxic biopolymer [17,23]. Furthermore, studies have been reporting that the daily intake of chitosan by humans (with doses varying from 3 g to 6 g) can promote its hypolipidemic activity. Then, chitosan added to gel-based foods could play a techno-functional and a biofunctional role, simultaneously.

In this paper, appearance, color, and rheological properties of carrageenan or starch hydrogels with partial replacement by chitosan were analysed. Moreover, the colorant Yellow sunset (INS 110) was added to the dispersed phases of carrageenan/chitosan or starch/chitosan hydrogels, in order to evaluate the release of the additive from these materials towards a sucrose aqueous solution. Results of this study aims to verify if the combination of chitosan with other gelling polysaccharides may be useful to modulate rheological and release properties of hydrogels.

2. Materials and methods

2.1. Materials

Chitosan (Medium Molecular Weight, Sigma-Aldrich Corporation, USA; Product ID = 448877; Batch number = #LBG4282V) from fresh shrimp shells *Pandalus borealis* was used in all the experiments. Before use, chitosan was washed three times with deionized water,

according to procedure described elsewhere [39]. This procedure aims to reduce water-soluble chitooligosaccharides content and salts residues. Washed chitosan was recovered using a vacuum filtration system, and qualitative paper (Cat No 1004 125, Whatman). Then, the remaining solid chitosan was frozen, lyophilized (Terroni, LS 3000, Brazil), and stored at 7 ± 2 °C (Consul, Pratice 410, Brazil) prior to further use. Carrageenan (Sigma-Aldrich Corporation, USA; predominantly κ carrageenan and lesser amounts of λ carrageenan), soluble starch (Vetec, Brazil), lactic acid (Impex Quimica, Spain; purity = 85%), sucrose (Vetec, Brazil), and Yellow sunset (INS 110) (Sigma-Aldrich Corporation, USA; purity = 90%) were analytical grade reagents, used as bought, without further purification. Deionized water (QUV3, Millipore, Italy; electrical resistivity ≅ 18.2 MΩ·cm^{-1}, at 25 ^{o}C) was used in all experiments.

2.1.1. Chitosan characterization

Chitosan degree of deacetylation (*DD*) was estimated by applying FT-IR spectroscopy approach [82,83]. FT-IR analyses were carried out directly on the chitosan powder using a spectrophotometer (600-IR, Varian, USA) equipped with an attenuated reflectance accessory (GladiATR, PIKE Technologies, USA), over the region of 450 - 3750 cm^{-1}, at an interval of 1.93 cm^{-1}. Acquired transmittance values (%) were converted to absorbance values (%), and normalized relatively to the highest corrected absorbance, and two regions (450 - 1850 cm^{-1} and 1850 - 3750 cm^{-1}) were created. Absorbances of peaks present in each region were calculated through deconvolution in Lorentzian components by PeakFit (v. 4.12, SeaSolve Software Inc., 1999-2003). Firstly, degree of acetylation (*DA*) was estimated using the empirical relationship between normalized absorbances of the peaks at wavenumbers 1320 and 1420 cm^{-1}, as presented in Equation 1 [82,83]. Then, *DD* was obtained by difference [DD(%) = 100% - DA(%)].

$$\mathrm{DA}(\%) = \frac{\left(\frac{A_{1320}}{A_{1420}} - 0.3822\right)}{0.03133} \quad (1)$$

In Eq. (1), A_{1320} and A_{1420} are the normalized absorbances of the peaks at wavenumbers 1320 cm^{-1} and 1420 cm^{-1}, respectively.

Chitosan presented *DD* = 74.4% (for details, see Supplementary Material), and this value is somehow inferior to that informed by the manufacturer (81.0%). The difference between the value obtained and the reported value may be related to elimination of water-soluble chitooligosaccharides (chitosan molecules with degrees of polymerization ≤ 20 and with *DD* usually ≥ 95.0%), during chitosan washing.

Viscometric average molar mass ($\bar{M}_V$) of chitosan also was estimated following an already standardized procedure [39,84,88]. Chitosan [0.05, 0.10, 0.15, 0.20, and 0.25 g·(100 g)$^{-1}$] was dispersed in acetic acid-sodium acetate buffer (0.2 mol L^{-1} acetic acid and 0.1 mol L^{-1} sodium acetate; pH = 4.41; and ionic strength = 0.1 mol L^{-1}) [12,84]. Flow times of each dispersion were measured in a Cannon-Fenske viscometer (model 513 10, Schott, Germany). From flow times data, average intrinsic viscosity ($[\bar{\eta}]$) was calculated, and viscometric-average molar mass ($\bar{M}_V$) could be estimated by the Mark-Houwink-Sakurada (MHS) relationship [84].

$$[\bar{\eta}] = K_{MHS} \cdot \bar{M}_V{}^{a} \quad (2)$$

In Eq. (2), *a* and K_{MHS} are the constants of MHS relationship.

Intrinsic viscosity of chitosan was estimated as $[\bar{\eta}]$ = 8.91 dL·g^{-1}, from the simple average between $[\eta]_H$ = 8.90 dL·g^{-1} and $[\eta]_K$ = 8.91 dL·g^{-1}. The constants *a* = 0.93 and K_{MHS} = 3.6·10^{-5} dL·g^{-1} of MHS relationship (Equation 2) were obtained according to the procedure described by Kasaai (2007) [84]. Then, viscometric-average molar mass ($\bar{M}_V$) of chitosan was estimated $\bar{M}_V$ = 640 ± 10 kDa, and its value is in accordance with the specification of chitosan molecular mass presented by Sigma-Aldrich [4].

2.2. Experimental design

Carrageenan or starch hydrogels were prepared, without or with a partial replacement of gelling agent by chitosan, as summarized in Table 1. All systems were replicated three times, and all measurements results were presented as average ± standard deviation.

Table 1 - Composition of carrageenan or starch hydrogels, without or with a partial replacement of gelling agent by 5.0%, 7.5% or 10.0% (w/v) chitosan

Carrageenan hydrogels	Carrageenan g·(100 mL)$^{-1}$	Chitosan g·(100 mL)$^{-1}$	Total g·(100 mL)$^{-1}$
100.0% carrageenan	1.50	0.00	1.50
95.0% carrageenan + 5.0% chitosan	1.43	0.08	1.50
92.5% carrageenan + 7.5% chitosan	1.39	0.11	1.50
90.0% carrageenan + 10.0% chitosan	1.35	0.15	1.50
Starch hydrogels	**Starch g·(100 mL)$^{-1}$**	**Chitosan g·(100 mL)$^{-1}$**	**Total g·(100 mL)$^{-1}$**
100.0% starch	10.00	0.00	10.00
95.0% starch + 5.0% chitosan	9.50	0.50	10.00
92.5% starch + 7.5% chitosan	9.25	0.75	10.00
90.0% starch + 10.0% chitosan	9.00	1.00	10.00

*The polysaccharides concentration used to prepare hydrogels were in accordance with that riquered by the biopolymers to perform their techno-functional action.

2.3. Preparation of polysaccharides dispersions and hydrogels

Firstly, a 50 mmol·L^{-1} lactic acid solution was prepared, colored with 0.02 g·(100 mL)$^{-1}$ Yellow sunset (INS 100). Next, 2.5 g·(100 mL)$^{-1}$ of chitosan was dispersed in this colored acidic solution, which was then kept under stirring in a thermostatic bath (TE-184, Tecnal, Brazil) at 25.0 ± 0.1 ^{o}C, during 24 h [12,38]. According to Table 1, carrageenan or starch powder were added to INS 110 acidic solution. Then, adequate amounts of polysaccharides dispersions were mixed during 1 min (DI25 Basic, Yellow Line, Germany), and heated up to 90 ^{o}C ± 1.0 ^{o}C using a heating plate for 3 min (TE-0851, Tecnal, Brazil). Finally, polysaccharides dispersion was

placed in centrifuge tubes (50 mL; 30 mm internal diameter and 115 mm height), and placed at 7.0 ± 1.0 °C (BOD SP500, SPlabor, Brazil) during 24 h.

2.4. Hydrogels characterization

2.4.1. Visual and colorimetric analyses

Hydrogels were visually examined and photographed, after 24 h of their preparation. Instrumental color analyses of hydrogles placed in Petri plates (49 mm internal diameter and 12 mm height) were performed based on CIE-Lab system (ColorQuest XE, HunterLab, USA). Results were presented in terms of *L*a*b** color coordinates. Positive values for *a** indicate a predominant reddish color component, while negative values a greenish color component; positive values for *b** a yellowish color component, and negative values indicate a blueish color component; and *L** = 0 indicate total opacity, while *L** = 100 maximum brightness [109].

2.4.2. Rheological analyses

Rheological measurements were performed using a rotational rheometer (DHR-1, TA Instruments, USA), equipped with a stainless steel plate-plate geometry sensor (diameter = 25 mm; gap = 10 mm), at 25.0 ± 0.1 °C. Hydrogels were removed from centrifuge tubes, and slices of 10 mm thickness were carefully cut using a stainless steel blade, and placed into plate-plate geometry, in order to proceed to transient and dynamic-oscillatory analyses.

Creep-recovery assays were performed by applying an instantaneous shear stress of 10 Pa (τ_0) on the hydrogel for 180 s (creep time), and were monitored for additional 180 s (recovery time). The Burgers' model expressed in terms of compliance (Equation 3) was fitted to the creep data (details about Burgers' model were presented in the SM).

$$J = J_0 + J_1\left[1 - \exp\left(\frac{-t}{\lambda_{ret}}\right)\right] + \frac{t}{\mu_0} \quad (3)$$

In Eq (3), J is the compliance $\left(\frac{\gamma(t)}{\tau_0}\right)$ or strain per stress unit, J_0 is the instantaneous elastic term, J_1 is the retarded elastic term, λ_{ret} is the retardation time, and μ_0 is the viscous term associated to newtonian viscosity.

In stress-relaxation assays, hydrogels were compressed so that a final axial deformation of 1.25% was reached. The stress required to maintain this deformation was recorded during 400 s. Then, the Maxwell's model (Equation 4) was fitted to relaxation curves.

$$\tau = \tau_0 \cdot \exp\left(\frac{-t}{\lambda_{ret}}\right) + \tau_{eq} \quad (4)$$

In Eq. (4) τ_0 is the decaying stress after the time (t), τ_{eq} is the equilibrium stress, and λ_{ret} is the retardation time.

For dynamic oscillatory assays, the linear viscoelastic range of the hydrogels was determined by initially performing a strain sweep (0.1 to 10%) at a constant frequency (1.59 Hz). Then, frequency sweeps were carried out from 0.1 to 50 Hz (at frequencies > 50 Hz materials became unsustainable) at constant strain amplitude = 0.125%, as determined by the linear viscoelastic range. Storage modulus (*G'*), loss modulus (*G''*), and tan δ were continuously recorded as a function of frequency.

2.4.3. Release of Yellow sunset (INS 110)

Hydrogels (20 mL) were formed in conical centrifuge tubes (50 mL), covered with 25 mL of a 20 g·(100 mL)$^{-1}$ sucrose solution, and stored at 7.0 ± 1.0 °C. Aliquots of this sucrose solution (400 µL) were periodically taken (0, 1, 2, 4, 8, 12, 24, 48, 72, 96, 120, 144, 168, 192, 216, 240, 264, and 312 h), and placed in a multiwall plate. UV absorbances of all solutions were measured using a plate reader (Biochrom Asys Expert Plus, Biochrom, United Kingdom), at 480 nm [110]. Then, Yellow sunset (INS 110) concentration could be determined (details were presented in the Supplementary Material). The real concentration was corrected to the existing volume of solution in each time (Equation 5), and the percentage of Yellow sunset released from hydrogels was calculated (Equation 6).

$$C_{Real} = \frac{V_T \cdot C}{V_E} \quad (5)$$

$$R\ (\%) = \frac{C_{Real}}{C_{Total}} \cdot 100\% \quad (6)$$

In Eq. (5) and (6), C_{Real} is the Yellow sunset (INS 110) corrected concentration, C is the INS 110 estimated concentration, V_T is the total solution volume in the tube (at the beginning of experiment), V_E is the existing volume in the tube at each time of the experiment, *R (%)* is the percentage INS 110 released, and C_{Total} is the total concentration of INS 110 within the hydrogels (at the beginning of the experiment).

The empirical Korsmeyer-Peppas's model [111–113] was adjusted to *R (%)* of INS 110 from hydrogels as a function of time, assuming a time-dependent Power law function (Equation 7).

$$R\ (\%) = k \cdot t^n \quad (7)$$

In Eq. (7), k is the constant of release that incorporates the structural/geometric characteristics of the matrix and n is the exponent of release for INS 110.

2.5. Statistical analyses

Statistical analyses were carried out using SAS software (version 9.3, SAS Institute Incorporation, USA). Color parameters (L*a*b*) were submitted to analyses of variance (ANOVA) to compare statistical differences ($p < 0.05$) between hydrogels without or with chitosan for each gelling agent. Nonlinear regression models were adjusted to creep or relaxation data as a function of time, according to Eq. (3) and (4). Linear regression models were adjusted to release kinetics of INS 110 as a function of time, as presented in Eq. (7). The coefficient of determination (R^2) and mean absolute percentage error (MAPE) (Eq. 8) were used to evaluate the adequacy of fitting in both cases.

$$MAPE = \frac{1}{n}\sum_{i=1}^{n}\left|\frac{(Y_i - \hat{Y}_i)}{Y_i}\right| \cdot 100\ \% \quad (8)$$

In Eq. 8, Y_i is the ith experimental score, $\hat{Y}_i$ is the i^{th} score predicted by applying the adjusted model, and n is the number of predicted/experimental score pairs. Models with R^2 values ≥ 0.9 and *MAPE* values ≤ 10% were considered adequate to experimental data fit.

3. Results and discussion

3.1. Appearance and color of carrageenan/chitosan and starch/chitosan hydrogels

Hydrogels with a partial replacement of gelling agents (carrageenan or starch) by 0.0%, 5.0%, 7.5% or 10.0% (w/v) chitosan, containing 0.02 g·(100 mL)$^{-1}$ of INS 110, were produced and photographed 24 h later (Figures 1A and 1B, respectively).

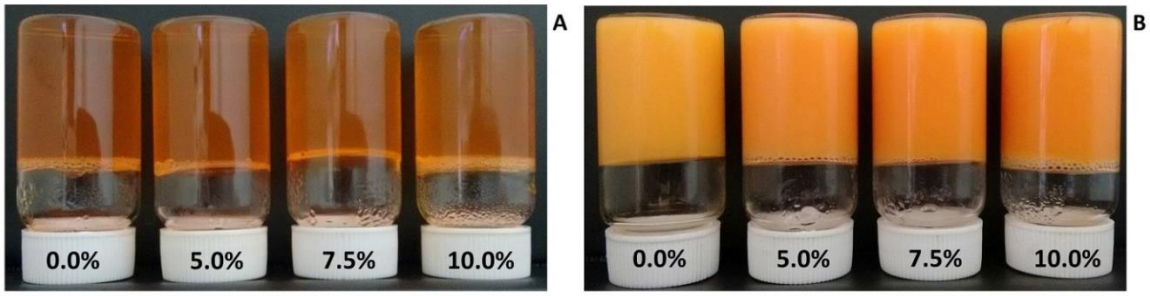

Figure 1 - Carrageenan (A) and starch (B) hydrogels, without or with a partial replacement of gelling agent by 5.0%, 7.5% or 10.0% (w/v) chitosan.
*In carrageenan hydrogels the total polysaccharide concentration was 1.5 g·(100 mL)$^{-1}$, and starch was 10.0 g·(100 mL)$^{-1}$.

Carrageenan hydrogels were translucent, presenting an orange/reddish tonality. Moreover, visually detectable differences were not observed among them. On the other hand, starch hydrogels were opaque, showing an orange tonality, with subtle visually detectable variations as the chitosan percentage substitution was increased. Specific gelation mechanisms of starch or carrageenan could explain the differences in the hydrogels optical properties [98]. Carrageenan gelification occurs in a two-step mechanism: *i*) from 75 ^{o}C to 80 ^{o}C, disperse carrageenans present random coil structures, as a result of electrostatic repulsions inter-chains; *ii*) carrageenan chains change conformation to helix structure during their cooling (or upon), while cations (Na^{+}, K^{+}, Ca^{2+}, for instance) stabilize junction zones between two helixes, creating a “shield effect” in the negatively charged sulfate groups, and forming a three-dimensional network [105]. Starch gelatinization begins with the collapse of the starch granule (swelling and partial or total disruption) in an aqueous media under heating (60 until 70 ^{o}C), promoting water intermolecular interactions with amylose and/or amylopectin [116]. The three-dimensional network is then created by the amylose double helices linked to each other using loops of amorphous amylose segments. Thus, amylopectin chains (and dispersed amylose chains) interacting with water molecules are the disperse phase entrapped by biopolymer network. Starch opaque gels result from the ternary phase separation occurring in the water-amylose-amylopectin system.

Instrumental color analyses (CIE-Lab) were also performed on all hydrogels, and results are presented in Table 2.

Table 2 - *L*a*b** color parameters to carrageenan or starch hydrogels, without or with a partial replacement of the gelling agent by 5.0%, 7.5% or 10.0% (w/v) chitosan.

Carrageenan hydrogels*	*a**	*b**	*L**
100.0% carrageenan	25.0 ± 1.0	43.8 ± 0.5	48.4 ± 0.3
95.0% carrageenan + 5.0% chitosan	26.1 ± 0.3	42.0 ± 2.0	47.8 ± 0.7
92.5% carrageenan + 7.5% chitosan	26.1 ± 0.4	43.6 ± 0.2	48.0 ± 0.4
90.0% carrageenan + 10.0% chitosan	26.0 ± 0.1	42.0 ± 1.0	47.4 ± 0.5
Starch hydrogels*	*a**	*b**	*L**
100.0% starch	21.3 ± 0.1	28.0 ± 2.0	50.0 ± 2.0
95.0% starch + 5.0% chitosan	21.3 ± 0.2	26.5 ± 0.8	50.0 ± 2.0
92.5% starch + 7.5% chitosan	22.0 ± 0.5	28.3 ± 0.1	52.0 ± 1.0
90.0% starch + 10.0% chitosan	22.0 ± 2.0	29.0 ± 5.0	53.0 ± 3.0

*In carrageenan hydrogels the total polysaccharide concentration was 1.5 g·(100 mL)$^{-1}$, and starch was 10.0 g·(100 mL)$^{-1}$.

**Significant differences (p > 0.05) were not observed by ANOVA for carrageenan or starch hydrogels without or with a partial replacement of gelling agents by chitosan.

Carrageenan or starch hydrogels without or with a partial replacement of gelling agent by 5.0%, 7.5% or 10.0% (w/v) chitosan did not show significant differences for *L*a*b** color coordinates (values were about 26.0, 42.0 and 48.0 in carrageenan, and about 22.0, 28.0 and 51.0 in starch hydrogels, respectively to *a**, *b** and *L**) by ANOVA (p > 0.05).

Interactions or reactions between different gelling agents change simultaneously the formation of 3D network and its solvent cross-linking ability, which are macroscopically observed by altering the color and opacity of the materials [114]. For instance, Sinthusamran et al. (2017) studied the fish gelatin (FG) (5.0% w/v) gels mixed with κ-carrageenan (CG) at different proportions (0.0%, 25.0%, 50.0%, 75.0% and 100.0% of total solid), and observed that the addition of carrageenan had an impact on *L* a*b** and color parameters of FG/CG mixed gels. Moreover, *L** was the color parameter mainly affected (71.0 for 100% FG and 48.0 for 25/75.0), and this result was attributed to the chemical interactions between gelatin and carrageenan chains [115].

Color analyses indicated that chitosan did not influence the color of polysaccharide hydrogels. Such findings are important for technological applications of carrageenan/chitosan and starch/chitosan hydrogels, since chitosan could offer advantages from a techno-functional point of view, since it is a macromolecule with several proven physiological properties. In this case, a partial replacement of the gelling agent by chitosan could be a strategy for the production of hydrogels with appearance and color closer to those prepared without it.

3.2. Rheological characterization of carrageenan/chitosan and starch/chitosan hydrogels

Transient compression tests (creep-recovery and stress-relaxation tests) and frequency sweeps were performed, in order to describe elastic and viscous components of carrageenan or

starch hydrogels with a partial replacement by chitosan. Creep-recovery curves of carrageenan or starch hydrogels without and with partial replacement of gelling agent by 5.0%, 7.5% or 10.0% (w/v) chitosan are presented in Figure 2.

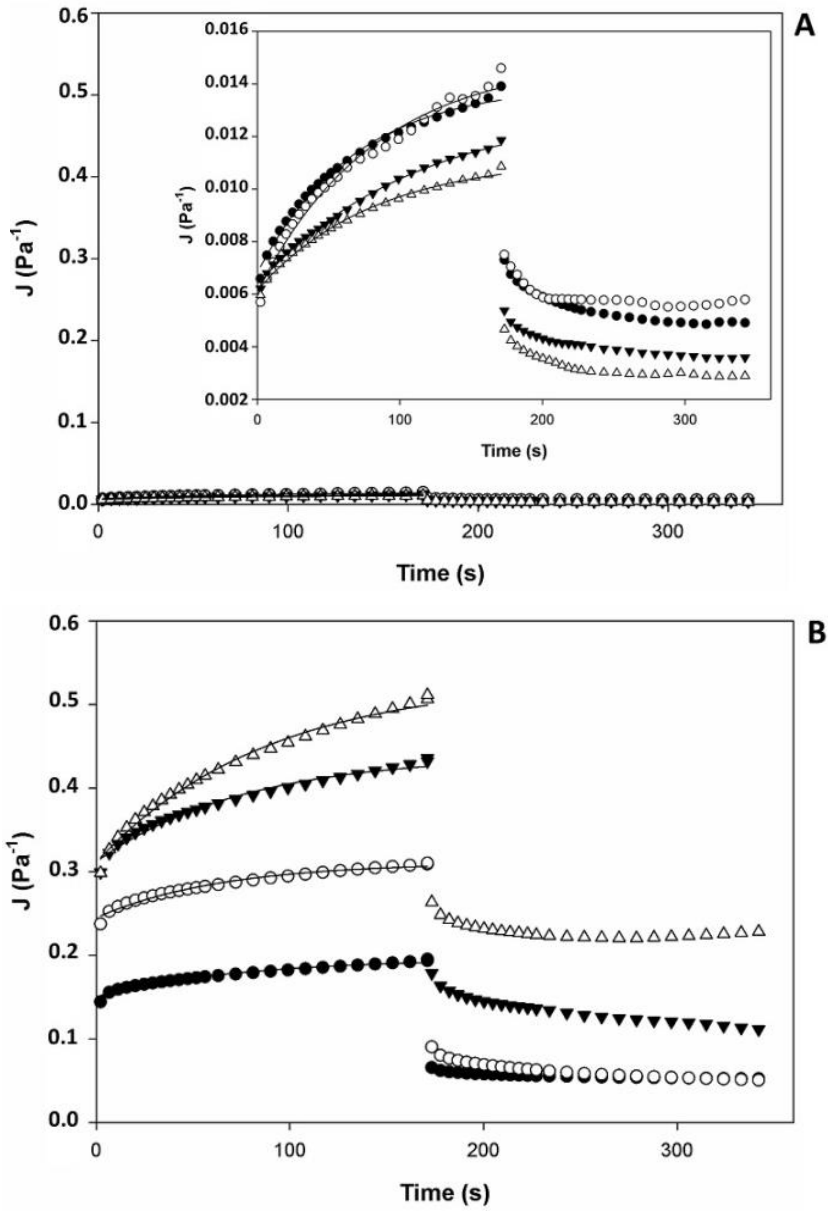

Figure 2 - Creep-recovery curves for carrageenan (A) and starch (B) hydrogels, without (●) or with a partial replacement of gelling agent by 5.0% (○); 7.5% (▼); or 10.0% w/v (Δ) chitosan.
*In carrageenan hydrogels the total polysaccharide concentration was 1.5 g·(100 mL)$^{-1}$, and starch was 10.0 g·(100 mL)$^{-1}$.

Carrageenan hydrogels without or with a partial replacement of gelling agent by 5.0%, 7.5% or 10.0% (w/v) chitosan presented compliance values varying from $6.0 \cdot 10^{-3}$ Pa^{-1} to $1.3 \cdot 10^{-2}$ Pa^{-1} (Figure 2-A), and these values were much lower than starch hydrogels (Figure 2-B). Starch hydrogels without chitosan showed strain values between $1.5 \cdot 10^{-1}$ Pa^{-1} and $2.0 \cdot 10^{-1}$ Pa^{-1} (Figure 2-B), and an increase in compliance values was observed accordingly as starch was replaced

by chitosan ($3.0 \cdot 10^{-2}$ Pa^{-1} to $3.0 \cdot 10^{-1}$ Pa^{-1} for 5.0% (w/v) of chitosan; $3.0 \cdot 10^{-1}$ Pa^{-1} to $4.0 \cdot 10^{-1}$ Pa^{-1} for 7.5% (w/v); and $3.0 \cdot 10^{-1}$ Pa^{-1} to $5.0 \cdot 10^{-1}$ Pa^{-1} for 10.0% (w/v)).

All materials showed typical curves of viscoelastic materials due to permanent deformation, after 180 s related to the recovery test. Then, in order to describe the viscoelasticity terms of elastic and viscous parameters, Burger's model (Equation 3) was adjusted to $J = f(t)$ data for creep curves of hydrogels. The third term of Burger's model related to a viscous behavior was not significant ($p > 0.05$), which is coherent with creep curves that did not present a long time viscous flow. Thus, the viscous parameter was negligible in the model. Elasticity parameters and adequacy of fitting of Burger's model for carrageenan and starch hydrogels are presented in Table 3 (p. 76).

In all cases, Burger's model was well-fitted to creep curves with $R^2 \geq 0.97$ and MAPE ≤ 2.1%, indicating the model reliability to describe such data. Model parameters were quite close in carrageenan hydrogels without or with a partial replacement of gelling agent by 5.0%, 7.5% or 10.0% (w/v) of chitosan ($6.0 \cdot 10^{-3}$ Pa^{-1} to J_0, $5.0 \cdot 10^{-3}$ Pa^{-1} to J_1 and $7.0 \cdot 10^{1}$ s to λ_{ret}). Starch hydrogels without chitosan presented a lower value for instantaneous elastic term ($J_0 = 1.5 \cdot 10^{-1}$ Pa^{-1}) than hydrogels prepared with a partial replacement of gelling agent for chitosan (J_0 about $3.0 \cdot 10^{-1}$ Pa^{-1}). This observation can indicate that chitosan could subtly decrease hydrogels resistance that undergo instantaneous stress (compression stress). In regards to the retarded elastic term (J_1 about $5.0 \cdot 10^{-2}$ Pa^{-1}), starch hydrogels without chitosan and with a partial replacement of gelling agent by 5.0% (w/v) chitosan presented similar values, while hydrogels containing a partial replacement of starch by 7.5% or 10.0% (w/v) chitosan were also similar and presented higher values (J_1 about $1.0 \cdot 10^{-1}$ Pa^{-1}). These observations were in accordance with creep curves (Figure 2 – B), since a more pronounced behavior in terms of retarded elastic term can be observed to starch hydrogels with a partial replacement of starch by 7.5% or 10.0% (w/v) chitosan. The increase of compliance as a function of time in terms of J_0 and J_1 is related to the energetic transition of the amylopectin-water intermolecular interactions. In addition, the reduction of water cross-linking in the interstices of amylose network is expected as a response to the stress instantaneously applied and kept over time [116]. In this case, the partial replacement of starch by chitosan may have reduced amylopectin-water interactions of starch hydrogels, allowing a higher conformational freedom to water molecules, and reducing the elasticity of the hydrogels.

However, from the magnitude of the variations observed, the increase of chitosan concentration in starch hydrogels may not have expressively impaired their final compliance. Starch hydrogels without chitosan and with a partial replacement of gelling agent by 5.0%, 7.5% or 10.0% (w/v) chitosan presented similar values for the retardation time (λ_{ret} about $7.0 \cdot 10^{1}$ s). In general, carrageenan and starch hydrogels presented expressive differences to three analyzed parameters (J_0, J_1 and λ_{ret}), which can be explained by the intrinsic characteristics of the gelification of each polysaccharide.

Table 3 - Model parameters and adequacy of fitting to Burger's model adjusted to creep data for carrageenan and starch hydrogels, without or with a partial replacement of gelling agent by 5.0%, 7.5% or 10.0% (w/v) chitosan

	Adjusted parameters			***Adequacy of fitting***	
Carrageenan hydrogels*	J_0 **(Pa^{-1})**	J_1 **(Pa^{-1})**	λ_{ret} **(s)**	R^2	**MAPE (%)**
100.0% carrageenan	$6.1 \cdot 10^{-3} \pm 6.0 \cdot 10^{-5}$	$5.0 \cdot 10^{-3} \pm 1.0 \cdot 10^{-4}$	$8.3 \cdot 10^{1} \pm 1.0 \cdot 10^{-1}$	0.99	2.1
95.0% carrageenan + 5.0% chitosan	$6.4 \cdot 10^{-3} \pm 5.0 \cdot 10^{-5}$	$6.8 \cdot 10^{-3} \pm 2.0 \cdot 10^{-4}$	$1.1 \cdot 10^{2} \pm 1.0 \cdot 10^{-1}$	0.99	0.8
92.5% carrageenan + 7.5% chitosan	$6.1 \cdot 10^{-3} \pm 1.0 \cdot 10^{-4}$	$8.9 \cdot 10^{-3} \pm 3.0 \cdot 10^{-4}$	$8.3 \cdot 10^{1} \pm 1.0 \cdot 10^{-1}$	0.99	2.1
90.0% carrageenan + 10.0% chitosan	$6.8 \cdot 10^{-3} \pm 1.0 \cdot 10^{-4}$	$7.2 \cdot 10^{-3} \pm 1.0 \cdot 10^{-4}$	$6.8 \cdot 10^{1} \pm 1.0 \cdot 10^{-1}$	0.99	1.1
Starch hydrogels*	J_0 **(Pa^{-1})**	J_1 **(Pa^{-1})**	λ_{ret} **(s)**	R^2	**MAPE (%)**
100.0% starch	$1.5 \cdot 10^{-1} \pm 1.0 \cdot 10^{-4}$	$4.5 \cdot 10^{-2} \pm 2.0 \cdot 10^{-3}$	$7.4 \cdot 10^{1} \pm 1.0 \cdot 10^{-1}$	0.97	0.9
95.0% starch + 5.0% chitosan	$2.4 \cdot 10^{-1} \pm 2.0 \cdot 10^{-4}$	$6.6 \cdot 10^{-2} \pm 2.0 \cdot 10^{-3}$	$6.4 \cdot 10^{1} \pm 1.0 \cdot 10^{-1}$	0.98	0.7
92.5% starch + 7.5% chitosan	$3.1 \cdot 10^{-1} \pm 3.0 \cdot 10^{-4}$	$1.3 \cdot 10^{-1} \pm 5.0 \cdot 10^{-3}$	$7.6 \cdot 10^{1} \pm 1.0 \cdot 10^{-1}$	0.99	0.9
90.0% starch + 10.0% chitosan	$3.1 \cdot 10^{-1} \pm 4.0 \cdot 10^{-4}$	$2.1 \cdot 10^{-1} \pm 7.0 \cdot 10^{-3}$	$8.7 \cdot 10^{1} \pm 1.0 \cdot 10^{-1}$	0.99	1.1

*In carrageenan hydrogels the total polysaccharide concentration was 1.5 g·(100 mL)$^{-1}$, and starch was 10.0 g·(100 mL)$^{-1}$.

Figure 3 shows the stress relaxation curves of carrageenan or starch hydrogels, without or with a partial replacement of gelling agent by 5.0%, 7.5% or 10.0% (w/v) chitosan, which were submitted to a controlled, constant axial deformation of 1.25%.

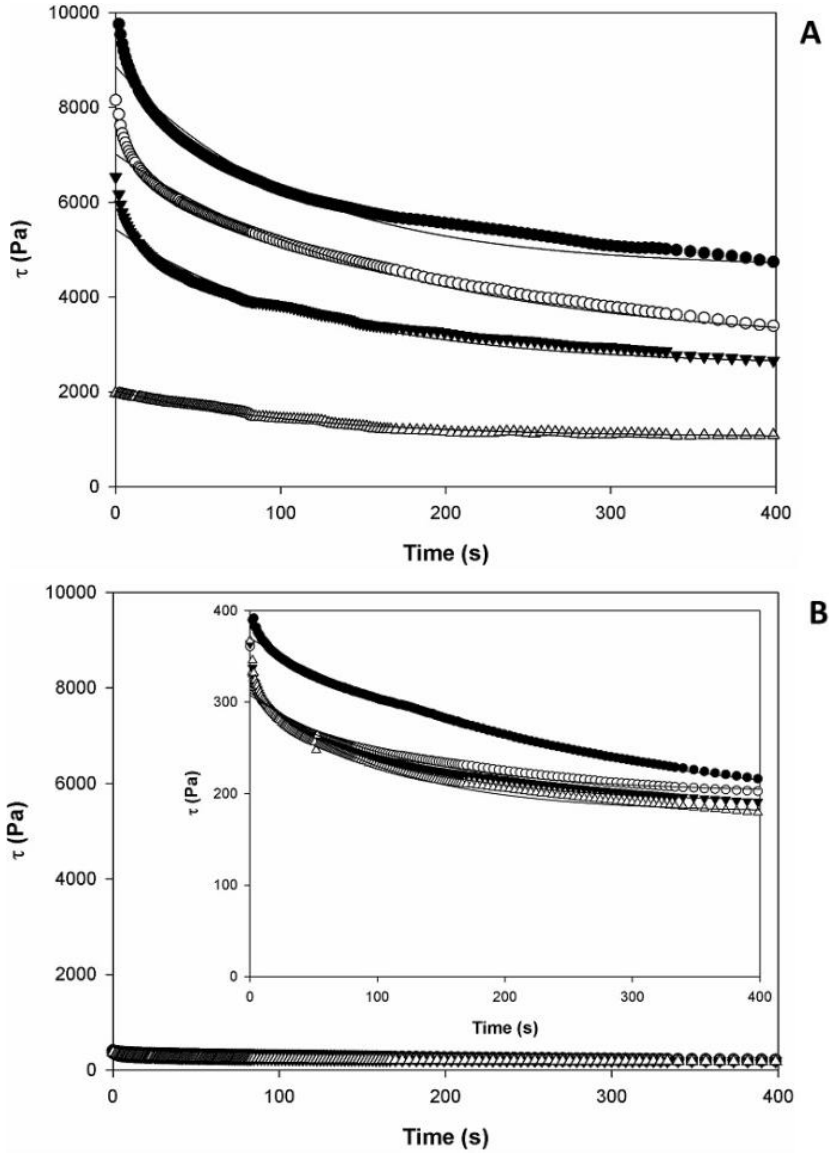

Figure 3 - Stress-relaxation curves for carrageenan (A) and starch (B) hydrogels, without (●) or with a partial replacement of the gelling agent by 5.0% (○); 7.5% (▼); or 10.0% w/v (Δ) of chitosan.

*In carrageenan hydrogels the total polysaccharide concentration was 1.5 g·(100 mL)$^{-1}$, and starch was 10.0 g·(100 mL)$^{-1}$.

Carrageenan hydrogels without or with a partial replacement of gelling agent by 5.0%, 7.5% or 10.0% (w/v) chitosan showed a decrease in values of initial stress as the chitosan concentration increased ($1.0 \cdot 10^4$ Pa, $8.0 \cdot 10^3$ Pa, $7.0 \cdot 10^3$ Pa, and $2.0 \cdot 10^3$ Pa, respectively to 0.0%, 5.0%, 7.5% and 10.0% (w/v) chitosan) (Figure 3 – A). Starch hydrogels without or with a partial replacement of gelling agent by 5.0%, 7.5% or 10.0% (w/v) chitosan presented similar

values of initial stress ($1.0 \cdot 10^2$ Pa). However, when compared to carrageenan gels, starch hydrogels showed lower initial stress values (Figure 3-B). In order to mathematically model the hydrogels relaxation as a function of time, the Maxwell's model (Equation 6) was adjusted to $\tau = f(t)$ data (Table 4), and results are presented in Table 4 (p. 79).

Adjusted models showed $R^2 \geq 0.96$ and MAPE ≤ 3.8 for all analyses, indicating a good adequacy of the Maxwell's model to describe the relaxation behavior of these hydrogels. Maxwell's model parameters presented similar values for carrageenan hydrogels without or with a partial replacement of gelling agent by 5.0%, 7.5% or 10.0% (w/v) chitosan ($1.0 \cdot 10^3$ Pa to τ_{eq}, $1.0 \cdot 10^3$ Pa to τ_0 and $1.0 \cdot 10^2$ s to λ_{ret}). Starch hydrogels without or with a partial replacement of gelling agent by 5.0, 7.5 or 10.0% (w/v) chitosan presented similar values in the model parameters (about $2.0 \cdot 10^2$ Pa to τ_{eq}, $1.0 \cdot 10^2$ Pa to τ_0 and $1.0 \cdot 10^2$ s to λ_{ret}), according to Figure 3 – B. Results suggested that the partial replacement of carrageenan or starch by chitosan in hydrogels did not promote expressive alterations of measured parameters during stress-relaxation tests.

Carrageenan hydrogels showed low compliance values as a function of time in the creep test. Then, high values of tension were expected for maintenance of these hydrogels during stress-relaxation tests, where a deformation is imposed to materials over time. On the other hand, the opposite behavior was expected for the hydrogels with or without a replacement of starch by chitosan; hydrogels containing starch presented higher compliance values as a function of time in the creep test than those with carrageenan. Thus, lower values of tension were expected for them, comparing with carrageenan hydrogels.

Table 4 - Model parameters and adequacy of fitting to Maxwell's model adjusted to relaxation data for carrageenan and starch hydrogels, without or with a partial replacement of the gelling agent by chitosan.

	Adjusted parameters			***Adequacy of fitting***	
Carrageenan hydrogels*	τ_{eq} **(Pa)**	τ_0 **(Pa)**	λ_{ret} **(s)**	R^2	**MAPE (%)**
100.0% carrageenan	$4.6 \cdot 10^3 \pm 5.0 \cdot 10^1$	$4.2 \cdot 10^3 \pm 6.0 \cdot 10^1$	$1.1 \cdot 10^2 \pm 4.0 \cdot 10^{-2}$	0.96	3.4
95.0% carrageenan + 5.0% chitosan	$3.0 \cdot 10^3 \pm 5.0 \cdot 10^1$	$4.0 \cdot 10^3 \pm 5.0 \cdot 10^1$	$1.7 \cdot 10^2 \pm 3.0 \cdot 10^{-2}$	0.98	2.6
92.5% carrageenan + 7.5% chitosan	$2.6 \cdot 10^3 \pm 4.0 \cdot 10^1$	$2.9 \cdot 10^3 \pm 4.0 \cdot 10^1$	$1.2 \cdot 10^2 \pm 4.0 \cdot 10^{-2}$	0.96	2.2
90.0% carrageenan + 10.0% chitosan	$1.1 \cdot 10^3 \pm 6.0 \cdot 10^0$	$9.7 \cdot 10^2 \pm 7.0 \cdot 10^0$	$1.1 \cdot 10^2 \pm 2.0 \cdot 10^{-2}$	0.98	1.9
Starch hydrogels*	τ_{eq} **(Pa)**	τ_0 **(Pa)**	λ_{ret} **(s)**	R^2	**MAPE (%)**
100.0% starch	$1.8 \cdot 10^2 \pm 3.0 \cdot 10^0$	$1.9 \cdot 10^2 \pm 2.0 \cdot 10^0$	$2.4 \cdot 10^2 \pm 2.0 \cdot 10^{-2}$	0.99	1.2
95.0% starch + 5.0% chitosan	$2.0 \cdot 10^2 \pm 1.0 \cdot 10^0$	$1.1 \cdot 10^2 \pm 1.0 \cdot 10^0$	$1.1 \cdot 10^2 \pm 3.0 \cdot 10^{-2}$	0.97	1.2
92.5% starch + 7.5% chitosan	$1.9 \cdot 10^2 \pm 1.0 \cdot 10^0$	$1.2 \cdot 10^2 \pm 2.0 \cdot 10^0$	$1.1 \cdot 10^2 \pm 3.0 \cdot 10^{-2}$	0.97	1.8
90.0% starch + 10.0% chitosan	$1.8 \cdot 10^2 \pm 1.0 \cdot 10^0$	$1.3 \cdot 10^2 \pm 2.0 \cdot 10^0$	$1.0 \cdot 10^2 \pm 3.0 \cdot 10^{-2}$	0.97	2.1

*In carrageenan hydrogels the total polysaccharide concentration was 1.5 $g \cdot (100\ mL)^{-1}$, and starch was 10.0 $g \cdot (100\ mL)^{-1}$.

In addition to transient compression tests (creep-recovery and stress-relaxation tests), frequency sweeps (0.1 to 50 Hz; 25.0 ± 0.1 ºC) of hydrogels were also performed, in order to gain additional information about their change in internal stress. The corresponding results (mechanical spectra) are represented in Figure 4.

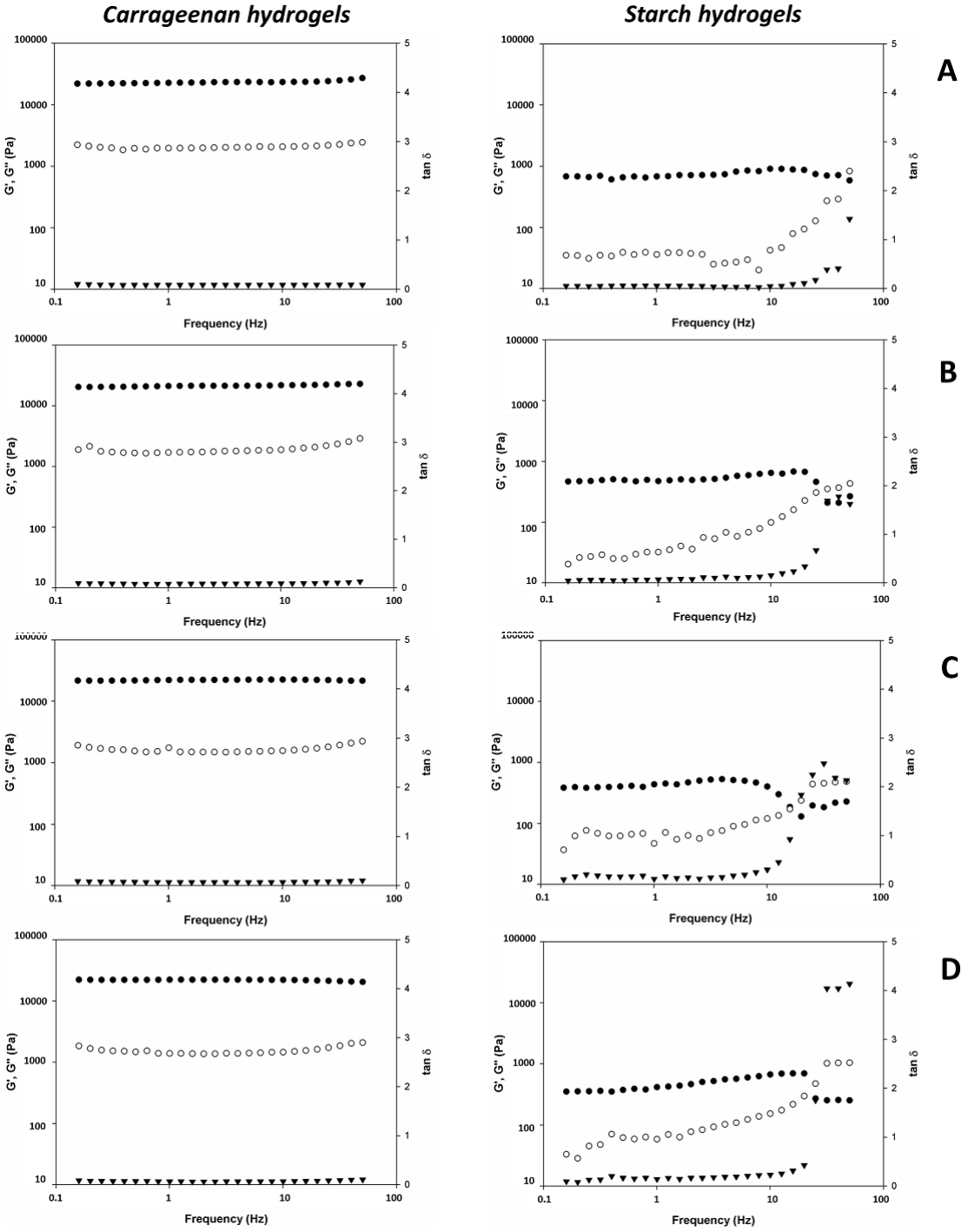

Figure 4 - Frequency sweeps from 0.1 to 50 Hz for carrageenan and starch hydrogels, without (A) and with replacement of the gelling agent by 5.0% (B); 7.5% (C); or 10.0% w/v (D) chitosan. *G'* (●), *G''* (○), and tan δ (▼).

*In carrageenan hydrogels the total polysaccharide concentration was 1.5 g·(100 mL)$^{-1}$, and starch was 10.0 g·(100 mL)$^{-1}$.

Elastic modulus ($1.1 \cdot 10^4$ Pa), viscous modulus ($1.1 \cdot 10^3$ Pa), and tan δ ($1.1 \cdot 10^0$) presented similar values in hydrogels without or with a partial replacement of carrageenan by 5.0%, 7.5% or 10.0% (w/v) chitosan, from 0.1 to 50 Hz. Carrageenan hydrogels showed *G'* > *G''* (about 10 times), which indicated a predominance of elastic character in the hydrogels. Furthermore, carrageenan hydrogels showed a behavior commonly found in "true gels", since *G'* and *G''* remained constant as a function of the frequency [54,117]. Results observed in frequency sweeps for carrageenan hydrogels were in accordance with those presented in transient tests: *i*) creep-recovery showed similar compliance values for materials without or with a partial replacement by 5.0%, 7.5% or 10.0% (w/v) chitosan; and *ii)* in stress-relaxation, carrageenan hydrogels were elastic and resistant when they were deformed. Thus, the predominantly elastic character of the carrageenan hydrogels without or with chitosan was observed in the tests under compression or shear stresses. Results presented in this study indicated that the partial replacement of carrageenan by chitosan could not change intermolecular interactions between colloidal network and water molecules, preserving the rheological parameters of the hydrogels.

Starch hydrogels presented differences in the mechanical spectra, when compared to those prepared using carrageenan. Hydrogels without or with a partial replacement of starch by 5.0%, 7.5% or 10.0% (w/v) presented low variations of both elastic ($8.0 \cdot 10^2$ Pa) and viscous modulus ($3.0 \cdot 10^2$ Pa), from 0.1 to 10 Hz. Moreover, the elastic character in starch hydrogels was also observed to be predominant, since *G'* > *G''* for all systems, from 0.1 to 10 Hz. Then, in starch hydrogel without chitosan, *G"* was increased progressively until it crossed *G'* (about 50 Hz). At the frequency range of 0.1 to 5 Hz, hydrogels with a partial replacement of starch by 5.0%, 7.5% or 10.0% (w/v) chitosan presented a similar behavior to each other and little variation of *G'* and *G''* values ($5.0 \cdot 10^2$ Pa to *G'* and $1.0 \cdot 10^2$ Pa to *G''*). Then, *G"* increased progressively until it crossed *G'* (about 20 Hz). These results indicate that starch hydrogels were more susceptible to shear than carrageenan hydrogels. The transition of *G'* and *G"* modulus as a function of frequency, along with the increase of *G"* surpassing *G'*, are suggesting a reorganization of water-polysaccharide interactions at a molecular level [118]. In this case, the colloidal network disruption and release of the solvent from interstices in starch hydrogels would be aggravated from replacement by chitosan. Moreover, the addition of chitosan seems to alter the interactions of amylopectin with water molecules, in starch hydrogels. As expected, hydrogels with a partial replacement of starch by 5.0%, 7.5% or 10.0% (w/v) chitosan also showed an increase in tan δ values, at > 5 Hz, when *G''* values were raised. Thus, tan δ values corroborated the hypothesis about colloidal network disruption mentioned above. Starch hydrogels were classified as "weak gels" [54], since *G'* and *G''* present variable values at frequencies > 5 Hz. Starch hydrogels with a partial replacement by 5.0%, 7.5% or 10.0% (w/v) chitosan showed alterations in their structure at frequencies > 5 Hz, and these observations were in accordance with creep-recovery tests, which showed higher compliance values as a function of time. Moreover, the compliance values were increased as the starch was replaced by chitosan, and hydrogels with 5.0% (w/v) chitosan presented lower compliance values than

others that were also partially replaced. At frequencies < 5 Hz, starch hydrogels without or with a partial replacement of gelling agent by 5.0%, 7.5% or 10.0% (w/v) chitosan presented a predominantly elastic character, in terms of *G'*, *G''* and tan δ.

Rheological results are relevant in the hydrogels characterization, since interactions between biopolymers can modify their elastic or viscous modulus. For instance, Sinthusamran et al. (2017) also studied the dynamic rheological properties of fish gelatin (FG) (5.0% (w/v)) gels containing κ-carrageenan (CG) at different levels (0.0%, 25.0%, 50.0%, 75.0% and 100.0% of total solid), and observed that the value of elastic modulus *G'* of FG/CG mixed gel decreased as CG content increased ($9.0 \cdot 10^3$ Pa for 0.0% (w/v) CG to $1.2 \cdot 10^3$ Pa for 75.0% (w/V)); while the *G''* of FG/CG mixed gel increased as CG content increased ($9.0 \cdot 10^1$ Pa – $4.0 \cdot 10^2$ Pa for 0.0% (w/v) CG to $1.2 \cdot 10^2$ Pa - $1.1 \cdot 10^3$ Pa for 75.0% (w/v)), at 0.01 to 100 Hz. Shortly, the substitution of FC for CG had a significant effect on the textural and viscoelastic properties of the materials. However, the replacement of carrageenan or starch by 5.0%, 7.5% or 10.0% (w/v) chitosan did not promote expressive changes on viscoelastic properties of the hydrogels studied by transient and oscillatory tests (< 5 Hz).

Thus, the present study showed that a partial replacement of gelling agents by chitosan did not promote changes in color or viscoelastic properties of hydrogels.

3.3. Release of INS 110 colorant by carrageenan/chitosan and starch/chitosan hydrogels

Yellow sunset (INS 110) is widely used as food additives to make more attractive foods due to its low risk to human health, when used in concentrations recommended by the main international institutions related to the consumers' health [119,120]. As other food colorants, the release of INS 100 from semi-solid systems towards fluids in contact with them usually occurs. Then, this experiment aimed to produce hydrogels with a partial replacement of carrageenan or starch by chitosan containing Yellow sunset (INS 110), in order to evaluate the release of this colorant when these hydrogels were covered with a sucrose solution 20.0% (w/v). Release (%) of Yellow sunset (INS 110) from hydrogels as a function of time is represented in Figure 5 (p. 83).

INS 110 release from carrageenan hydrogels (Figure 5-A), without or with a partial replacement of gelling agent by chitosan presented a similar behavior during the first 12 h, varying from 0.0% to 10.0%. Carrageenan hydrogel without chitosan released 32.0% of INS 110 to sucrose solution, whereas this value was 27.0% for hydrogels with a partial replacement by 5.0%, 7.5% and 10.0% (w/v) chitosan, after 120 h. From 120 h to 312 h, the release of INS 110 was increased for all carrageenan hydrogels, and the system without chitosan reached up 43.0%. The release of INS 110 increased accordingly as the partial replacement of carrageenan for chitosan was raised on hydrogels: 35.0% for 5.0% (w/v), 37.0% for 7.5% (w/v), and 40.0% for 10.0% (w/v) chitosan, after 312 h. Thus, the Yellow sunset (INS 110) release was reduced in 19%, 18%, and 6%, respectively for 5.0%, 7.5% and 10.0% (w/v) chitosan added to carrageenan hydrogels.

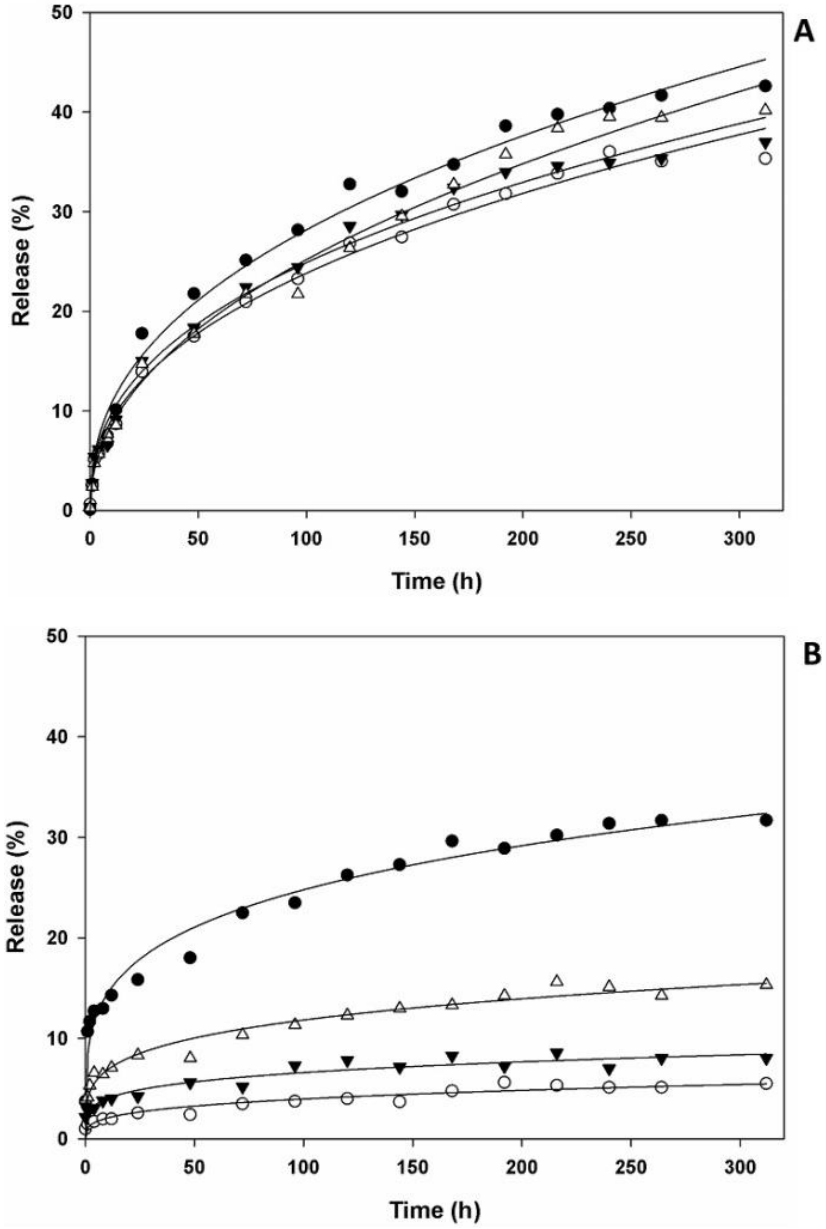

Figure 5 - Release (%) of Yellow sunset (INS 110) from carrageenan (A) and starch (B) hydrogels, without (●) or with a partial replacement of the gelling agent by 5.0% (○); 7.5% (▼); or 10.0% w/v (Δ) chitosan.

*In carrageenan hydrogels the total polysaccharide concentration was 1.5 g·(100 mL)$^{-1}$, and starch was 10.0 g·(100 mL)$^{-1}$.

Hydrogels without or with a starch partial replacement by 5.0%, 7.5% or 10.0% (w/v) chitosan presented different behavior to INS 110 release (Figure 5-B). Starch hydrogel without chitosan released 26.0% of INS 110 to sucrose solution, while hydrogels containing a partial replacement of starch by 5.0%, 7.5% and 10.0% (w/v) chitosan presented 4.0%, 8.0%, and 12.0% of release, after 120 h. The release of INS 110 was increased in all starch hydrogels after 312 h, and starch hydrogel without chitosan released 33.0% Yellow sunset (INS 110) to sucrose solution. INS 110 release was increased according to the partial replacement of starch

for chitosan was raised on hydrogels: 6.0% for 5.0% (w/v), 8.0% for 7.5% (w/v), and 15.0% for 10.0% (w/v) chitosan, after 312 h. This is an important observation, since Yellow unset (INS 110) release was reduced 492%, 305%, and 114% with a partial replacement of starch agent for 5.0%, 7.5% or 10.0% (w/v) chitosan, respectively. These results demonstrate that the partial replacement of starch by chitosan in hydrogels promotes a better retention in the Yellow sunset (INS 110), when compared to systems formulated with carrageenan replaced at the same concentrations by 5.0%, 7.5% and 10.0% (w/v) chitosan. In order to describe the release kinetics of Yellow sunset (INS 110) from different carrageenan/chitosan and starch/chitosan hydrogels to a sucrose solution, the Korsmeyer-Peppas' model (Equation 13) was adjusted to release curves. Model parameters and adequacy of fitting of Korsmeyer-Peppas' model for carrageenan and starch hydrogels are presented in Table 5.

Table 5 - Model parameters and adequacy of fitting to Korsmeyer-Peppas' model adjusted to release of Yellow sunset (INS 110) from carrageenan and starch hydrogels, without or with a partial replacement of the gelling agent by chitosan

	Adjusted parameters		***Adequacy of fitting***	
Carrageenan hydrogels*	***k* (h^{-1})**	***n***	***R^2***	**MAPE (%)**
100.0% carrageenan	4.1 ± 0.4	0.42 ± 0.02	0.99	7.1
95.0% carrageenan + 5.0% chitosan	3.5 ± 0.3	0.42 ± 0.02	0.99	6.6
92.5% carrageenan + 7.5% chitosan	3.5 ± 0.3	0.40 ± 0.02	0.99	8.8
90.0% carrageenan + 10.0% chitosan	2.9 ± 0.3	0.47 ± 0.02	0.99	6.0
Starch hydrogels*	***k* (h^{-1})**	***n***	***R^2***	**MAPE (%)**
100.0% starch	8.4 ± 0.6	0.24 ± 0.02	0.97	6.5
95.0% starch + 5.0% chitosan	1.1 ± 0.2	0.28 ± 0.03	0.90	8.3
92.5% starch + 7.5% chitosan	2.4 ± 0.3	0.22 ± 0.03	0.87	7.4
90.0% starch + 10.0% chitosan	4.0 ± 0.5	0.24 ± 0.02	0.90	5.5

*In carrageenan hydrogels the total polysaccharide concentration was 1.5 g·(100 mL)$^{-1}$, and starch was 10.0 g·(100 mL)$^{-1}$.

In Table 5, the Korsmeyer-Peppas' model was well-fitted to creep curves presenting $R^2 \geq 0.91$ and MAPE ≤ 10.0%, which indicates a good reliability to describe matematically the release of INS 100 in carrageenan and starch hydrogels, without or with chitosan. In Korsmeyer-Peppas' model, *k* is the constant of release, which gives information about the increase in the Yellow sunset release (INS 110) as a function of time. Carrageenan hydrogels without or with a replacement of this gelling agent by chitosan presented *k* values from 2.93 to 4.14 (h^{-1}), demonstrating a similar release of INS 100 between these systems. Moreover, *n* is the exponent of release for INS 110 in Korsmeyer-Peppas' model, and this term predicts that

the effective release would decrease with increasing time (n < 1.0). Carrageenan and carrageenan/chitosan hydrogels also presented similar n values (from 0.40 to 0.47), indicating that for all systems the release of INS 110 was similarly reduced as a function of time. Chitosan added to carrageenan hydrogels seemed not to have changed the INS 110 release to sucrose solution 20.0% (w/v), since expressive differences cannot be observed between hydrogels without or with a partial replacement of carrageenan by 5.0%, 7.5% or 10.0% (w/v) chitosan.

On the other hand, starch gel without chitosan presented k = 8.40 (h^{-1}), while hydrogels with a partial replacement of starch by chitosan showed lower values (k = 1.09 h^{-1} for 5.0% (w/v); k = 2.44 h^{-1} for 7.5% (w/v); and k = 3.97 h^{-1} for 10.0% (w/v) chitosan). These results were in accordance with the release curves presented in Figure 5-B, since a higher concentration of Yellow sunset was released for starch hydrogel without chitosan. Starch and starch/chitosan hydrogels showed similar n values (from 0.22 to 0.28), which indicated that INS 110 release was similar as a function of time for these systems. Hydrogels with lower substitutions of starch by 5.0% and 7.5% (w/v) chitosan presented the highest percentages of Yellow sunset (INS 110) retention. These observations might be explained by the hypothesis that some chitosan chains in the starch hydrogels were positioned within the interstices of the colloidal network, along with the amylose and amylopectin chains, contributing to the cross-linking of the INS 110 present in the solvent. In this case, the increase in starch substitution percentage for 10.0% (w/v) chitosan could cause the diffusion of some part of the chitosan from the interstices to the colloidal network along with the amylose chains, reducing the retention of INS 110, as well as hindering the hydrogel formation.

Modification to Korsmeyer-Peppas's model (Eq. 7) have been proposed [121–124]. In Equation 8, the latency (l), *i. e*. the time required for the release of compound from the matrix to be initiated ,was added to the Korsmeyer-Peppas's model. Furthermore, another modification to Korsmeyer-Peppas's model considering an immediate release of the compound (burst effect) can also be used [113,122].

$$R(\%) = k \cdot (t - l)^n \quad (8)$$

$$R(\%) = k \cdot t^n + b \quad (9)$$

In Eq. (8) and (9), k is the constant of release, n is the exponent of release, l is the latency time, and b is the burst effect term.

Models for *R (%)* as a function of time presented in the Eq. (8) and (9) were adjusted to INS 110 release data. However, l and b terms were not significant (p > 0.05) for all systems, indicating that *R (%) = f(t)* of INS 110 from hydrogels without or with a partial replacement of gelling agent for chitosan (5.0%, 7.5% or 10.0% w/v) did not present a latency time and/or the burst effect.

Finally, the replacement of starch by chitosan did not promote major changes in the visual, color and viscoelastic characteristics of the resulting hydrogels, but altered the Yellow sunset (INS 110) release. The partial replacement of starch by chitosan may be a new strategy to increase the retention of compounds in hydrogels matrices. Moreover, chitosan is a

polysaccharide with several biofunctional properties, which could offer advantages beyond the techno-functional role. Thus, chitosan can be seen as a functional alternative for the food industry.

4. Conclusion

Hydrogels without or with a partial replacement of carrageenan or starch by 5.0%, 7.5% or 10.0% (w/v) chitosan have neither showed significant differences for color parameters nor expressive changes for viscoelastic properties, according to transient tests and frequency sweeps (< 5 Hz). Chitosan did not expressively alter Yellow sunset (INS 110) release from carrageenan hydrogels(about 40%) to an aqueous phase. However, a partial replacement of starch by 5.0%. 7.5% and 10.0% (w/v) chitosan in hydrogels altered INS 110 release after 316 h (5%, 8% and 15%, respectively), when compared to starch hydrogel without chitosan. Thus, our findings pointed out that the replecement of starch by chitosan did not promote major changes on color and viscoelastic characteristics of hydrogels, but altered drastically the INS 110 release. Therefore, the replacement of gelling agents by chitosan has demonstrated to be a potential strategy to reduce INS 110 release from starch hydrogels, in which this biopolymer may act simultaneously as a biofunctional and a technico-functional agent.

3. CONCLUSÃO GERAL

Interações atrativas mais intensas foram estabelecidas entre os contra-ânions glicolato e lactato e as cadeias de quitosano, quando comparados ao acetato ou propionato, de acordo com as análises de FT-IR. Contudo, dispersões de quitosano contendo os ácidos acético, glicólico, propiônico ou lático apresentaram, apenas, sutis variações em suas propriedades físicas e nos valores de diâmetro médio e potencial ζ de suas cadeias dispersas, para uma determinada concentração dos ácido orgânicos. Uma baixa concentração de quitosano (0,1% m/v) promoveu o aumento da viscosidade das dispersões, em pelo menos quatro vezes, quando comparadas aos meios aquosos ácidos sem a adição de nenhum polissacarídeo. Além disso, a dispersão do quitosano pode ser realizada em meios aquosos, o que favorece a utilização do biopolímero para fins tecnológicos.

A combinação da homogeneização ultrassônica com o emulsificante Tween 20 mostrou-se eficiente na formação de gotículas de óleo, sendo o seu desempenho influenciado pelo aumento do espessamento dos sistemas, que foi causado pelo quitosano. Além disso, emulsões contendo ≥ 0,5% (m/m) de quitosano apresentaram um maior espessamento e uma menor desestabilização cinética (durante 28 dias) e frente a estresses ambientais. Emulsões O/A preparadas usando quitosano disperso em meios aquosos contendo diferentes ácidos (acético, glicólico, propiônico ou lático) não apresentaram alterações expressivas em termos de espessamento ou desestabilização (cinética e frente a estresses ambientais), para uma dada concentração de quitosano.

Hidrogéis de carragena ou amido contendo uma substituição parcial do agente gelificante por quitosano (5,0%, 7,5% e 10,0% m/v) não apresentaram alterações expressivas em termos de aspecto visual, cor e propriedades viscoelásticas. Contudo, a substituição parcial de amido por quitosano reduziu a liberação do corante amarelo crepúsculo (INS 110) para uma solução de sacarose em contato com os hidrogéis durante 316 h.

A técnico-funcionalidade do quitosano em meios aquosos ácidos foi demonstrada por sua ação espessante em dispersões aquosas e estabilizante em emulsões O/A. Além disso, hdrogéis de amido contendo o quitosano modularam a liberação de um corante alimentício para uma solução de sacarose. Assim, o impacto promissor do quitosano em sistemas-modelo foi demonstrado apontando, por conseguinte, para a utilização do biopolímero em aplicações alimentícias, nas quais ele poderia atuar simultaneamente como agente biofuncional ou técnico-funcional.

4. REFERÊNCIAS

[1] S. Islam, M.A. Bhuiyan, M.N. Islam, Chitin and Chitosan: Structure, Properties and Applications in Biomedical Engineering, Journal of Polymers and the Environment. 25 (2017) 854–866.

[2] I. Hamed, F. Ozogul, J.M. Regenstein, Industrial applications of crustacean by-products (chitin, chitosan, and chitooligosaccharides): A review, Trends in Food Science & Technology. 48 (2016) 40–50.

[3] M. Dash, F. Chiellini, R.M. Ottenbrite, E. Chiellini, Chitosan - A versatile semi-synthetic polymer in biomedical applications, Progress in Polymer Science. 36 (2011) 981–1014.

[4] Sigma-Aldrich, Chitosan Medium Molecular Weight, (2019) 1. https://www.sigmaaldrich.com/catalog/product/aldrich/448877?lang=pt&region=BR.

[5] A. Muxika, A. Etxabide, J. Uranga, P. Guerrero, K. De Caba, International Journal of Biological Macromolecules Chitosan as a bioactive polymer: Processing , properties and applications, International Journal of Biological Macromolecules. 105 (2017) 1358–1368.

[6] C. Muanprasat, V. Chatsudthipong, Chitosan oligosaccharide : Biological activities and potential therapeutic applications, Pharmacology and Therapeutics. 170 (2017) 80–97.

[7] M. Hosseinnejad, S.M. Jafari, Evaluation of different factors affecting antimicrobial properties of chitosan, International Journal of Biological Macromolecules. 85 (2016) 467–475.

[8] I. Younes, M. Rinaudo, Chitin and Chitosan Preparation from Marine Sources. Structure, Properties and Applications, Marine Drugs. 13 (2015) 1133–1174.

[9] Sigma-Aldrich, Chitosan High Molecular Weight, (2019) 1. https://www.sigmaaldrich.com/catalog/product/aldrich/419419?lang=pt&region=BR.

[10] Sigma-Aldrich, Chitosan Low Molecular Weight, (2019) 1. https://www.sigmaaldrich.com/catalog/product/aldrich/448869?lang=pt&region=BR.

[11] R.C.F. Cheung, T.B. Ng, J.H. Wong, W.Y. Chan, Chitosan: An Update on Potential Biomedical and Pharmaceutical Applications, Marine Drugs. 13 (2015) 5156–5186.

[12] M.L. Amorim, G.M.D. Ferreira, L. S. Soares, W.A. S. Soares, A.M. Ramos, J.S. R. Coimbra, L.H.M. Silva, E.B. Oliveira, Physicochemical Aspects of Chitosan Dispersibility in Acidic Aqueous Media: Effects of the Food Acid Counter-Anion, Food Biophysics. 11 (2016) 388–399.

[13] U. Klinkesorn, The Role of Chitosan in Emulsion Formation and Stabilization The Role of Chitosan in Emulsion Formation and Stabilization, Food Reviews International. 29 (2013) 371–393.

[14] H.A.R. Suleria, G. Gobe, P. Masci, S.A. Osborne, Marine bioactive compounds and health promoting perspectives ; innovation pathways for drug discovery, Trends in Food Science & Technology. 50 (2016) 44–55.

[15] S. Abdel-Aleem, M. El-Aidie, A Review on Chitosan: Ecofriendly Multiple Potential Applications in the Food Industry, International Journal of Advancement in Life Sciences Research. 1 (2018) 1–14.

[16] M. Ahmad, K. Manzoor, S. Singh, S. Ikram, Chitosan centered bionanocomposites for medical specialty and curative applications: A review, International Journal of Pharmaceutics. 529 (2017) 200–217.

[17] A. Oryan, S. Sahvieh, International Journal of Biological Macromolecules Effectiveness of chitosan scaffold in skin , bone and cartilage healing, International Journal of Biological Macromolecules. 104 (2017) 1003–1011.

[18] S.K. Shukla, A.K. Mishra, O. A. Arotiba, B.B. Mamba, Chitosan-based nanomaterials: A state-of-the-art review, International Journal of Biological Macromolecules. 59 (2013) 46–58.

[19] S. Dehghani, S. Vali, J.M. Regenstein, Edible films and coatings in seafood preservation: A review, Food Chemistry. 240 (2018) 505–513.

[20] I. Bano, M. Arshad, T. Yasin, M. Afzal, M. Younus, Chitosan: A potential biopolymer for wound management, International Journal of Biological Macromolecules. 102 (2017) 380–383.

[21] H.P.S.A. Khalil, C.K. Saurabh, Y.Y. Tye, T.K. Lai, A.M. Easa, E. Rosamah, M.R.N. Fazita, M.I. Syakir, A.S. Adnan, H.M. Fizree, N.A.S. Aprilia, A. Banerjee, Seaweed based sustainable films and composites for food and pharmaceutical applications: A review, Renewable and Sustainable Energy Reviews. 77 (2017) 353–362.

[22] A. Anitha, S. Sowmya, P.T.S. Kumar, S. Deepthi, K.P. Chennazhi, H. Ehrlich, M. Tsurkan, R. Jayakumar, Chitin and chitosan in selected biomedical applications, Progress in Polymer Science. 39 (2014) 1644–1667.

[23] D.-H. Ngo, T.-S. Vo, D.-N. Ngo, K.-H. Kang, J.-Y. Je, H.N.-D. Pham, H.-G. Byun, S.-K. Kim, Biological effects of chitosan and its derivatives, Food Hydrocolloids. 51 (2015) 200–216.

[24] E. Szymańska, K. Winnicka, Stability of Chitosan-A Challenge for Pharmaceutical and Biomedical Applications, Marine Drugs. 13 (2015) 1819–1846.

[25] N. Bhardwaj, D. Devi, B.B. Mandal, Tissue-Engineered Cartilage: The Crossroads of Biomaterials, Cells and Stimulating Factors, Macromolecular Bioscience. 15 (2015) 153–182.

[26] M. Kurek, S. Galus, F. Debeaufort, Surface, mechanical and barrier properties of bio-based composite films based on chitosan and whey protein, Food Packaging and Shelf Life. 1 (2014) 56–67.

[27] R.A. Shiekh, M.A. Malik, S.A. Al-Thabaiti, M.A. Shieck, Chitosan as a Novel Edible Coating for Fresh Fruits, Food Science Technology Research. 19 (2013) 139–155.

[28] A.M. Patti, N. Katsiki, D. Nikolic, K. Al-Rasadi, M. Rizzo, Nutraceuticals in lipid-lowering treatment: a narrative review on the role of chitosan., Angiology. 66 (2015) 416–21.

[29] L. Chiappisi, M. Gradzielski, Co-assembly in chitosan-surfactant mixtures: thermodynamics , structures , interfacial properties and applications, Advances in Colloid and Interface Science. 220 (2015) 92–107.

[30] M.S. Rodríguez, L.A. Albertengo, E. Agulló, Emulsification capacity of chitosan, Carbohydrate Polymers. 48 (2002) 271–276.

[31] A. Martínez, E. Chornet, D. Rodrigue, Steady-shear rheology of concentrated chitosan solutions, Journal of Texture Studies. 35 (2004) 53–74.

[32] C. Anchisi, A.M. Maccioni, M.C. Meloni, Physical properties of chitosan dispersions in glycolic acid, IL Farmaco. 59 (2004) 557–561.

[33] N. Calero, J. Muñoz, P. Ramírez, A. Guerrero, Flow behaviour, linear viscoelasticity and surface properties of chitosan aqueous solutions, Food Hydrocolloids. 24 (2010) 659–666.

[34] X. Li, W. Xia, Effects of concentration, degree of deacetylation and molecular weight on emulsifying properties of chitosan, International Journal of Biological Macromolecules. 48 (2011) 768–772.

[35] C.S.F. Picone, R.L. Cunha, Chitosan-gellan electrostatic complexes: Influence of preparation conditions and surfactant presence, Carbohydrate Polymers. 94 (2013) 695–703.

[36] J. Mikešová, J. Hašek, G. Tishchenko, P. Morganti, Rheological study of chitosan acetate solutions containing chitin nanofibrils, Carbohydrate Polymers. 112 (2014) 753–757.

[37] L. Zavaleta-Avejar, E. Bosquez-Molina, M. Gimeno, J.P. Pérez-Orozco, K. Shirai, Rheological and antioxidant power studies of enzymatically grafted chitosan with a hydrophobic alkyl side chain, Food Hydrocolloids. 39 (2014) 113–119.

[38] L.S. Soares, J.T. Faria, M.L. Amorim, J.M. Araújo, L.A. Minim, J.S.R. Coimbra, A.V.N.C. Teixeira, E.B. Oliveira, Rheological and Physicochemical Studies on Emulsions Formulated with Chitosan Previously Dispersed in Aqueous Solutions of Lactic Acid, Food Biophysics. 12 (2017) 109–118.

[39] L.S. Soares, R.B. Perim, E.S. Alvarenga, L.M. Guimarães, A.V.N.C. Teixeira, J.S.R. Coimbra, E.B. Oliveira, Insights on physicochemical aspects of chitosan dispersion in aqueous solutions of acetic, glycolic, propionic or lactic acid, International Journal of Biological Macromolecules. 128 (2019) 140–148.

[40] J. Wu, L. Zhang, Dissolution behavior and conformation change of chitosan in concentrated chitosan hydrochloric acid solution and comparison with dilute and semidilute solutions, International Journal of Biological Macromolecules. 121 (2019) 1101–1108.

[41] J. Liu, H. Pu, S. Liu, J. Kan, C. Jin, Synthesis, characterization, bioactivity and potential application of phenolic acid grafted chitosan: A review, Carbohydrate Polymers. 174 (2017) 999–1017.

[42] D.J. McClements, Food Emulsions - Principles, Practices, and Techniques, 3rd ed., CRC Press, Boca Raton, 2016.

[43] R.C. Santana, F.A. Perrechil, R.L. Cunha, High- and Low-Energy Emulsifications for Food Applications: A Focus on Process Parameters, Food Engineering Reviews. 5 (2013) 107–122.

[44] A.W. Adamson, A.P. Gast, Physical Chemistry of Surfaces, 6th ed., John Wiley & Songs, Inc., New York, 1997.

[45] J.J. Morelli, G. Szajer, Analysis of Surfactants: Part I, Journal of Surfactants and Detergents. 3 (2000) 539–552.

[46] G. Kume, M. Gallotti, G. Nunes, Review on Anionic/Cationic Surfactant Mixtures, Journal of Surfactants and Detergents. 11 (2008) 1–11.

[47] E. Scholten, T. Moschakis, C.G. Biliaderis, Biopolymer composites for engineering food structures to control product functionality, Food Structure. 1 (2014) 39–54.

[48] D. Saha, S. Bhattacharya, Hydrocolloids as thickening and gelling agents in food: a critical review, Journal of Food Science and Technology. 47 (2010) 587–597.

[49] S. Ogawa, E.A. Decker, D.J. McClements, Production and Characterization of O/W Emulsions Containing Cationic Droplets Stabilized by Lecithin- Chitosan Membranes, Journal of Agricultural and Food Chemistry. 51 (2003) 2806–2812.

[50] S. Mun, E.A. Decker, D.J. McClements, Influence of Droplet Characteristics on the Formation of Oil-in-Water Emulsions Stabilized by Surfactant-Chitosan Layers, Langmuir. 1 (2005) 6228–6234.

[51] U. Klinkesorn, Y. Namatsila, Influence of chitosan and NaCl on physicochemical properties of low-acid tuna oil-in-water emulsions stabilized by non-ionic surfactant, Food Hydrocolloids. 23 (2009) 1374–1380.

[52] T. Kaasgaard, D. Keller, Chitosan coating improves retention and redispersibility of freeze-dried flavor oll emulsions, Journal of Agricultural and Food Chemistry. 58 (2010) 2446–2454.

[53] E. Colombo, F. Cavalieri, M. Ashokkumar, Role of Counterions in Controlling the Properties of Ultrasonically Generated Chitosan-Stabilized Oil-in-Water Emulsions, Applied Materials & Interfaces. 7 (2015) 12972–12980.

[54] M.A. Rao, Rheology of Fluid, Semisolid, and Solid Foods, 3rd ed., Springer, New York, 2013.

[55] T.R. Cuadros, J.M. Aguilera, Gels as Precursors of Porous Matrices for Use in Foods: a Review, Food Biophysics. 10 (2015) 487–499.

[56] R. Curvello, V.S. Raghuwanshi, G. Garnier, Engineering nanocellulose hydrogels for biomedical applications, Advances in Colloid and Interface Science. 267 (2019) 47–61.

[57] S. Graham, P. Facal, A. Blencowe, Thermoresponsive polysaccharides and their thermoreversible physical hydrogel networks, Carbohydrate Polymers. 207 (2019) 143–159.

[58] A. Martínez-Ruvalcaba, E. Chornet, D. Rodrigue, Viscoelastic properties of dispersed chitosan/xanthan hydrogels, Carbohydrate Polymers. 67 (2007) 586–595.

[59] J.C. Raguzzoni, I. Delgadillo, J.A. Lopes, Influence of a cationic polysaccharide on starch functionality, Carbohydrate Polymers. 150 (2016) 369–377.

[60] J. Nie, Z. Wang, Q. Hu, Difference between Chitosan Hydrogels via Alkaline and Acidic Solvent Systems, Nature Publishing Group. 6 (2016) 1–8.

[61] T. Furuike, D. Komoto, H. Hashimoto, H. Tamura, Preparation of chitosan hydrogel and its solubility in organic acids, International Journal of Biological Macromolecules. 104 (2017) 1620–1625.

[62] Y. Chen, F. Wang, N. Zhang, Y. Li, B. Cheng, Y. Zheng, Preparation of a 6-OH quaternized chitosan derivative through click reaction and its application to novel thermally induced / polyelectrolyte complex hydrogels, Colloids and Surfaces B: Biointerfaces. 158 (2017) 431–440.

[63] M. Abrami, C. Siviello, G. Grassi, D. Larobina, M. Grassi, Investigation on the thermal gelation of Chitosan/β-Glycerophosphate solutions, Carbohydrate Polymers. 214 (2019) 110–116.

[64] D. Komoto, T. Furuike, H. Tamura, Preparation of polyelectrolyte complex gel of sodium alginate with chitosan using basic solution of chitosan, International Journal of Biological Macromolecules. 126 (2019) 54–59.

[65] T. Ramasamy, T. Hiep, J. Yeon, H. Jun, J. Hwan, C. Soon, H. Choi, J. Oh, Layer-by-layer coated lipid – polymer hybrid nanoparticles designed for use in anticancer drug delivery, Carbohydrate Polymers. 102 (2014) 653–661.

[66] B.R. Thompson, V.N. Paunov, T.S. Horozov, S.D. Stoyanov, An ultra melt-resistant hydrogel from food grade carbohydrates, RSC Advances. 7 (2017) 45535–45544.

[67] R.G. Jones, J. Kahovec, R. Stepto, E.S. Wilks, M. Hess, T. Kitayama, W.V. Metanomski, Compendium of Polymer Terminology and Nomenclature, 1st ed., RSC Publiching, Cambridge, 2008.

[68] F. Chemat, Zill-e-Huma, M.K. Khan, Applications of ultrasound in food technology: Processing , preservation and extraction, Ultrasonics Sonochemistry. 18 (2011) 813–835.

[69] M. Sivakumar, S.Y. Tang, K.W. Tan, Cavitation technology-A greener processing technique for the generation of pharmaceutical nanoemulsions, Ultrasonics Sonochemistry. 21 (2014) 2069–2083.

[70] A.R. Jambrak, Physical Properties of Sonicated Products: A New Era for Novel Ingredients, in: D. Bermudez-Aguirre (Ed.), Ultrasound: Advances in Food Processing and Preservation, 1st ed., Academic Press, Cambridge, 2017: pp. 237–265.

[71] D. Bermúdez-Aguirre, T. Mobbs, G. V Barbosa-Cánovas, Ultrasound Applications in Food Processing, in: H. Feng, G. V Barbosa-Cánovas, J. Weiss (Eds.), Ultrasound Technologies for Food and Bioprocessing, 1st ed., Springer, 2011: pp. 65–106.

[72] O. Behrend, K. Ax, H. Schubert, Influence of continuous phase viscosity on emulsification by ultrasound, Ultrasonics Sonochemistry. 7 (2000) 77–85.

[73] J.J. Morelli, G. Szajer, Analysis of Surfactants: Part II, Journal of Surfactants and Detergents. 4 (2001) 75–83.

[74] I. Kralova, J. Sjöblom, Surfactants Used in Food Industry : A Review, 1 (2017) 1363–1383.

[75] J.-M. Li, S.-P. Nie, The functional and nutritional aspects of hydrocolloids in foods, Food Hydrocolloids. 53 (2014) 46–61.

[76] H. El Knidri, R. Belaabed, A. Addaou, A. Laajeb, A. Lahsini, Extraction , chemical modi fi cation and characterization of chitin and chitosan, International Journal of Biological Macromolecules. 120 (2018) 1181–1189.

[77] F. Garavand, M. Rouhi, S. Hadi, I. Cacciotti, Improving the integrity of natural biopolymer films used in food packaging by crosslinking approach: A review, International Journal of Biological Macromolecules. 104 (2017) 687–707.

[78] A. Verlee, S. Mincke, C. V Stevens, Recent developments in antibacterial and antifungal chitosan and its derivatives, Carbohydrate Polymers. 164 (2017) 268–283.

[79] A. Busilacchi, A. Gigante, M. Mattioli-Belmonte, S. Manzotti, R.A.A. Muzzarelli, Chitosan stabilizes platelet growth factors and modulates stem cell differentiation toward tissue regeneration., Carbohydrate Polymers. 98 (2013) 665–76.

[80] D. Zhao, S. Yu, B. Sun, S. Gao, S. Guo, K. Zhao, Biomedical Applications of Chitosan and Its Derivative Nanoparticles, Polymers. 10 (2018) 462–481.

[81] M. Rinaudo, Chitin and chitosan: Properties and applications, Progress in Polymer Science. 31 (2006) 603–632.

[82] M.R. Kasaai, A review of several reported procedures to determine the degree of N-acetylation for chitin and chitosan using infrared spectroscopy, Carbohydrate Polymers. 71 (2008) 497–508.

[83] J. Brugnerotto, J. Lizardi, F.M. Goycoolea, W. Argülles-Monal, J. Desbrières, M. Rinaudo, An infrared investigation in relation with chitin and chitosan characterization, Polymer. 42 (2001) 3569–3580.

[84] M.R. Kasaai, Calculation of Mark-Houwink-Sakurada (MHS) equation viscometric constants for chitosan in any solvent-temperature system using experimental reported viscometric constants data, Carbohydrate Polymers. 68 (2007) 477–488.

[85] M.P.M. Costa, M.C. Delpech, I. de M. Ferreira, M.T. de M. Cruz, J.A. Castanharo, M.D. Cruz, Evaluation of single-point equations to determine intrinsic viscosity of sodium alginate and chitosan with high deacetylation degree, Polymer Testing. 63 (2017) 427–433.

[86] A.M.T. Lago, I.C.O. Neves, N.L. Oliveira, D.A. Botrel, L.A. Minim, J.V. de Resende, Ultrasound-assisted oil-in-water nanoemulsion produced from Pereskia aculeata Miller mucilage, Ultrasonics Sonochemistry. 50 (2019) 339–353.

[87] W. Brown, Dynamic Light Scattering: The Method and Some Applications, 1st ed., Clarendon Press, Oxford, 1993.

[88] Z.R. Nieto Galván, L.S. Soares, A.E.A. Medeiros, N.F.F. Soares, A.M. Ramos, J.S.R. Coimbra, E.B. Oliveira, Rheological Properties of Aqueous Dispersions of Xanthan Gum Containing Different Chloride Salts Are Impacted by both Sizes and Net Electric Charges of the Cations, Food Biophysics. 13 (2018) 186–197.

[89] M. Kaszuba, M.T. Connah, F.K. McNeil-Watson, U. Nobbmann, Resolving Concentrated Particle Size Mixtures Using Dynamic Light Scattering, Particle & Particle Systems Characterization. 1 (2007) 159–162.

[90] R.C. Santana, F.A. Perrechil, A.C.K. Sato, R.L. Cunha, Emulsifying properties of collagen fibers: Effect of pH, protein concentration and homogenization pressure, Food Hydrocolloids. 25 (2011) 604–612.

[91] B.C. Tatar, G. Sumnu, S. Sahin, Rheology of Emulsions, in: J. Ahmed, P. Ptaszek, S. Basu (Eds.), Advances in Food Rheology and Its Applications, 1st ed., Woodhead Publishing, Cambridge, 2017: pp. 437–457.

[92] D.J. Mcclements, S.M. Jafari, General Aspects of Nanoemulsions and Their Formulation, in: D.J. Mcclements (Ed.), Nanoemulsions, 1st ed., Academic Press, Cambridge, 2018: pp. 3–20.

[93] S. Ghosh, J.N.C. Ã, Factors affecting the freeze-thaw stability of emulsions, Food Hydrocolloids. 22 (2008) 105–111.

[94] S. Ghosh, D. Rousseau, Freeze – thaw stability of water-in-oil emulsions, Journal of Colloid And Interface Science. 339 (2009) 91–102.

[95] S. Aldrich, Tween 20, (2019) 1–2. https://www.sigmaaldrich.com/catalog/substance/tween20123459005645 11?lang=pt&region=BR.

[96] A. Teo, K.K.T. Gog, J. Wen, I. Oey, S. Ko, K. Hae-Soo, J.L. Sung, Physicochemical properties of whey protein, lactoferrin and Tween 20 stabilised nanoemulsions: Effect of temperature, pH and salt, Food Chemistry. 197 (2015) 297–306.

[97] K. Dunn, Surfactants and Polymers Containing Oxyethylene Groups Show a Complex Behavior, in: B. Kronberg, K. Holmberg, B. Lindman (Eds.), Surface Chemistry of Surfactants and Polymers, 1st ed., John Wiley & Songs, 2014: pp. 137–152.

[98] D. Saha, S. Bhattacharya, Hydrocolloids as thickening and gelling agents in food : a critical review, 47 (2010) 587–597.

[99] A. Mohraz, Interfacial routes to colloidal gelation, Current Opinion in Colloid & Interface Science. 25 (2016) 89–97.

[100] E.A. Foegeding, Rheology and sensory texture of biopolymer gels, Current Opinion in Colloid & Interface Science. 12 (2007) 242–250.

[101] W.A. Laftah, S. Hashim, A.N. Ibrahim, W.A. Laftah, S. Hashim, A.N. Ibrahim, Polymer Hydrogels: A Review, Polymer-Plastics Technology and Engineering. 50 (2017) 1475–1486.

[102] F.M. Clydesdale, Color perception and food quality, Journal of Food Quality. 14 (1991) 61–74.
[103] P. Singham, P. Birwal, B.K. Yadav, Importance of Objective and Subjective Measurement of Food Quality and their Inter-relationship, Food Processing & Technology. 6 (2015) 1–9.
[104] C. Spence, On the psychological impact of food colour, Flavour. 4 (2015) 1–16.
[105] W. Wijaya, A.R. Patel, A.D. Setiowati, P. Van Der Meeren, Trends in Food Science & Technology Functional colloids from proteins and polysaccharides for food applications, Trends in Food Science & Technology. 68 (2017) 56–69.
[106] Y. Zheng, J. Monty, R.J. Linhardt, Polysaccharide-based nanocomposites and their applications, Carbohydrate Research. 405 (2015) 23–32.
[107] J. Liu, S. Willfor, C. Xu, A review of bioactive plant polysaccharides: Biological activities, functionalization, and biomedical applications, Bioactive Carbohydrates and Dietary Fibre. 5 (2015) 31–61.
[108] G. Zhu, L. Sheng, Q. Tong, Food Hydrocolloids Preparation and characterization of carboxymethyl-gellan and pullulan blend films, Food Hydrocolloids. 35 (2014) 341–347.
[109] P.B. Pathare, U.L. Opara, F.A.-J. Al-said, Colour Measurement and Analysis in Fresh and Processed Foods : A Review, Food Bioprocess Technology. 6 (2013) 36–60.
[110] Sigma-Aldrich, Yellow Sunset FCF, (2019) 1. https://www.sigmaaldrich.com/catalog/product/aldrich/465224?lang=pt&region=BR.
[111] R.W. Korsmqer, R. Gumy, E. Doelker, P. Buri, N.A. Peppas, Mechanisms of solute release from porous hydrophilic polymers, International Journal of Pharmaceutics. 15 (1983) 25–35.
[112] R.W. Korsmeyer, N.A. Peppas, Effect of the morphology of hydrophilic polymeric, Journal of Membrane Science. 9 (1981) 211–227.
[113] L. Chien-Chi, A.T. Metters, Hydrogels in controlled release formulations: Network design and mathematical modeling, Advanced Drug Delivery Reviews. 58 (2006) 1379–1408.
[114] X. Shen, J.L. Shamshina, P. Berton, R.D. Rogers, Hydrogels based on cellulose and chitin: fabrication, properties, and applications, Green Chemistry. 1 (2016) 53–75.
[115] S. Sinthusamran, S. Benjakul, P.J. Swedlund, Y. Hemar, Physical and rheological properties of fish gelatin gel as influenced by κ-carrageenan, Food Bioscience. 20 (2017) 88–95.
[116] A.C. Bertolini, STARCHES Characterization, Properties, and Applications, 1st ed., CRC Press, New York, 2010.

[117] J.F. Steffe, Rheological Methods in Food Process Engineering, 2nd ed., Freeman Press, East Lansing, 1996.
[118] J. BeMiller, T. Whistler, Starch: Chemistry and Tchnology, 3rd ed., Academic Press, New York, 2009.
[119] K. Rovina, P. Perumal, S. Siddiquee, Trends in Analytical Chemistry Methods for the analysis of Sunset Yellow FCF (E110) in food and beverage products- a review, Trends in Analytical Chemistry. 85 (2016) 47–56.
[120] G. Feketea, S. Tsabouri, Common food colorants and allergic reactions in children: Myth or reality?, Food Chemistry. 230 (2017) 578–588.
[121] J.L. Ford, M.H. Rubinstein, M. F, J.E. Hogan, P.J. Edgar, Importance of drug type, tablet shape and added diluents on drug release kinetics from hydroxypropylmethylcellulose matrix tablets, International Journal of Pharmaceutics. 40 (1987) 223–234.
[122] J.L. Ford, K. Mitchell, P. Rowe, D.J. Armstrong, P.N.C. Elliott, C. Rostron, J.E. Hogan, Mathematical modelling of drug release from hydroxypropylmethylcellulose matrices : Effect of temperature, International Journal of Pharmaceutics. 71 (1991) 95–104.
[123] H. Kim, R. Fassihi, Application of Binary Polymer System in Drug Release Rate Modulation. 2. Influence of Formulation Variables and Hydrodynamic Conditions on Release Kinetics, Journal oF Pharmaceutical Sciences. 86 (1997) 323–328.
[124] R.S. Harland, A. Gazzaniga, M.E. Sangalli, P. Colombo, N.A. Peppas, Drug/Polymer Matrix Swelling and Dissolution, Pharmaceutical Research. 5 (1988) 488–494.
[125] S. Sahin, S.G. Sumnu, Physical Properties of Foods, 1st ed., Springer, New York, 2006.

APÊNDICE I: Supplementary Material (SM) for "Insights on physicochemical aspects of chitosan dispersion in aqueous solutions of acetic, glycolic, propionic or lactic acid"

Lucas de Souza Soares[1,✉], Rayza Badiani Perim[1], Elson Santiago de Alvarenga[2], Luciano de Moura Guimarães[3], Alvaro Vianna Novaes de Carvalho Teixeira[3], Jane Sélia dos Reis Coimbra[1], Eduardo Basílio de Oliveira[1,✉]

[1] Departamento de Tecnologia de Alimentos (DTA), Universidade Federal de Viçosa (UFV), Campus Universitário, Postal code 36570-900, Viçosa, MG, Brazil.

[2] Departamento de Química (DEQ), Universidade Federal de Viçosa (UFV), Campus Universitário, Postal code 36570-900, Viçosa, MG, Brazil.

[3] Departamento de Física (DPF), Universidade Federal de Viçosa (UFV), Campus Universitário, Postal code 36570-900, Viçosa, MG, Brazil.

Corresponding authors:

✉ Eduardo Basílio de Oliveira, Departamento de Tecnologia de Alimentos (DTA), Universidade Federal de Viçosa (UFV), Campus Universitário, Postal code 36570-900, Viçosa, MG, Brazil; phone: +55 31 3899 2228; e-mail: eduardo.basilio@ufv.br.

✉ Lucas de Souza Soares, Departamento de Tecnologia de Alimentos (DTA), Universidade Federal de Viçosa (UFV), Campus Universitário, Postal code 36570-900, Viçosa, MG, Brazil; phone: +55 31 97111 8854; e-mail: lucassoares.ufv@gmail.com.

SUMARY

ABBREVIATIONS AND SYMBOLS

A	First constant of Mark-Houwink-Sakurada relationship (dimensionless)
A_2	Second virial coefficient $(cm^3 \cdot mol) \cdot g^{-2}$
c	Concentration $(g \cdot mL^{-1})$
dn/dc	Refractive index increment $(mg \cdot mL^{-1})$
$g^{(2)}(t)$	Normalized temporal intensity correlation functions
I	Scattering intensity
I_0	Laser intensity
K_{MHS}	Second constant of Mark-Houwink-Sakurada relationship $(dL \cdot g^{-1})$
k	Optical constant
$\bar{M}_V$	Viscometric-average molar mass (kDa)
$\bar{M}_W$	Weight-average molar mass (kDa)
n_0	Refraction index (dimensionless)
N_A	Avogadro number (mol^{-1})
q	Scattering vector modulus
r	Distance between the sample and the detector (m)
R_G	Gyration radius (nm)
R_Θ	Rayleigh ratio
Θ	Scattering angle (º)
λ	Wave-length (nm)
τ	Shear stress (Pa)
$\dot{\gamma}$	Shear rate (s^{-1})
η_{sp}	Specific viscosities (dimensionless)
η_r	Relative viscosity (dimensionless)
$[\eta]_H$	Huggins intrinsic viscosity $(dL \cdot g^{-1})$
$[\eta]_K$	Kraemer intrinsic viscosity $(dL \cdot g^{-1})$
$\overline{[\eta]}$	Average intrinsic viscosity $(dL \cdot g^{-1})$

I. Electrical conductivity from chitosan

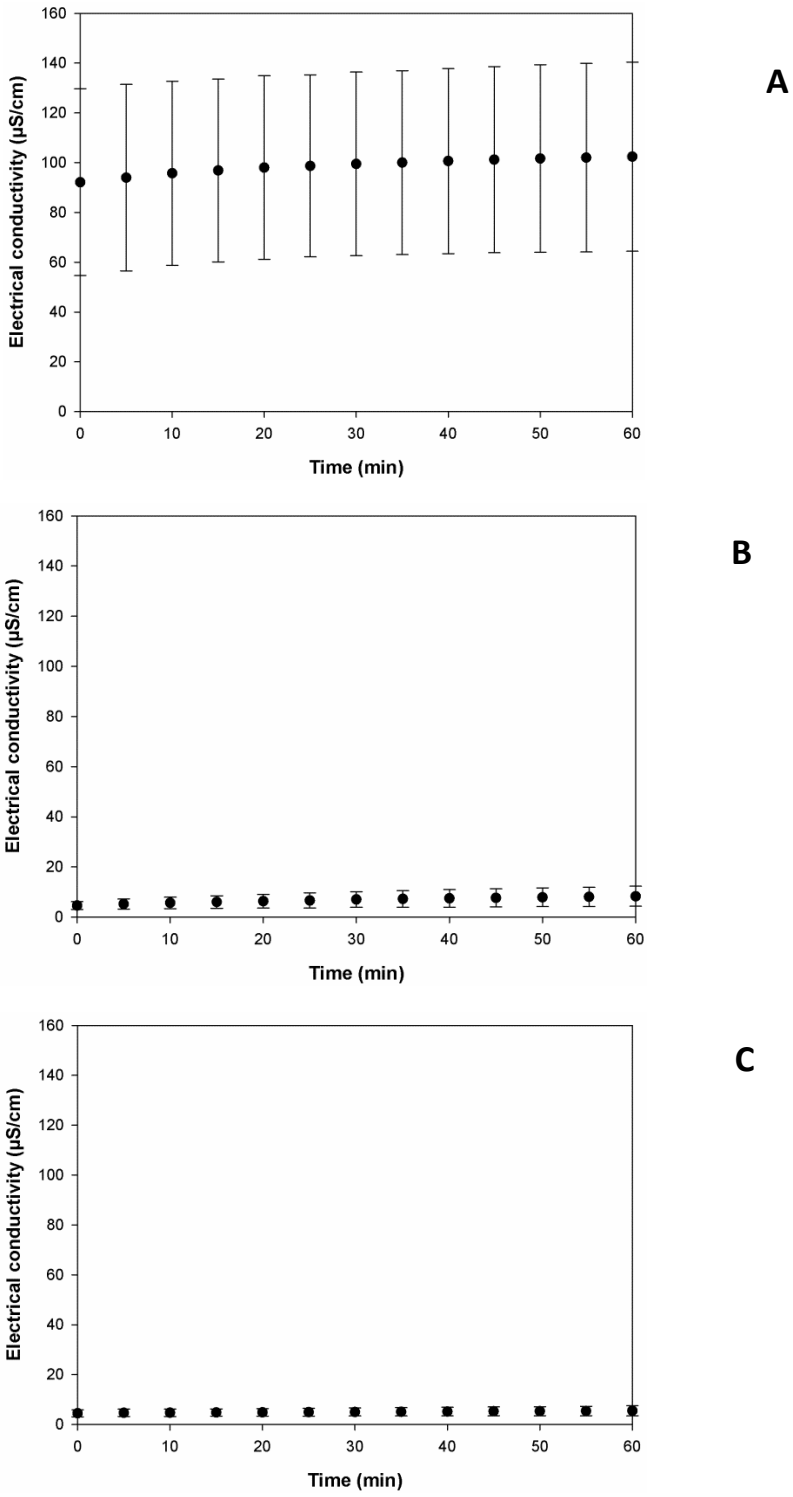

Figure SM1 -Electrical conductivity from chitosan washed three times (A, B, and C) with deionized water

II. Deacetylation degree

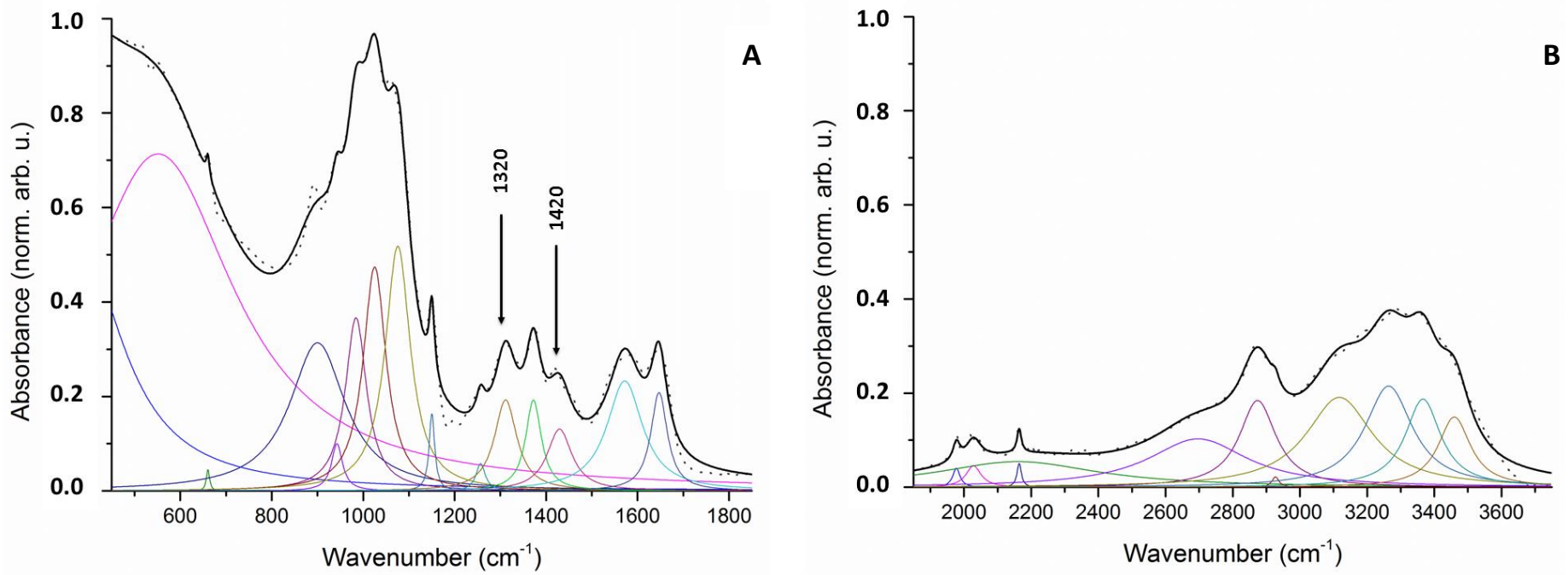

Figure SM2 - FT-IR spectra from chitosan to 450 - 1850 cm^{-1} (A) and 1850 - 3750 cm^{-1} (B). Absorbance from FT-IR spectra (··) and absorbance calculated through deconvolution in Lorentzian components (-).

III. Viscosimetric-average molar mass

From the flow times of chitosan dispersions [0.1, 0.2, 0.3, 0.4, and 0.5 g·(100 mL)$^{-1}$ in 50 mmol·L^{-1} lactic acid solution] measured in a Cannon-Fenske viscometer (model 513 20, Schott, Germany), specific (η_{sp}) (Equation 1) and relative viscosities (η_r) (Equation 2) were calculated.

$$\eta_{sp} = \frac{t - t_0}{t_0} \quad (1)$$

$$\eta_r = \eta_{sp} + 1 \quad (2)$$

Where, t is the flow time of the chitosan dispersions and t_0 is the flow time of lactic acid solution, in Equations 1 and 2.

Then, the average intrinsic viscosity ($\overline{[\eta]}$) was calculated as the average between the Huggins ($[\eta]_H$) and Kraemer ($[\eta]_K$) intrinsic viscosities (Figure SM3), which were obtained by extrapolating Equations 3 and 4, respectively, to infinite dilution (c → 0).

$$\frac{\eta_{sp}}{c} = [\eta]_H + k_1[\eta]^2 c \quad (3)$$

$$\frac{\ln(\eta_r)}{c} = [\eta]_K - k_1'[\eta]^2 c \quad (4)$$

Where k_1 and k'_1 are the Huggins and Kraemer constants, and c is the concentration of chitosan in the diluted dispersions.

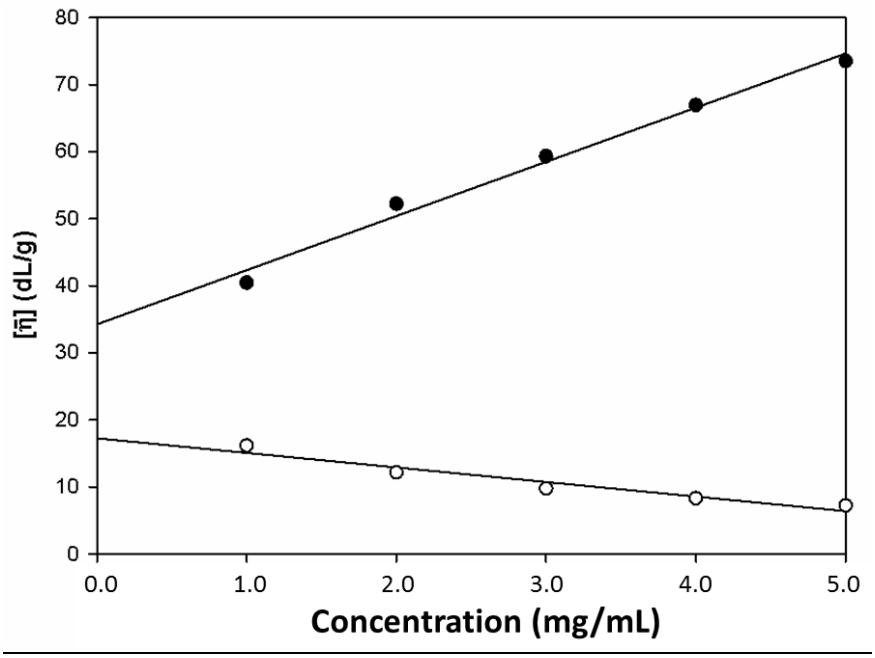

Figure SM3 – Extrapolation to infinite dilution ([chitosan] → 0) of Huggins and Kraemer empirical models adjusted to viscometric-average experimental data from chitosan aqueous dispersions. (●) $\frac{\eta_{sp}}{c} = k_1[80.8]^2 \cdot c + [34.3]$; R^2 = 0.99, (○) $\frac{\ln \eta_r}{c} = k'_1[-21.7]^2 \cdot c + [17.3]$; R^2 = 0.93.

IV. Weight-average molar mass

Light intensity measurements were derived according to the classical Rayleigh-Debye relationship (Equation 1).

$$\frac{k \cdot c}{\Delta R_\theta} = \frac{1}{\bar{M}_W}\left(1 + \frac{q^2\langle {R_G}^2\rangle}{3}\right) + 2A_2 \cdot c \quad (1)$$

Where k is an optical constant (Equation 2), c is the concentration (w/V), ΔR_Θ is the Rayleigh ratio in excess (Equation 3), $\bar{M}_W$ is the weight-average molar mass, q is the scattering vector modulus (as showed to Equation 11), $\langle R_G^2 \rangle$ is the root-mean square average radius of gyration, and A_2 is the 2nd virial coefficient.

$$k = \frac{2\pi^2 \cdot n_0 \cdot (\mathrm{d}n/\mathrm{d}c)^2}{N_A \cdot \lambda^4} \quad (2)$$

Where n_0 is the refractive index of the reference solvent, (dn/dc) is the refractive index increment with the increasing of the polymer concentration, N_A is the Avogadro contant, and λ is the wave-length.

Then, the refractive index increment (dn/dc) was estimated (0.2000 ± 0.0090 mg·mL^{-1}) using a differential refractometer (BI-DNDC, Brookhaven, USA). Five dispersions of chitosan (concentrations 1.000, 2.000, 3.000, 4.000, and 5.000 mg·mL^{-1}) in 50 mmol·L^{-1} lactic acid were analyzed to determine (dn/dc) value; 50 mmol·L^{-1} lactic acid solution was used also as solvent reference during the measures (Figure SM4).

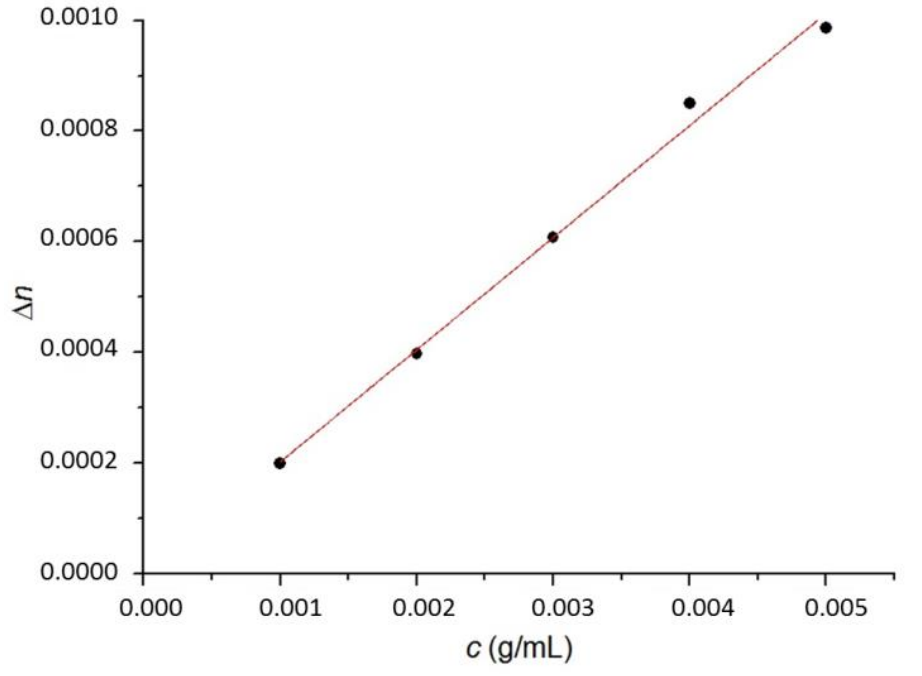

Figure SM4 - Δn as function of the chitosan concentration (1.000, 2.000, 3.000, 4.000, and 5.000 mg·mL^{-1} in 50 mmol·L^{-1} lactic acid) used to estimate (dn/dc) value.

Rayleigh ratio in excess (ΔR_Θ) was defined as (Equation 3):

$$\Delta R_\theta = R_{\theta,dispersion} - R_{\theta,solvent} \quad (3)$$

Where R_Θ is the Rayleigh ratio (as showed in Equation 4), and θ is the angle of detection (as showed in Equation 5).

$$R_\theta \equiv \frac{r^2 \cdot i}{I_0} \quad (4)$$

Where r is the distance between the sample and the detector, i is the scattering intensity, and I_0 is the laser intensity.

$$q = \frac{4\pi n_0}{\lambda} \sin\frac{\theta}{2} \quad (5)$$

From ΔR_Θ estimated values a Zimm plot was elaborated to determine the weight-average molar mass (Figure SM5).

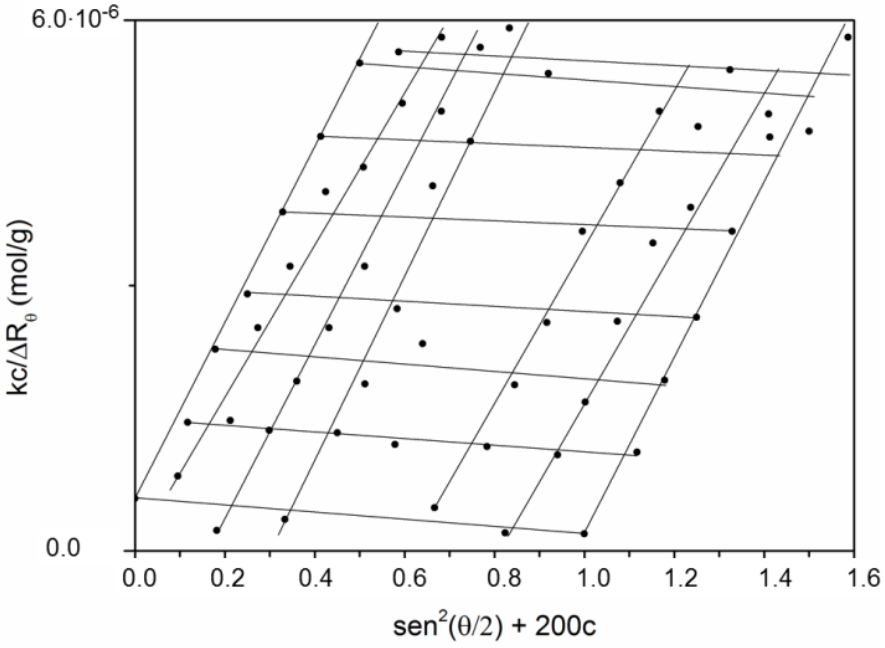

Figure SM5 - Zimm plot to chitosan concentration (0.476, 0.909, 1.667, 2.307, 3.333, 4.118, and 5.000 mg·mL^{-1} in 50 mmol·L^{-1} lactic acid) used to determine the weight-average molar mass.

V. Refractive index of the dispersions containing chitosan

Table SM1 - Refractive index of 0.1 g·(100 mL)$^{-1}$ chitosan dispersed in different concentrations of acetic, glycolic, propionic, and lactic acid.

Acid concentration (mmol·L^{-1})	Acetic	Glycolic	Propionic	Lactic
10	1.3326 ± 0.0002	1.3325 ± 0.0001	1.3325 ± 0.0000	1.3327 ± 0.0003
20	1.3330 ± 0.0001	1.3326 ± 0.0002	1.3328 ± 0.0002	1.3329 ± 0.0004
30	1.3331 ± 0.0001	1.3328 ± 0.0003	1.3330 ± 0.0001	1.3329 ± 0.0002
40	1.3331 ± 0.0001	1.3329 ± 0.0002	1.3332 ± 0.0001	1.3330 ± 0.0004
50	1.3330 ± 0.0000	1.3329 ± 0.0002	1.3332 ± 0.0000	1.3332 ± 0.0002

VI. PDI

Table SM2 - PDI values from d_h values of 0,1 g·(100 mL)$^{-1}$ chitosan dispersed in different concentrations of organic acid.

Acid concentration (mmol·L^{-1})	Acetic	Glycolic	Propionic	Lactic
10	0.04 ± 0.01	0.09 ± 0.01	0.03 ± 0.01	0.07 ± 0.01
20	0.04 ± 0.01	0.04 ± 0.01	0.10 ± 0.01	0.03 ± 0.01
30	0.06 ± 0.02	0.10 ± 0.04	0.06 ± 0.03	0.03 ± 0.01
40	0.05 ± 0.02	0.08 ± 0.04	0.05 ± 0.04	0.09 ± 0.05
50	0.03 ± 0.01	0.09 ± 0.06	0.05 ± 0.03	0.07 ± 0.03

VII. Rheograms of the dispersions

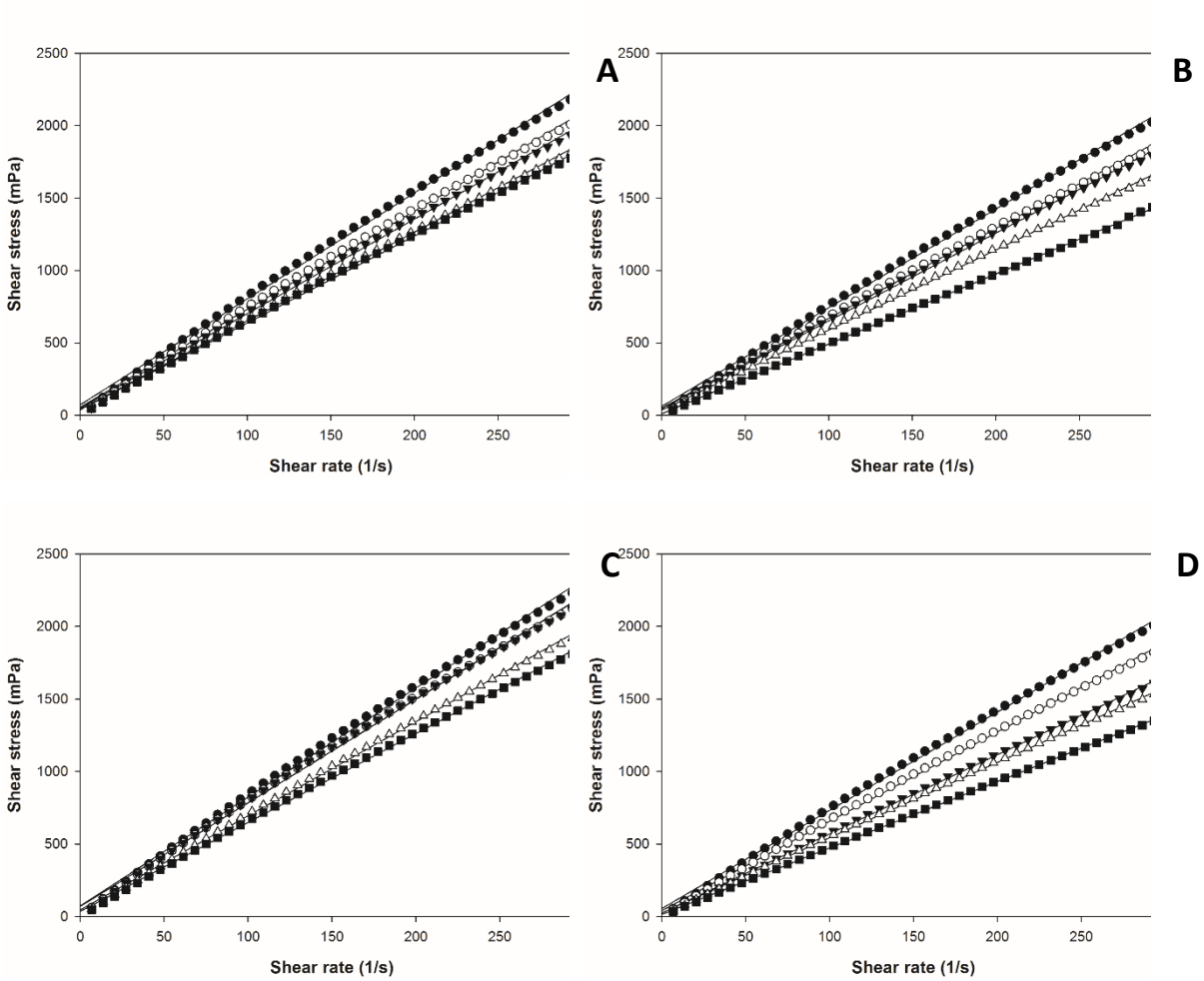

Figure SM5 - Flow curves of (●) 10 mmol·L^{-1} (○) 20 mmol·L^{-1}, (▲) 30 mmol·L^{-1}, (Δ) 40 mmol·L^{-1}, and (▪) 50 mmol·L^{-1} to acetic (A), glycolic (B), propionic (C), and lactic acid (D).

VIII. Statistical analyses to fitted the Newtonian model to experimental $\tau = f(\dot{\gamma})$ data

Table SM3 - Nonlinear OLS Summary of Residual Errors to Newtonian Model adjusted to experimental data

System	DF Model	DF Error	MSE	R^2	MAPE (%)	*System*	DF Model	DF Error	MSE	R^2	MAPE (%)
AA 10	1	131	13193.3	0.97	5.29	GA 10	1	131	21132.1	0.94	4.89
AA 20	1	131	10061.9	0.97	4.48	GA 20	1	131	6728.2	0.98	4.35
AA 30	1	131	19441.8	0.94	3.97	GA 30	1	131	2853.9	0.99	4.07
AA 40	1	131	16866.0	0.94	3.62	GA 40	1	131	993.0	0.99	3.70
AA 50	1	131	14600.2	0.95	3.46	GA 50	1	131	11133.6	0.94	1.54
PA 10	1	131	4486.9	0.99	6.16	LA 10	1	131	13614.6	0.96	4.48
PA 20	1	131	4202.6	0.99	5.23	LA 20	1	131	7587.6	0.97	3.81
PA 30	1	131	2790.9	0.99	4.79	LA 30	1	131	1319.0	0.99	2.57
PA 40	1	131	16423.1	0.95	3.94	LA 40	1	131	2509.4	0.99	2.87
PA 50	1	131	7915.4	0.97	3.28	LA 50	1	131	7454.8	0.96	2.13

Table SM4 - Nonlinear OLS Parameter Estimates to Newtonian Model adjusted to experimental data

System	μ (mPa·s)	Std. Error	t Value	Pr > |t|	*System*	μ (mPa·s)	Std. Error	t Value	Pr > |t|
AA 10	7.7 ± 0.6	0.0568	135.29	< 0.0001	GA 10	7.1 ± 0.8	0.0718	99.17	< 0.0001
AA 20	7.1 ± 0.4	0.0496	142.29	< 0.0001	GA 20	6.5 ± 0.2	0.0405	159.23	< 0.0001
AA 30	6.8 ± 0.5	0.0689	98.34	< 0.0001	GA 30	6.3 ± 0.3	0.0264	238.41	< 0.0001
AA 40	6.3 ± 0.7	0.0642	98.60	< 0.0001	GA 40	5.7 ± 0.1	0.0156	366.99	< 0.0001
AA 50	6.2 ± 0.7	0.0597	103.70	< 0.0001	GA 50	4.9 ± 0.6	0.0521	93.62	< 0.0001
PA 10	7.7 ± 0.3	0.0331	233.98	< 0.0001	LA 10	7.0 ± 0.6	0.0577	122.21	< 0.0001
PA 20	7.5 ± 0.1	0.0320	234.42	< 0.0001	LA 20	6.4 ± 0.5	0.0430	147.84	< 0.0001
PA 30	7.4 ± 0.1	0.0261	284.32	< 0.0001	LA 30	5.6 ± 0.1	0.0179	310.80	< 0.0001
PA 40	6.7 ± 0.7	0.0633	106.05	< 0.0001	LA 40	5.3 ± 0.3	0.0248	214.61	< 0.0001
PA 50	6.3 ± 0.5	0.0440	143.50	< 0.0001	LA 50	4.7 ± 0.5	0.0427	109.15	< 0.0001

IX. FI-IR spectra

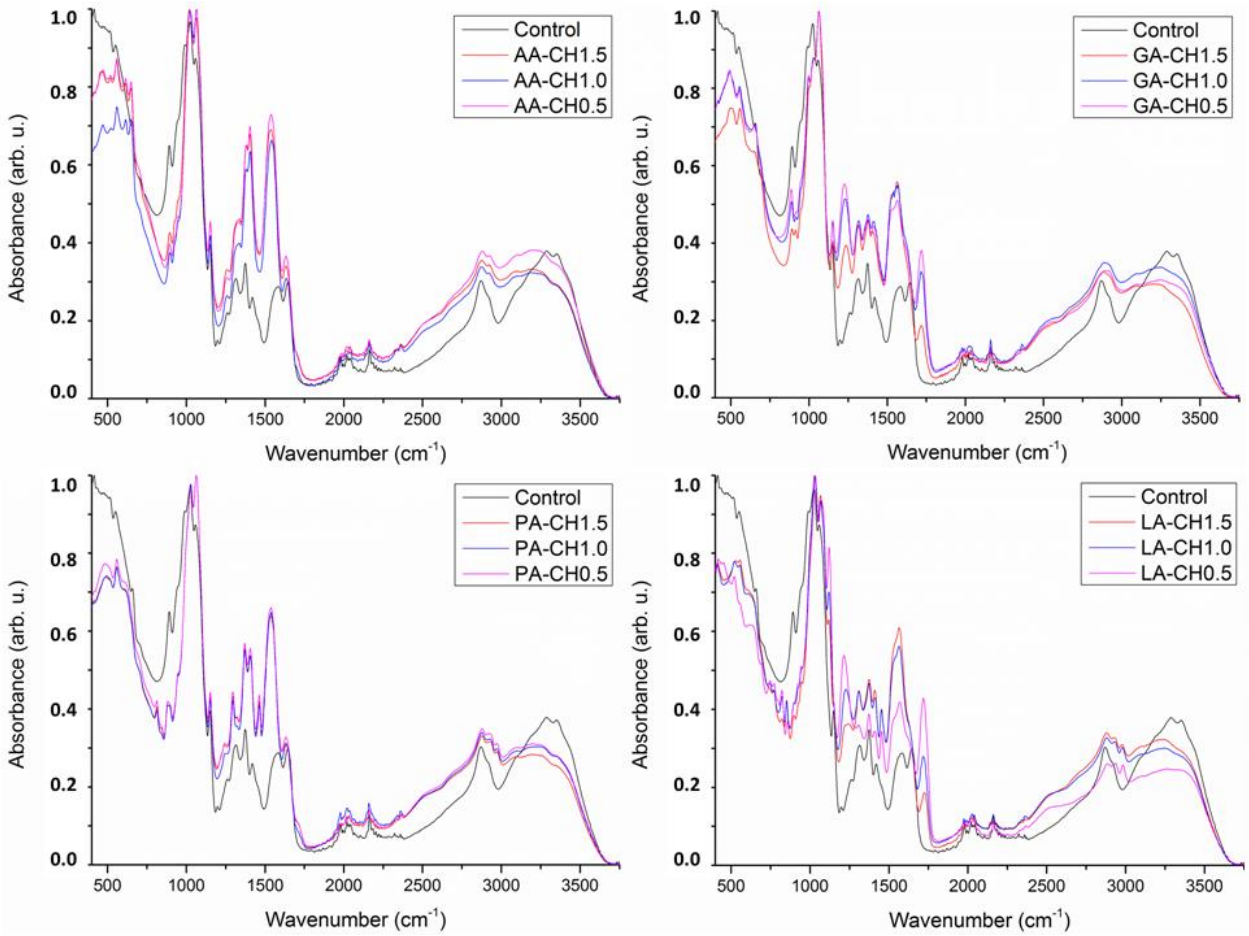

Figure SM6 - FT-IR of lyophilized dispersions containing chitosan [0.5, 1.0, and 1.5 g·(100 mL)$^{-1}$] in 100 mmol·L^{-1} acid solutions (AA, GA, PA, or LA).

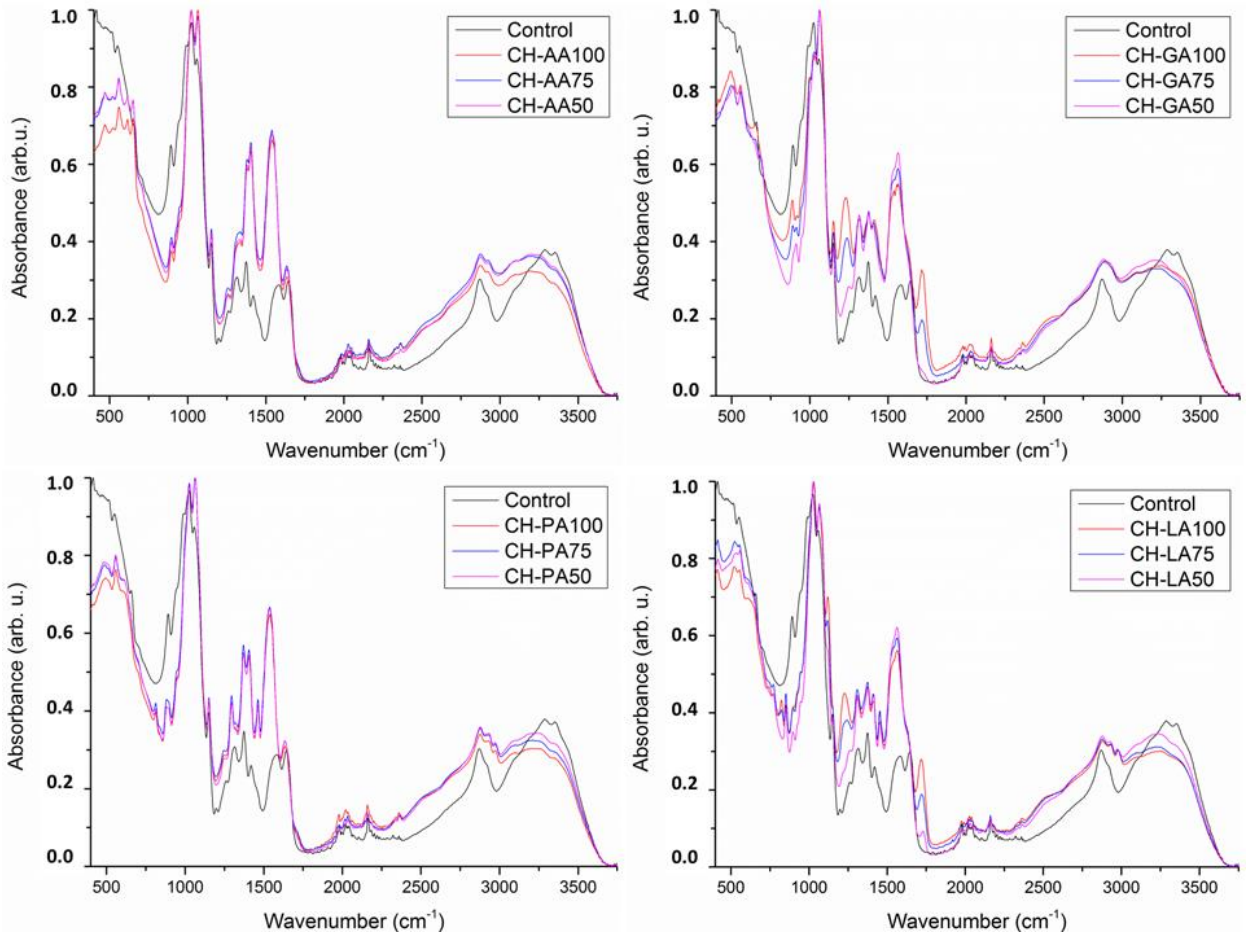

Figure SM7 - FT-IR spectra of lyophilized dispersions containing chitosan [1.0 g·(100 mL)$^{-1}$] in 50, 75, or 100 mmol·L^{-1} acid solutions (AA, GA, PA, or LA).

Table SM5 - Normalized absorbance (arb. u.) calculated through deconvolution in Lorentzian components to chitosan powder and lyophilized dispersions containing chitosan [1.0 g·(100 mL)$^{-1}$] in 50, 75, or 100 mmol·L^{-1} acid solutions (AA or GA)

Chitosan powder		CH dispersed in AA						CH dispersed in GA					
-		50 mmol·L^{-1}		75 mmol·L^{-1}		100 mmol·L^{-1}		50 mmol·L^{-1}		75 mmol·L^{-1}		100 mmol·L^{-1}	
Peak	Abs	Peak	Abs	Peak	Abs	Peak	Abs	Peak	Abs	Peak	Abs	Peak	Abs
900	0.6154	894	0.3985	893	0.4107	893	0.3748	905	0.3887	897	0.4368	888	0.4975
943	0.7123	937	0.4503	937	0.4595	936	0.4206	948	0.4156	950	0.4961	943	0.5219
1076	0.8478	1074	0.9493	1074	0.9548	1074	0.9743	1068	0.9938	1069	0.9945	1089	0.9999
1150	0.4133	1154	0.4261	1154	0.4364	1154	0.4230	1154	0.3861	1153	0.4302	1152	0.4590
1257	0.2228	1250	0.2579	1250	0.2508	1251	0.2600	1243	0.2776	1234	0.4139	1230	0.5219
1319	0.3064	1319	0.4071	1318	0.4256	1318	0.3987	1313	0.4698	1314	0.4704	1315	0.4613
1372	0.3447	1374	0.5777	1374	0.5955	1374	0.5705	1372	0.4652	1371	0.4704	1370	0.4662
1419	0.2589	1406	0.6327	1406	0.6440	1405	0.6228	1417	0.4219	1419	0.4334	1422	0.4464
1572	0.3013	1539	0.6980	1538	0.7060	1539	0.6847	1572	0.6253	1569	0.5867	1567	0.5468
1647	0.3157	1642	0.3410	1642	0.3467	1642	0.3203	1633	0.3614	1632	0.3614	1631	0.3846
2874	0.2976	2886	0.3570	2887	0.3642	2886	0.3349	2885	0.3548	2886	0.3486	2888	0.3509
3460	0.2761	3465	0.2500	3464	0.2452	3459	0.2165	3460	0.2232	3460	0.2287	3425	0.2401

Table SM6 - Normalized absorbance (arb. u.) calculated through deconvolution in Lorentzian components to chitosan powder and lyophilized dispersions containing chitosan [1.0 g·(100 mL)$^{-1}$] in 50, 75, or 100 mmol·L^{-1} acid solutions (PA or LA)

Chitosan powder		CH dispersed in AA						CH dispersed in GA					
-		50 mmol·L^{-1}		75 mmol·L^{-1}		100 mmol·L^{-1}		50 mmol·L^{-1}		75 mmol·L^{-1}		100 mmol·L^{-1}	
Peak	Abs	Peak	Abs	Peak	Abs	Peak	Abs	Peak	Abs	Peak	Abs	Peak	Abs
900	0.6154	889	0.4190	888	0.4377	888	0.4175	897	0.3372	896	0.4090	895	0.4121
943	0.7123	943	0.4655	942	0.4901	942	0.4722	945	0.4152	942	0.4904	943	0.4918
1076	0.8478	1073	0.9638	1072	0.9687	1072	0.9620	1072	0.9342	1074	0.9219	1075	0.9296
1150	0.4133	1154	0.4320	1154	0.4357	1154	0.4245	1154	0.3864	1154	0.4103	1154	0.4139
1257	0.2228	1247	0.2788	1239	0.2905	1246	0.2860	1220	0.2465	1235	0.3889	1228	0.4608
1319	0.3064	1324	0.3511	1322	0.5550	1324	0.3546	1310	0.4318	1309	0.4560	1309	0.4396
1372	0.3447	1370	0.5444	1370	0.5517	1370	0.5444	1372	0.4591	1372	0.4739	1373	0.4627
1419	0.2589	1408	0.5428	1409	0.6176	1408	0.5361	1413	0.4480	1414	0.4517	1414	0.4335
1572	0.3013	1538	0.6843	1519	0.6176	1537	0.6628	1573	0.6071	1569	0.5894	1570	0.5568
1647	0.3157	1642	0.3340	1640	0.3311	1642	0.3170	1636	0.3445	1638	0.2529	1635	0.3477
2874	0.2976	2871	0.3491	2875	0.3495	2868	0.3336	2892	0.3361	2875	0.3280	2877	0.3234
3460	0.2761	3465	0.2362	3474	0.2103	3462	0.2122	3421	0.2813	3462	0.2157	3414	0.2613

YAHOO! MAIL
Localizar mensagens, documentos, fotos ou pessoas
Página inicial

Escrever

Entrada
Não lidos
Favoritos
Rascunhos
Enviados
Arquivo
Spam
Lixeira
Menos

Visualizações Mostrar

Pastas Ocultar
Nova pasta
CBCTA
CNPEN
Comprovantes
Espectros FT-IR
Formatura
Graduação - ...
Livros
Monitoria
Pibic
Pós-grad IFMG
SAUNI
Termodinâmi...
UBER
UFV
vagner tebaldi

Voltar | Arquivar | Mover | Apagar | Spam

eduardo basilio <eduardobasilio.ufv@gmail.com> 13 de mai às 09:18
Para: Lucas Souza

---------- Forwarded message ---------
De: <jfk@chembiotech.couk>
Date: qui, 9 de mai de 2019 às 17:01
Subject: Re: Enquiry: Authorization for including a published article within academic thesis
To: <eduardo.basilio@ufv.br>, <c.abinesh@elsevier.com>

Dear Clement - can you deal with this one please according to Elsevier protocol = I Have not objection - Many thanks,
With kind regards,

From: eduardo.basilio@ufv.br
To: jfk@chembiotech.couk
Date sent: 22 Apr 2019 12:20:04 +0100
Subject: Enquiry: Authorization for including a published article within academic thesis

> The following enquiry was sent via the Elsevier Journal website:
>
> -- Sender --
> First Name: Eduardo Basílio
> Last Name: de Oliveira
> Email: eduardo.basilio@ufv.br
>
> -- Message --
> Dear Dr Kennedy
>
> I hope this message finds you well.
>
> We had the honour of publishing our most recent article in the
> International Journal of Biological Macromolecules
> (https://doi.org/10.1016/j.ijbiomac.2019.01.106). This article was
> born as a part of the doctorate research of Lucas de Souza Soares
> (1st author), under my advisement.
>
> Next month, Lucas will defend his thesis. The purpose of the present
> message is ask you, as editor-in-chef, if we could incorporate the
> above mentionned article, as published by IJBIOMAC, within Lucas'
> thesis. This thesis will be presented to a jury of professors and,
> if approved, its final version will be available in the academic
> library of our university (http://www.bbt.ufv.br/).
>
> If we have your authorization to present this article as a part of

> Lucas' thesis, the complete reference of the journal IJBIOMAC will
> be adequatelly presented, and your message giving such autorization
> will be attached to it. Moreover, we emphasize that the sole purpose
> of this thesis is academic.
>
> We thanks you a lot for your attention, and we hope you can give us
> a positive response.
>
> Best regards,
>
> Eduardo
>
> _____
> Eduardo Basílio de Oliveira
> Associate Professor
> Food Technology Department
> Universidade Federal de Viçosa (UFV)
> 36.570.900 - Viçosa, MG - Brazil

Livre de vírus. www.avg.com.

APÊNDICE II: Supplementary Material (SM) for "Chitosan dispersed in aqueous solutions of acetic, glycolic, propionic or lactic acid as a thickener/stabilizer agent of O/W emulsions produced by ultrasonic homogenization"

SUMARY

I. Deacetylation degree

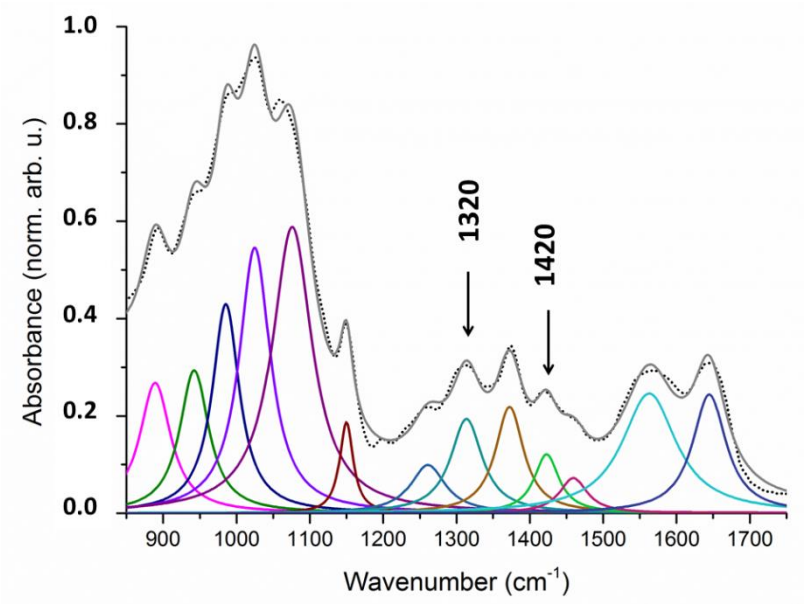

Figure SM1 - FT-IR spectra from chitosan to 850 - 1750 cm^{-1}. Absorbance from FT-IR spectra (··) and absorbance calculated through deconvolution in Lorentzian components (-).

II. Viscometric-average molar mass ($\bar{M}_V$) of chitosan

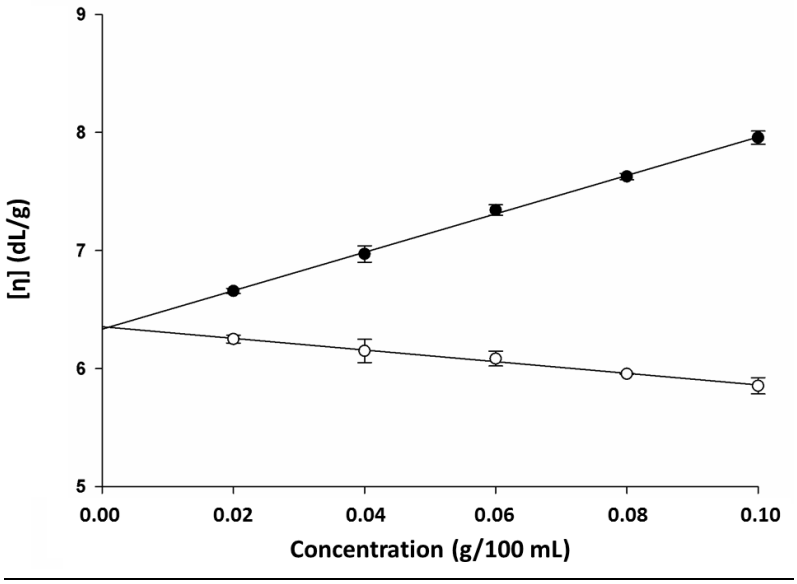

Figure SM2 – Extrapolation to infinite dilution (c → 0) of Huggins and Kraemer empirical models adjusted to viscometric average experimental data from chitosan aqueous dispersions. (●) $\frac{\eta_{sp}}{c} = k_1[16.3]^2 \cdot c + [6.3]$; R^2 = 0.999, (○) $\frac{\ln \eta_r}{c} = k'_1[-17.3]^2 \cdot c + [6.0]$; R^2 = 0.930.

III. Rheograms of the emulsions

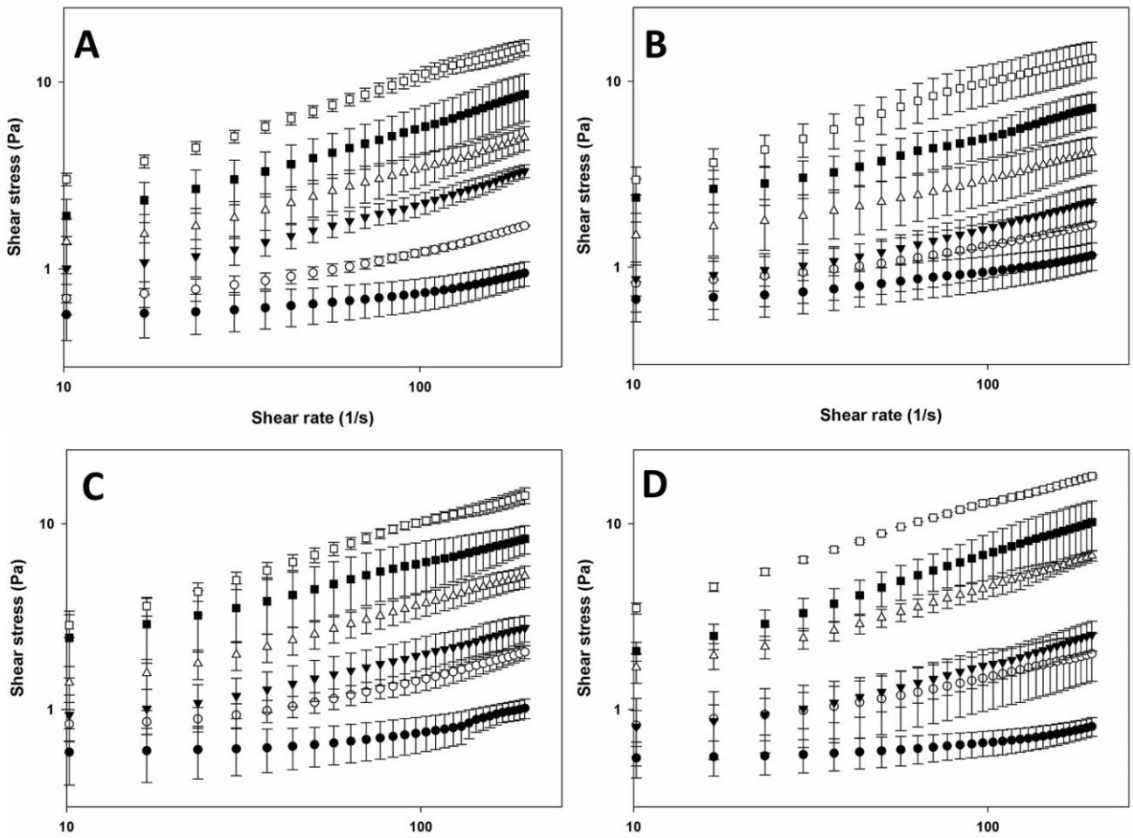

Figure SM3 - Flow curves of emulsions prepared with a continuous phase containing acetic (A), glycolic (B), propionic (C), and lactic acid (D), and (●) 0.000 g·(100 g)$^{-1}$, (○) 0.125 g·(100 g)$^{-1}$, (▼) 0.250 g·(100 g)$^{-1}$, (Δ) 0.500 g·(100 g)$^{-1}$, (■) 0.750 g·(100 g)$^{-1}$, and (□) 1.000 g·(100 g)$^{-1}$ chitosan, previously dispersed.

I. Statistical analyses to fitted the Ostwald de Waele Model to experimental $\tau = f(\dot{\gamma})$ data

Table SM1 - Nonlinear OLS Summary of Residual Errors to Ostwald de Waele Model adjusted to experimental data

Emulsion	DF Model	DF Error	MSE	Emulsion	DF Model	DF Error	MSE
AA 0.000 g·(100 g)$^{-1}$	2	88	0.001	GA 0.000 g·(100 g)$^{-1}$	2	88	0.001
AA 0.125 g·(100 g)$^{-1}$	2	88	0.005	GA 0.125 g·(100 g)$^{-1}$	2	88	0.005
AA 0.250 g·(100 g)$^{-1}$	2	88	0.016	GA 0.250 g·(100 g)$^{-1}$	2	88	0.008
AA 0.500 g·(100 g)$^{-1}$	2	88	0.018	GA 0.500 g·(100 g)$^{-1}$	2	88	0.017
AA 0.750 g·(100 g)$^{-1}$	2	88	0.021	GA 0.750 g·(100 g)$^{-1}$	2	88	0.049
AA 1.000 g·(100 g)$^{-1}$	2	88	0.044	GA 1.000 g·(100 g)$^{-1}$	2	88	0.049
PA 0.000 g·(100 g)$^{-1}$	2	88	0.002	LA 0.000 g·(100 g)$^{-1}$	2	88	0.001
PA 0.125 g·(100 g)$^{-1}$	2	88	0.011	LA 0.125 g·(100 g)$^{-1}$	2	88	0.004
PA 0.250 g·(100 g)$^{-1}$	2	88	0.011	LA 0.250 g·(100 g)$^{-1}$	2	88	0.001
PA 0.500 g·(100 g)$^{-1}$	2	88	0.014	LA 0.500 g·(100 g)$^{-1}$	2	88	0.019
PA 0.750 g·(100 g)$^{-1}$	2	88	0.011	LA 0.750 g·(100 g)$^{-1}$	2	88	0.014
PA 1.000 g·(100 g)$^{-1}$	2	88	0.036	LA 1.000 g·(100 g)$^{-1}$	2	88	0.049

Table SM2 - Nonlinear OLS Parameter Estimates to Ostwald de Waele Model adjusted to experimental data

Emulsion	Parameter	t Value	Pr > |t|	Emulsion	Parameter	t Value	Pr > |t|
AA 0.000 g·(100 g)$^{-1}$	K (Pa·s^n)	16.3	< 0.0001	GA 0.000 g·(100 g)$^{-1}$	K (Pa·s^n)	32.8	< 0.0001
	n	15.9	< 0.0001		n	21.5	< 0.0001
AA 0.125 g·(100 g)$^{-1}$	K (Pa·s^n)	11.9	< 0.0001	GA 0.125 g·(100 g)$^{-1}$	K (Pa·s^n)	15.2	< 0.0001
	n	19.5	< 0.0001		n	19.8	< 0.0001
AA 0.250 g·(100 g)$^{-1}$	K (Pa·s^n)	10.7	< 0.0001	GA 0.250 g·(100 g)$^{-1}$	K (Pa·s^n)	11.7	< 0.0001
	n	24.8	< 0.0001		n	21.5	< 0.0001
AA 0.500 g·(100 g)$^{-1}$	K (Pa·s^n)	15.1	< 0.0001	GA 0.500 g·(100 g)$^{-1}$	K (Pa·s^n)	14.9	< 0.0001
	n	35.4	< 0.0001		n	28.2	< 0.0001
AA 0.750 g·(100 g)$^{-1}$	K (Pa·s^n)	21.6	< 0.0001	GA 0.750 g·(100 g)$^{-1}$	K (Pa·s^n)	14.2	< 0.0001
	n	58.2	< 0.0001		n	29.7	< 0.0001
AA 1.000 g·(100 g)$^{-1}$	K (Pa·s^n)	27.3	< 0.0001	GA 1.000 g·(100 g)$^{-1}$	K (Pa·s^n)	24.8	< 0.0001
	n	75.1	< 0.0001		n	60.3	< 0.0001
PA 0.000 g·(100 g)$^{-1}$	K (Pa·s^n)	11.0	< 0.0001	LA 0.000 g·(100 g)$^{-1}$	K (Pa·s^n)	20.4	< 0.0001
	n	15.5	< 0.0001		n	14.4	< 0.0001
PA 0.125 g·(100 g)$^{-1}$	K (Pa·s^n)	9.6	< 0.0001	LA 0.125 g·(100 g)$^{-1}$	K (Pa·s^n)	15.5	< 0.0001
	n	16.7	< 0.0001		n	25.4	< 0.0001
PA 0.250 g·(100 g)$^{-1}$	K (Pa·s^n)	12.0	< 0.0001	LA 0.250 g·(100 g)$^{-1}$	K (Pa·s^n)	11.2	< 0.0001
	n	23.4	< 0.0001		n	24.4	< 0.0001
PA 0.500 g·(100 g)$^{-1}$	K (Pa·s^n)	17.8	< 0.0001	LA 0.500 g·(100 g)$^{-1}$	K (Pa·s^n)	18.6	< 0.0001
	n	42.7	< 0.0001		n	47.4	< 0.0001
PA 0.750 g·(100 g)$^{-1}$	K (Pa·s^n)	35.2	< 0.0001	LA 0.750 g·(100 g)$^{-1}$	K (Pa·s^n)	30.8	< 0.0001
	n	73.0	< 0.0001		n	86.4	< 0.0001
PA 1.000 g·(100 g)$^{-1}$	K (Pa·s^n)	28.9	< 0.0001	LA 1.000 g·(100 g)$^{-1}$	K (Pa·s^n)	31.7	< 0.0001
	n	74.4	< 0.0001		n	81.0	< 0.0001

APÊNDICE III: Supplementary Material (SM) for "Partial replacement of gelling agents by chitosan: impact on the color, viscoelastic properties, and release of Yellow sunset (INS 110) from carrageenan or starch hydrogels"

SUMARY

ABBREVIATIONS AND SYMBOLS

a^*	position between red and green in the CIELab coordinates
Abs	UV absorbance measured (arb. unit)
b^*	position between Yellow and blue in the CIELab coordinates
c^*	chroma or relative saturation in the CIELab coordinates
C	Yellow sunset (INS 110) concentration ($g \cdot (100\ g)^{-1}$)
G_0	elastic modulus in creep-recovery test (Pa)
G_1	retarded elastic modulus in creep-recovery test (Pa)
G'	storage modulus (Pa)
G''	loss modulus (Pa)
h^*	hue angle in the CIELab coordinates (°)
L^*	luminosity in the CIELab coordinates
J	compliance or strain per stress unit in creep-recovery tests (Pa^{-1})
J_0	instantaneous elastic term in creep-recovery tests (Pa^{-1})
J_1	retarded elastic term in creep-recovery tests (Pa^{-1})
R	release of Yellow sunset (INS 110) (%)
t	time (s)
tan δ	tangent of the phase shift (°)
γ	strain (%)
λ_{ret}	retardation time (s)
μ_0	viscous modulus associated with Newtonian viscosity (Pa)
η_{sp}	specific viscosities (dimensionless)
η_r	relative viscosity (dimensionless)
τ_0	stress (Pa)
$[\eta]$	average intrinsic viscosity ($dL \cdot g^{-1}$)

I. Degree of acetylation

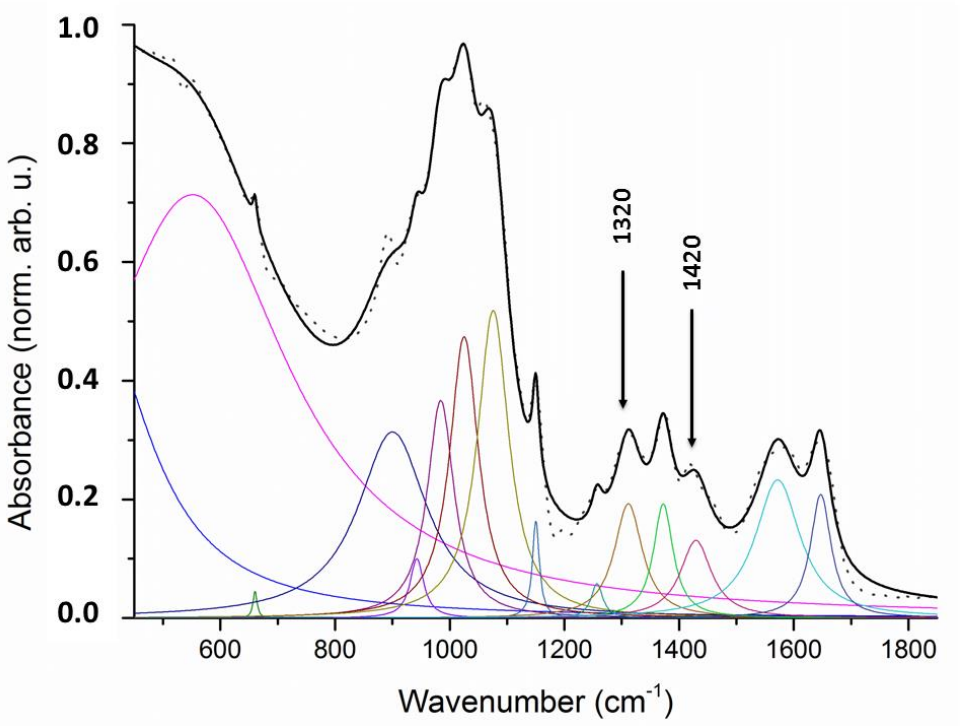

Figure SM1 - Chitosan FT-IR spectra from 450 to 1850 cm^{-1}. Absorbance from FT-IR spectra (··) and absorbance calculated through deconvolution in Lorentzian components (-).

II. Viscometric-average molar mass ($\bar{M}_V$) of chitosan

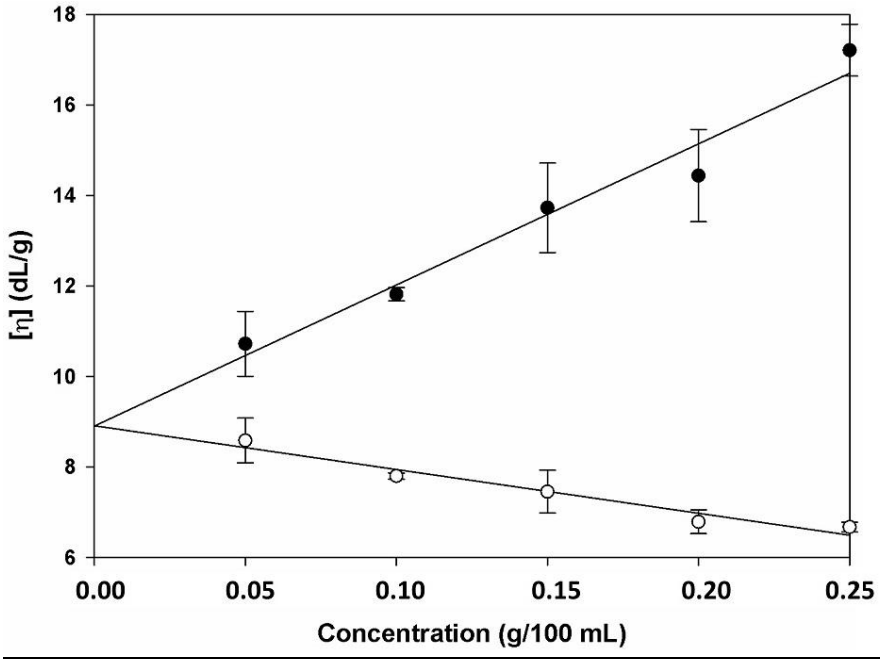

Figure SM2 - Extrapolation to infinite dilution ([chitosan] → 0) of Huggins and Kraemer empirical models adjusted to viscometric-average experimental data from chitosan aqueous dispersions. (●) $\frac{\eta_{sp}}{c} = k_1[31.20]^2 \cdot c + [8.90]$; R^2 = 0.97, (○) $\frac{\ln \eta_r}{c} = k'_1[-9.67]^2 \cdot c + [8.91]$; R^2 = 0.95.

III. Color analyses

From L*a*b* values previously determined, chroma (c^*) and hue angle (h^*) were calculated [109] (Equations SM1 and SM2). Results for c^* and h^* were presented in Table SM1.

$$c^* = \sqrt{a^2 + b^2} \quad \text{(SM1)}$$

$$h^* = \tan^{-1}\left(\frac{b}{a}\right) \quad \text{(SM2)}$$

Table SM1 - c^* and h^* color parameters to carrageenan and starch hydrogels, without or with a partial replacement of the gelling agent by 5.0, 7.5 or 10.0 (w/v) chitosan.

Carrageenan gels*	c^*	h^*
100.0% carrageenan	50.9 ± 0.2	1.0 ± 0.2
95.0% carrageenan + 5.0% chitosan	50.0 ± 1.0	1.0 ± 0.2
92.5% carrageenan + 7.5% chitosan	50.8 ± 0.1	1.0 ± 0.1
90.0% carrageenan + 10.0% chitosan	49.4 ± 0.9	1.0 ± 0.1
Starch gels**	c^*	h^*
100.0% starch	35.0 ± 2.0	0.9 ± 0.3
95.0% starch + 5.0% chitosan	34.0 ± 0.8	0.9 ± 0.1
92.5% starch + 7.5% chitosan	36.0 ± 0.3	0.9 ± 0.1
90.0% starch + 10.0% chitosan	36.0 ± 1.0	0.9 ± 0.1

IV. Burger's model

The Burgers model (Equation 3) fitted to the creep data [125] was described in terms of compliance (Equations SM3, SM4 and SM5).

$$\gamma = \frac{\tau_0}{G_0} + \frac{\tau_0}{G_1}\left(1 - \exp\left(\frac{-t}{(\lambda_{ret})}\right)\right) + \frac{\tau_0}{\mu_0} \cdot t \quad \text{(SM3)}$$

$$\frac{\gamma}{\tau_0} = \frac{1}{G_0} + \frac{1}{G_1}\left(1 - \exp\left(\frac{-t}{(\lambda_{ret})}\right)\right) + \frac{t}{\mu_0} \quad \text{(SM4)}$$

$$J = J_0 + J_1\left(1 - \exp\left(\frac{-t}{(\lambda_{ret})}\right)\right) + \frac{t}{\mu_0} \quad \text{(SM5)}$$

In Eq. (SM3), (SM4) and (SM5), γ is the total strain at time, G_0 is the elastic modulus, G_1 is the retarded elastic modulus, μ_0 is the viscous modulus associated with Newtonian viscosity, λ_{ret} is the retardation time, J is the compliance or strain per stress unit, J_0 is the instantaneous elastic term, and J_1 is the retarded elastic term.

V. Strain sweeps

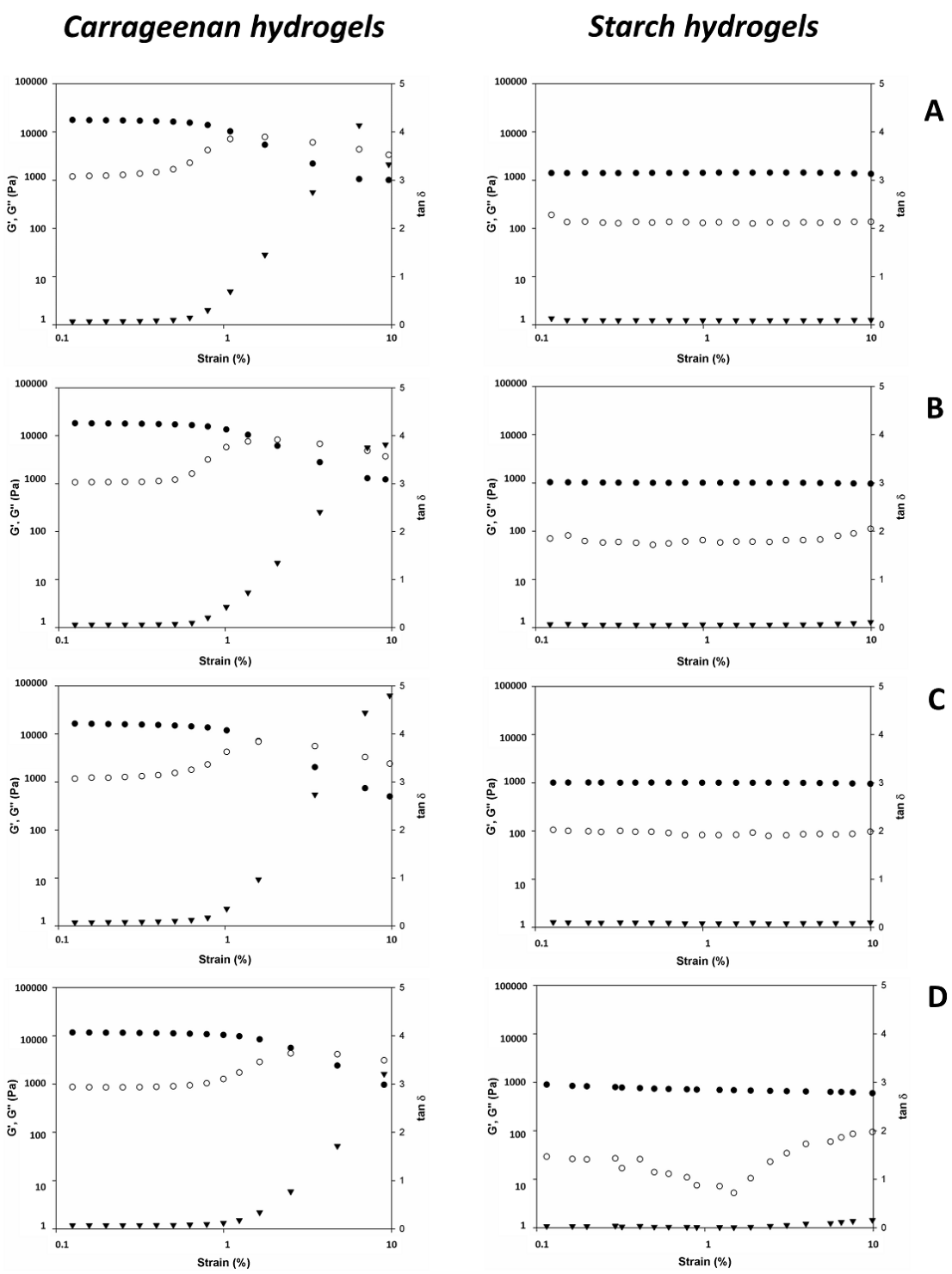

*In carrageenan gels the total polysaccharide concentration was 1.5 g·(100 mL)$^{-1}$.

**In starch gels the total polysaccharide concentration was 10.0 g·(100 mL)$^{-1}$.

Figure SM3 – Deformation sweeps from 0.1to 10.0% (at 1.59 Hz) for carrageenan and starch hydrogels, without and with replacement of the gelling agent by 5.0%, 7.5% or 10.0% (w/v) chitosan. *G'* (●), *G''* (○), and tan δ (▼).

VI. Release of Yellow sunset (INS 110) from the gels

A standard curve was built to measure the concentrations of colorant in the fluid phase in contact with the gels. For this purpose, 0.02% (w/v) Yellow sunset (INS 110) was dissolved into the sucrose solution (20.0% w/v). Colored sucrose solution was sequentially diluted (1:1; 1:5; 1:10; 1:15; 1:20; 1:25; and 1:50), in order to obtain different concentrations (*C*) of the INS 110. The UV absorbances of all of these solutions were measures using a microplate reader (Biochrom Asys Expert Plus, Biochrom, United Kingdom), at 480 nm [110]. Then, the correlation $Abs_{480nm} = f(C)$ could be deduced (Equation SM3).

$$Abs = 93.954 \cdot C \ (R^2 = 0.9777) \quad \text{(SM6)}$$

Where, *Abs* is the UV absorbance measured, and *C* is the Yellow sunset (INS 110) concentration.

VII. Statistical analyses

Table SM2 - ANOVA used to evaluate a*, b*, L*, c*, and h* of carrageenan gels

	DF	Mean Square	F Value	Pr > F
a*	3	0.1074	0.24	0.8671
b*	3	2.8991	2.17	0.1690
L*	3	0.5673	1.49	0.2889
c*	3	1.8419	1.92	0.2051
h*	3	0.0005	1.46	0.2967

Table SM3 - ANOVA used to evaluate a*, b*, L*, c*, and h* of starch gels

	DF	Mean Square	F Value	Pr > F
a*	3	0.8432	2.39	0.1443
b*	3	3.2873	1.61	0.2610
L*	3	6.6028	1.62	0.2601
c*	3	2.5678	0.04	0.9902
h*	3	0.0005	1.05	0.4224

Table SM4 - Nonlinear OLS Summary of Residual Errors to Burgers' Model adjusted to carrageenan data

	DF Model	DF Error	MSE
100.0% carrageenan	2	16	$7.0 \cdot 10^{-3}$
95.0% carrageenan + 5.0% chitosan	2	16	$8.0 \cdot 10^{-3}$
92.5% carrageenan + 7.5% chitosan	2	16	$1.0 \cdot 10^{-2}$
90.0% carrageenan + 10.0% chitosan	2	16	$1.1 \cdot 10^{-2}$

Table SM5 - Nonlinear OLS Parameter Estimates to Burger's model adjusted to carrageenan data

	Parameter	t Value	Approx Pr > |t|
100.0% carrageenan	J_0	107.02	< 0.0001
	J_1	51.15	< 0.0001
	λ_{ret}	11.70	< 0.0001
95.0% carrageenan + 5.0% chitosan	J_0	120.60	< 0.0001
	J_1	38.62	< 0.0001
	λ_{ret}	17.02	< 0.0001
92.5% carrageenan + 7.5% chitosan	J_0	35.61	< 0.0001
	J_1	29.27	< 0.0001
	λ_{ret}	10.32	< 0.0001
90.0% carrageenan + 10.0% chitosan	J_0	67.53	< 0.0001
	J_1	55.17	< 0.0001
	λ_{ret}	17.76	< 0.0001

Table SM6 - Nonlinear OLS Summary of Residual Errors to Burgers' Model adjusted to starch data

	DF Model	DF Error	MSE
100.0% starch	2	16	$2.7 \cdot 10^{-1}$
95.0% starch + 5.0% chitosan	2	16	$7.0 \cdot 10^{-1}$
92.5% starch + 7.5% chitosan	2	16	$1.3 \cdot 10^{0}$
90.0% starch + 10.0% chitosan	2	16	$1.6 \cdot 10^{0}$

Table SM7 - Nonlinear OLS Parameter Estimates to Burger's model adjusted to starch data

	Parameter	t Value	Approx Pr > |t|
100.0% starch	J_0	109.93	< 0.0001
	J_1	22.71	< 0.0001
	λ_{ret}	7.52	< 0.0001
95.0% starch + 5.0% chitosan	J_0	132.07	< 0.0001
	J_1	29.99	< 0.0001
	λ_{ret}	9.56	< 0.0001
92.5% starch + 7.5% chitosan	J_0	100.05	< 0.0001
	J_1	26.88	< 0.0001
	λ_{ret}	9.02	< 0.0001
90.0% starch + 10.0% chitosan	J_0	89.88	< 0.0001
	J_1	31.96	< 0.0001
	λ_{ret}	11.70	< 0.0001

Table SM8 - Nonlinear OLS Summary of Residual Errors to Maxwell's Model adjusted to carrageenan data

	DF Model	DF Error	MSE
100.0% carrageenan	2	16	$2.6 \cdot 10^9$
95.0% carrageenan + 5.0% chitosan	2	16	$1.6 \cdot 10^9$
92.5% carrageenan + 7.5% chitosan	2	16	$9.3 \cdot 10^8$
90.0% carrageenan + 10.0% chitosan	2	16	$1.4 \cdot 10^8$

Table SM9 - Nonlinear OLS Parameter Estimates to Maxwell's model adjusted to carrageenan data

	Parameter	t Value	Approx Pr > |t|
100.0% carrageenan	τ_0	99.33	< 0.0001
	τ_{eq}	68.37	< 0.0001
	λ_{ret}	25.89	< 0.0001
95.0% carrageenan + 5.0% chitosan	τ_0	57.91	< 0.0001
	τ_{eq}	83.57	< 0.0001
	λ_{ret}	28.30	< 0.0001
92.5% carrageenan + 7.5% chitosan	τ_0	72.28	< 0.0001
	τ_{eq}	67.82	< 0.0001
	λ_{ret}	24.47	< 0.0001
90.0% carrageenan + 10.0% chitosan	τ_0	186.50	< 0.0001
	τ_{eq}	132.50	< 0.0001
	λ_{ret}	49.59	< 0.0001

Table SM10 - Nonlinear OLS Summary of Residual Errors to Maxwell's Model adjusted to starch data

	DF Model	DF Error	MSE
100.0% starch	2	16	$5.6 \cdot 10^6$
95.0% starch + 5.0% chitosan	2	16	$3.9 \cdot 10^6$
92.5% starch + 7.5% chitosan	2	16	$3.7 \cdot 10^6$
90.0% starch + 10.0% chitosan	2	16	$3.5 \cdot 10^6$

Table SM11 - Nonlinear OLS Parameter Estimates to Maxwell's model adjusted to starch data

	Parameter	t Value	Approx Pr > |t|
100.0% starch	τ_0	68.48	< 0.0001
	τ_{eq}	84.49	< 0.0001
	λ_{ret}	32.76	< 0.0001
95.0% starch + 5.0% chitosan	τ_0	176.97	< 0.0001
	τ_{eq}	74.05	< 0.0001
	λ_{ret}	27.24	< 0.0001
92.5% starch + 7.5% chitosan	τ_0	162.34	< 0.0001
	τ_{eq}	77.16	< 0.0001
	λ_{ret}	29.09	< 0.0001
90.0% starch + 10.0% chitosan	τ_0	145.23	< 0.0001
	τ_{eq}	78.61	< 0.0001
	λ_{ret}	30.24	< 0.0001

Table SM12 - Nonlinear OLS Summary of Residual Errors to Korsmeyer-Peppa's model adjusted to carrageenan data

	DF Model	DF Error	MSE
100.0% carrageenan	2	16	$7.0 \cdot 10^3$
95.0% carrageenan + 5.0% chitosan	2	16	$5.0 \cdot 10^3$
92.5% carrageenan + 7.5% chitosan	2	16	$5.4 \cdot 10^3$
90.0% carrageenan + 10.0% chitosan	2	16	$5.9 \cdot 10^3$

Table SM13 - Nonlinear OLS Parameter Estimates to Korsmeyer-Peppa's model adjusted to carrageenan data

	Parameter	t Value	Approx Pr > |t|
100.0% carrageenan	*k*	11.11	< 0.0001
	n	23.88	0.0002
95.0% carrageenan + 5.0% chitosan	*k*	12.10	< 0.0001
	n	26.11	< 0.0001
92.5% carrageenan + 7.5% chitosan	*k*	11.20	< 0.0001
	n	23.34	< 0.0001
90.0% carrageenan + 10.0% chitosan	*k*	9.70	< 0.0001
	n	23.52	< 0.0001

Table SM14 - Nonlinear OLS Summary of Residual Errors to Korsmeyer-Peppa's model adjusted to starch data

	DF Model	DF Error	MSE
100.0% starch	2	16	$4.7 \cdot 10^3$
95.0% starch + 5.0% chitosan	2	16	$1.2 \cdot 10^2$
92.5% starch + 7.5% chitosan	2	16	$3.3 \cdot 10^2$
90.0% starch + 10.0% chitosan	2	16	$1.1 \cdot 10^3$

Table SM15 - Nonlinear OLS Parameter Estimates to Korsmeyer-Peppa's model adjusted to starch data

	Parameter	t Value	Approx Pr > |t|
100.0% starch	*k*	13.25	< 0.0001
	n	15.33	< 0.0001
95.0% starch + 5.0% chitosan	*k*	6.28	< 0.0001
	n	8.84	< 0.0001
92.5% starch + 7.5% chitosan	*k*	7.47	< 0.0001
	n	7.89	< 0.0001
90.0% starch + 10.0% chitosan	*k*	8.37	< 0.0001
	n	9.79	< 0.0001